

Modulating the glycolytic or Wnt- β -catenin signaling
pathway to generate EBV-specific human CD8⁺ cytotoxic
T lymphocytes with stem cell memory and
central memory properties (EBV-CTL_{SCM/CM})

Dissertation
Zur Erlangung des Grades
Doktor der Naturwissenschaften

Am Fachbereich Biologie
Der Johannes Gutenberg-Universität Mainz

Iuliia Weber

geboren am 01.02.1985
in Tschernonograd

Mainz, 2017

Eidesstattliche Erklärung

„Ich erkläre, dass ich die vorgelegte Thesis selbstständig, ohne unerlaubte fremde Hilfe und nur mit den Hilfen angefertigt habe, die ich in der Thesis angegeben habe. Alle Textstellen, die wörtlich oder sinngemäß aus veröffentlichten oder nicht veröffentlichten Schriften entnommen sind, und alle Angaben, die auf mündlichen Auskünften beruhen, sind als solche kenntlich gemacht. Bei den von mir durchgeführten Untersuchungen habe ich die Grundsätze guter wissenschaftlicher Praxis, wie sie in der Satzung der Johannes Gutenberg-Universität Mainz zur Sicherung guter wissenschaftlicher Praxis niedergelegt sind, eingehalten.“

Mainz, den.....

Dekan:

1. Berichterstatter:

2. Berichterstatter:

Tag der mündlichen Prüfung: 26.01.2017

Table of contents

1.	Abstract.....	1
2.	Introduction	3
2.1	Biology of CD8 ⁺ T lymphocyte immune response.....	3
2.2	CD8 ⁺ T cell memory formation	4
2.3	Characterization of CD8 ⁺ memory T cells.....	5
2.4	Wnt- β -catenin signaling pathway	6
2.5	mTOR signaling pathway	7
2.6	Metabolic profiles of T lymphocytes	10
2.7	Biology of Epstein-Barr virus infection.....	13
2.7.1	Lytic life cycle.....	14
2.7.2	Latent life cycle	15
2.7.3	Association of EBV with malignancies and PTLD.....	16
2.8	The clinical potential of T stem cell memory cells.....	18
2.9	Aim of this study	21
3.	Methods and Materials	22
3.1	Materials	22
3.1.1	Equipment.....	22
3.1.2	Consumables.....	23
3.1.3	Chemicals.....	23
3.1.4	Kits	24
3.1.5	Cytokines.....	24
3.1.6	Media and additives	25
3.1.7	Antibodies.....	25
3.1.8	Primers	26
3.1.9	Cell culture medium and buffer	27
3.1.10	Cells.....	29
3.2	Methods.....	30
3.2.1	Isolation of peripheral blood mononucleated cells from buffy coats.....	30
3.2.2	Isolation of naïve and total CD8 ⁺ T cells from PBMC	30

3.2.3	Generation of mature dendritic cells from PBMC	31
3.2.4	Generation of EBV-specific DC	31
3.2.5	Generation of EBV-specific PBMC	31
3.2.6	Production of EBV transformed B cells	32
3.2.7	Generation of EBV-specific CTL _{SCM/CM}	32
3.2.8	Freezing of cells.....	33
3.2.9	Thawing of cells	33
3.2.10	Generation of EBV supernatant from B95-8 cells	33
3.2.11	Cell surface marker analysis with flow cytometry	33
3.2.12	Analysis of the glucose consumption of <i>in vitro</i> generated CTL _{SCM/CM}	34
3.2.13	Analysis of the lactate production of <i>in vitro</i> generated CTL _{SCM/CM}	35
3.2.14	OCR and ECAR measurements of <i>in vitro</i> generated CTL _{SCM/CM}	36
3.2.15	Polymerase chain reaction (PCR)	37
3.2.16	IFN- γ ELISpot assay	37
3.2.17	The transmigration assay.....	38
3.2.18	Chromium-51 release assay	39
3.2.19	<i>In vivo</i> analysis on survival of CTL _{SCM/CM} in the absence of antigen.....	40
3.2.20	Adoptive T cell transfer in EBV-engrafted mice	41
3.2.21	Isolation and preparation of peripheral blood and organs from NSG-mice	41
4.	Results	43
4.1	Phenotype of <i>in vitro</i> generated EBV-CTL _{SCM/CM} using RAPA.....	43
4.2	Phenotype of <i>in vitro</i> generated EBV-CTL _{SCM/CM} using 2-DG	45
4.3	Phenotype of <i>in vitro</i> generated EBV-CTL _{SCM/CM} using TWS119.....	48
4.4	Proliferative capacity of EBV-CTL _{SCM/CM}	50
4.5	Phenotypic characterization of <i>in vitro</i> generated B-LCL.....	51
4.6	<i>In vitro</i> EBV reactivity of EBV-CTL _{SCM/CM} cells	52
4.7	Manipulation of T cell metabolism	55
4.8	Metabolic features of EBV-CTL _{SCM/CM} cells cultured with 2-DG and TWS119	58
4.9	Expression of Lef-1 and Tcf-7 in 2-DG/TWS119 treated EBV-CTL _{SCM/CM}	61
4.10	<i>In vitro</i> transmigration capacity of 2-DG/TWS119 treated EBV-CTL _{SCM/CM}	63

4.11	<i>In vivo</i> survival of EBV-CTL _{SCM/CM} cells cultured with 2-DG and TWS119.....	64
4.12	<i>In vivo</i> EBV reactivity of EBV-CTL _{SCM/CM} cultured with 2-DG.....	65
4.13	<i>In vivo</i> EBV reactivity of TWS119 treated EBV-CTL _{SCM/CM} cells	67
5.	Discussion.....	70
5.1	Phenotype and <i>in vitro</i> reactivity of EBV-specific CTL _{SCM/CM} cells generated under the impact of RAPA.....	70
5.2	Phenotype and <i>in vitro</i> reactivity of EBV-specific CTL _{SCM/CM} cells generated in presence of 2-DG.....	71
5.3	Phenotype and <i>in vitro</i> reactivity of EBV-specific CTL _{SCM/CM} cells generated in presence of TWS119	72
5.4	Similar phenotype but different functionality of EBV-specific CTL _{SCM/CM} cells generated by three different inhibitors	73
5.5	Metabolism profiles and migration potential of 2-DG treated CTL _{SCM/CM}	74
5.6	Metabolism profiles and migration potential of TWS119 treated CTL _{SCM/CM}	76
5.7	Adoptive transfer of 2-DG and TWS119 treated EBV-specific CTL _{SCM/CM} cells into B-LCL engrafted NSG-mice.....	77
6.	Summary and outlook	80
7.	References.....	82
8.	Appendix.....	92
8.1	Abbreviations	92
8.1	Index of figures	95
8.2	Index of tables	97
9.	Addendum.....	98
9.1	Acknowledgments.....	98
9.2	Curriculum vitae.....	99

1. Abstract

Post-transplant lymphoproliferative disease (PTLD) is a serious and life threatening disease driven by Epstein Barr Virus (EBV) in immunocompromised patients undergoing hematopoietic stem cell transplantation (HSCT). High dose chemotherapy or whole-body irradiation treatment severely impairs the immune system and increases the risk of opportunistic and recurrent infections, particularly caused by persistent viruses of the herpesvirus family such as cytomegalovirus (CMV) and EBV (Gottschalk et al. 2005). Currently, donor-derived memory virus-specific T cells are applied as antiviral treatment. However, the *in vitro* generation and adoptive transfer of EBV-specific CD8⁺ cytotoxic T lymphocytes (CTL) displaying stem cell memory (EBV-CTL_{SCM}) and central memory (EBV-CTL_{CM}) characteristics might be an interesting option to improve antiviral immunity since CTL_{SCM/CM} cells have been shown to have a prolonged long-lifespan and increased self-renewal capacity as compared to effector memory and effector T cells (Cieri et al. 2012); (Biasco et al. 2015).

Moreover, EBV-specific memory T cells might be an attractive tool to generate genetically modified T_{SCM} or T_{CM} cells such as e.g. CD19-CAR modified T_{SCM} or T_{CM} cells as reported by Sabatino and colleagues (Sabatino et al. 2016).

Therefore, the aim of this proof of concept study was to explore different approaches to generate antigen specific T_{SCM}⁺ and T_{CM}⁺ like T cells *in vitro*. Naïve CD45RA⁺ CD8⁺ T cells isolated from peripheral blood mononuclear cells (PBMC) of healthy donors were repetitively stimulated with EBV-specific peptides while pharmacologically treated with rapamycin, 2-deoxy glucose (2-DG) or TWS119. All drugs were shown to modulate T cell differentiation resulting in T cells that preferentially express the markers CD45RA, CD95, CD62L and CCR7 reported to define T lymphocytes with stem cell memory and central memory-like properties (He, Kato, Jiang, Daniel R Wahl, et al. 2011); (Sukumar et al. 2013); (Gattinoni et al. 2009).

Accordingly, treatment with all three drugs resulted in the expression of T_{SCM}⁺ and T_{CM}⁺ like phenotype. However, our studies revealed that rapamycin also strongly inhibited cell proliferation and antigen specificity, and therefore its further application was discontinued. Results from metabolic assays demonstrated that both 2-DG and TWS119 treated naïve CD8⁺ T cells (EBV-CTL_{SCM/CM} cells) exhibited a T_{SCM}⁺ and T_{CM}⁺ like quiescent metabolism by mainly utilizing oxidative phosphorylation (OXPHOS) to generate ATP. In addition, EBV-CTL_{SCM/CM} cells preferentially expressed the homing markers CCR7 and CD62L and showed increased migration capacity when compared to T_{EFF}. 2-DG treated EBV-CTL_{SCM/CM} cells were capable of secreting IFN- γ *in vitro* in the presence of EBV infected B cells (B-LCL) but unfortunately failed to elicit cytolytic activity to the same targets when tested in chromium-51 release assays. In contrast, TWS119 treated EBV-CTL_{SCM/CM} cells showed superior IFN- γ production *in vitro* and 40% cytotoxicity towards B-LCL in chromium-51 release assay.

To test for their long-term survival in the absence of antigen EBV-reactive CTL_{SCM/CM} cells were transferred into NOD/SCID-IL2Rcy^{null} (NSG)-mice and supplemented with human ILR13-Fc (IL-15 with extended half-life). Small amounts of 2-DG treated EBV-CTL_{SCM/CM} cells (1.8 %) could be detected in the peripheral blood of these mice at two weeks after transfer, suggesting that 2-DG treated EBV-CTL_{SCM/CM} cells failed to survive and persist for an extended time period *in vivo* in the absence of antigen, although NSG mice might not provide optimal conditions for long-term survival due to an impaired immunological micromilieu.

Finally, *in vivo* studies demonstrated that upon adoptive transfer of EBV-reactive CTL_{SCM/CM} cells into NOD/SCID-IL2Rcy^{null} (NSG)-mice engrafted with MHC-matched, EBV-immortalized human B cells (B-LCL) very poor survival of 2-DG treated EBV-CTL_{SCM/CM} cells could be detected, even though, the antigen (B-LCL) was present in the system. Tumor progression was equally rapid in control mice and in mice, who had received T cells. Thus, 2-DG treated EBV-CTL_{SCM/CM} cells failed to induce an anti-tumor response towards B cell lymphoma.

In contrast, TWS119 treated EBV-CTL_{SCM/CM} cells showed better long-term survival as about 30% of TWS119 treated CTL_{SCM/CM} cells could be detected in spleen and blood of mice sacrificed on day 28. Moreover, TWS119 treated EBV-CTL_{SCM/CM} cells elicited a profound anti-lymphoma response and tumor mice that had received TWS119 EBV-CTL_{SCM/CM} cells could be shown to survive for up to 80 days. As we detected small amounts of tumor in individual sacrificed recipients these results suggest, that TWS119 treated EBV-CTL_{SCM/CM} cells controlled tumor growth but apparently were not able to confer complete tumor regression.

In conclusion, treating naive CD45RA⁺ CD8⁺ T cells with TWS119 was more successful as compared to rapamycin and 2-DG. EBV-specific CTL_{SCM/CM} cells generated under the impact of TWS119 showed a T_{SCM}⁻ and T_{CM}⁻ like phenotype, increased migration capacity and quiescent metabolism *in vitro*. Moreover, CTL_{SCM/CM} cells showed superior *in vitro* and *in vivo* antigen recognition and long-term survival in NSG-mice in absence of the antigen.

In the future, *in vitro* generated CTL_{SCM/CM} cells might be an interesting approach to prevent opportunistic and recurrent viral infection in immunosuppressed patients after HSCT. Furthermore, as viral-specific CTL_{SCM/CM} cells can be transduced with genetically modified TCR (Cieri et al. 2012) or chimeric-antigen receptor (CAR) (Sabatino et al. 2016), these T cells could serve as a valuable tool to improve adoptive cellular immunotherapy.

2. Introduction

2.1 Biology of CD8⁺ T lymphocyte immune response

The human immune system comprises both innate and adaptive immunity. The innate immune system contains cells and proteins that are always present and ready to fight pathogens at the site of infection. The main components of the innate immune system are: physical epithelial barriers, phagocytic leukocytes, dendritic cells (DC), natural killer cells (NK) and circulating plasma proteins.

The adaptive immune system is activated against pathogens that are able to overcome innate immune defenses. Components of the adaptive immune system include humoral immunity, mediated by antibodies produced by B lymphocytes and cell-mediated immunity, composed of a primary response induced by naive T cells, formation of T lymphocytes with effector functions, and persistence of antigen-specific memory T cells.

In the thymus the immature CD4⁺CD8⁺ double-positive T cells are screened for TCR reactivity to self-peptides bound to major histocompatibility complex (MHC) of specific antigen presenting cells (APC), such as thymic cortical epithelial cells. During the process of negative selection, T cells with high affinity to self MHC molecules are eradicated, whereas cells with low affinity to these ligands receive a weak T cell receptor (TCR) signal that induces the double-positive cells to differentiate into either mature CD4⁺CD8⁻ or CD4⁻CD8⁺ single-positive T cells (positive selection).

Once CD8⁺ T lymphocytes have completed their development, they enter the bloodstream to reach the peripheral lymphoid organs. CD8⁺ T cells that have not encountered a specific antigen are defined as naive T cells (T_N). They circulate from the bloodstream into lymph nodes, spleen and mucosa-associated lymphoid tissues and back to the blood, whereby they get into contact with dendritic cells (DC). DC capture antigens at the sites of infection, generate antigenic peptides, present them on the cell surface in the context of MHC molecules and migrate into the secondary lymphoid organs to recruit naive T cells. DC are unique “professional APCs” since they express costimulatory molecules such as e.g. members of B7 and TNF family, on the cell surface. These costimulatory molecules effectively contribute to a full T cell activation. Upon antigen recognition on the surface of APC, T cells start proliferating and undergo clonal expansion before they differentiate into T stem cell memory cells (T_{SCM}), T central memory cells (T_{CM}), T effector memory cells (T_{EM}) and finally into T effector cells (T_{EFF}) of identical antigen specificity. Effector T cells exit into the efferent lymphatics, enter the bloodstream and migrate to the site of infection. The effector T cells disappear after antigen elimination but memory T cells will remain to give a quicker and stronger response to reinfections (Mackay et al. 2000); (Théry & Amigorena 2001).

2.2 CD8⁺ T cell memory formation

An enrichment of memory T cells throughout a human's life can be divided into three phases: memory generation, memory homeostasis and immunosenescence, as illustrated in Figure 1 (Farber et al. 2014).

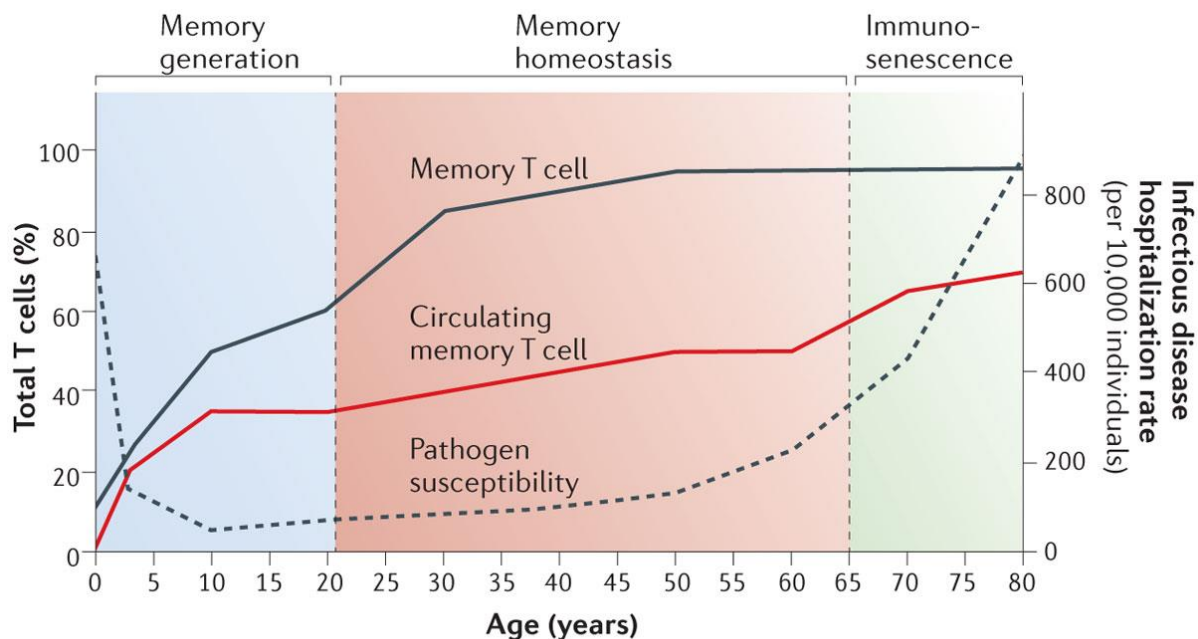


Figure 1: Memory T cell frequency, pathogen susceptibility and mortality throughout human life. Memory T cells are mostly generated during young adulthood. In the second phase, the expansion of memory T cells reaches plateau and remains stable throughout adulthood. In the third phase, T cells show senescent changes.

All T cells in a newborn organism are believed to be “young” and naïve, whereby individuals of the age between 0 and 20 years have the highest susceptibility to pathogens, shown by infectious disease hospitalization rate (Christensen et al. 2009). Accordingly, most of memory T cells are generated in the early adulthood in response to exposure to the various antigens.

The second phase of memory homeostasis (30-65 years) is characterized by a stable number of circulating memory T cells against different antigens (Saule et al. 2006), which ceases a pathogen susceptibility of an individual, as measured by infectious disease hospitalization rate (Christensen et al. 2009).

At the age of 65-70, individuals become more susceptible to pathogens, as reported by infectious disease hospitalization rate (Christensen et al. 2009), which is caused by immunosenescence and by general physiological decline. During the immunosenescence stage, the diversity of T cells is compromised by involution of the thymus and ongoing conversion of T_N into memory T cells due to exposure to a range of antigens, thus, resulting in reduced number of naïve T cells.

2.3 Characterization of CD8⁺ memory T cells

According to the “linear” or “developmental” model proposed by Restifo (Restifo 2014), as illustrated in Figure 2, naive T cells give a rise to all memory subsets in human and mouse organism, unlike the previous model, which proposed that memory T cells originate from T_{EFF} (Kaech & Ahmed 2001).

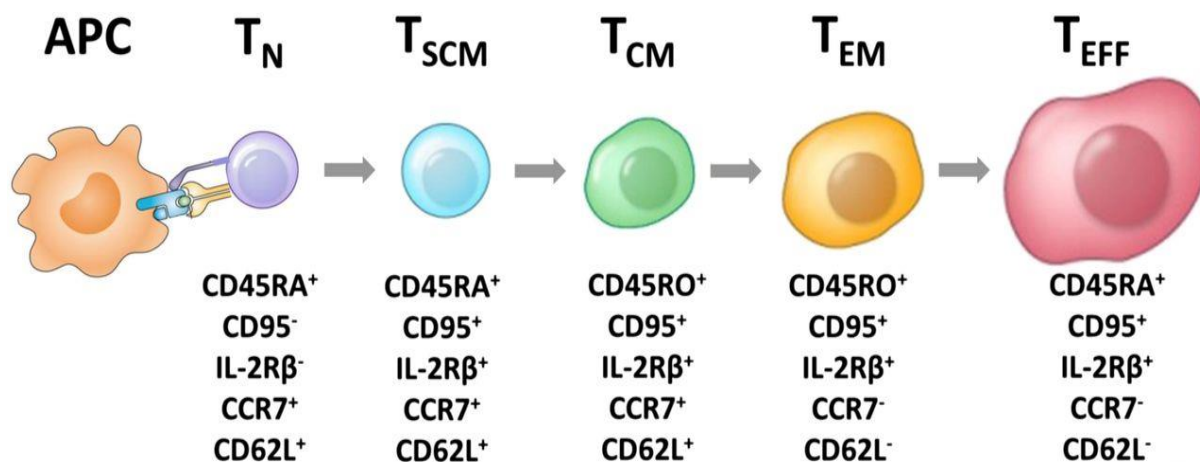


Figure 2: “Linear” or “developmental” model of T cell differentiation. After T_N cells are primed by APCs, they undergo a differentiation pathway, generating T_{SCM}, T_{CM}, T_{EM} and T_{EFF}. APC, antigen-presenting cell; T_{CM}, central memory T cell; T_{EFF}, effector T cell; T_{EM}, effector memory T cell; T_N, naive T cell; T_{SCM}, T memory stem cell.

The accrued memory T cell population is very heterogeneous, including T stem cell memory cells (T_{SCM}), T central memory cells (T_{CM}) and T effector memory cells (T_{EM}). According to their differentiation stage, memory T cells express different markers on their cell surface (see Figure 2). Normally, human CD8⁺ memory T cells are defined by the expression of the CD45RO isoform and lack of CD45RA. However, T_{SCM} cells resemble T_N cells as they are characterized by the expression of CD45RA⁺, costimulatory molecules such as CD27⁺ and CD28⁺, and are highly positive for the homing markers CCR7 and CD62L since both subsets predominantly reside in the lymphoid organs. Central memory T cells that traffic to lymphoid tissue exhibit lower expression levels of CCR7 and CD62L while effector memory T cells and effector T cells, which migrate to multiple peripheral tissue sites, are negative for CCR7 and CD62L. Human T_{SCM} and T_{CM} were identified by Gattinoni et al. (Gattinoni et al. 2011a) to be highly positive for CD95 and CD122 (IL-2Rβ), which might initially be distracting as the Fas-receptor CD95 is primarily associated with a proapoptotic function. However, the outcome of CD95L–CD95 interaction depends on the differentiation stage of the cell, as observed in various organ systems. CD95 e.g. activates apoptosis in terminally differentiated neurons, but it promotes cell proliferation in neuronal progenitors and cancer stem cells by inducing Wnt-β-catenin and mammalian target of rapamycin (mTOR) cascade signaling pathways (Beier & Schulz 2009). Considering the emerging role of Wnt-β-catenin signaling and mTOR

signaling cascade in the formation and maintenance of memory CD8⁺ T cells, CD95 might be very important for their self-renewal and persistence.

T_{SCM} have a multipotent capacity to form other memory subsets, including T_{CM} and T_{EM} and highly lytic effector T cells. Furthermore, their superior survival potential and self-renewal capacity enables them to persist over longer period of time and to give rapid rise to effector T cells in the case of reinfection (Gattinoni et al. 2011a); (Stemberger et al. 2014). T_{SCM} maintain their self-renewal capacity and multipotency by limited proliferation and differentiation, which are regulated by different signaling pathways, amongst others, Wnt- β -catenin pathway (Gattinoni et al. 2009) and mTOR signaling cascade (Chi 2012); (Xu et al. 2012).

2.4 Wnt- β -catenin signaling pathway

The Wnt- β -catenin signaling is known to play an important role in early T cell development in thymus, where it is regulated by high expression of intracellular activating signaling molecules such as e.g. β -catenin, plakoglobin and long forms of T cell factor-1 (Tcf-1) (Weerkamp et al. 2006). T cell factor-7 (Tcf-7) and lymphoid enhancer-binding factor-1 (Lef-1) are transcription factors of the Wnt- β -catenin signaling pathway, and their expression declines during differentiation of naive T cells towards T effector cells in humans (Willinger et al. 2006a) and mice (Gattinoni et al. 2009). In addition, Lef-1 and Tcf-7 were detected in high levels in T cells with an ability to form memory cells *in vivo* (Hinrichs et al. 2008).

Wnt- β -catenin signaling pathway stabilizes β -catenin, which associates with Tcf-7 and Lef-1 proteins to form transcriptional activation complexes that regulate Wnt-target genes (Willinger et al. 2006b).

In the absence of Wnt-ligand (see Figure 3A), cytoplasmic β -catenin is bound by two scaffolding proteins in the destruction complex (tumor suppressors adenomatous polyposis coli and axin), following phosphorylation of Ser45 by CK1, and subsequently of Ser33, Ser37 and Thr41 by glycogen synthase kinase-3 (Gsk3 β). The phosphorylated β -catenin is then targeted for degradation by the proteasome. In the nucleus, Tcf-7 acts as transcriptional repressor complex to silence Wnt-target genes (Staal et al. 2008).

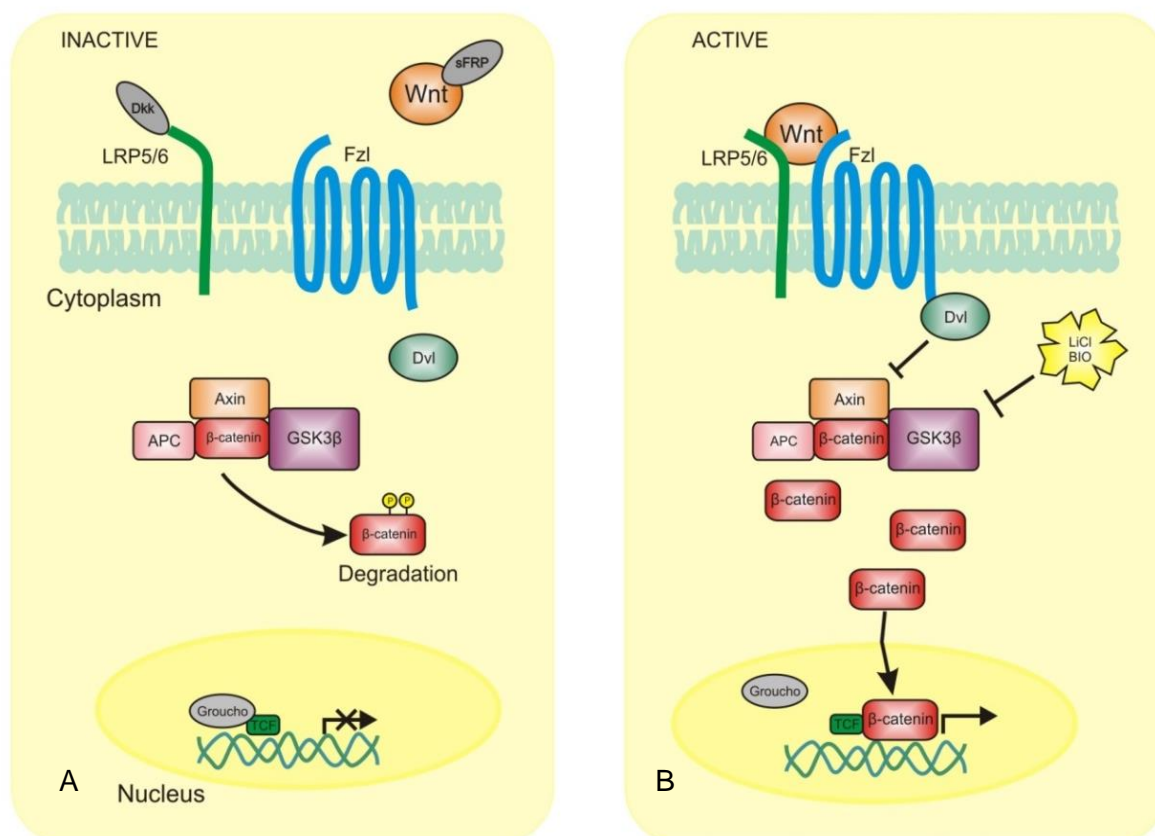


Figure 3: Active and inactive stage of Wnt- β -catenin signaling. A. Inactive stage of Wnt- β -catenin signaling: β -catenin is phosphorylated and degraded by proteasome, resulting in Tcf-7 assembling a transcriptional suppressor of Wnt-target genes. B. Active stage of Wnt-signaling: activated DVL inhibits Gsk3 β , which allows β -catenin to escape proteosomal degradation. β -catenin translocates into nucleus and interacts with Tcf-7 and Lef-1, which results in the transcription of Wnt-target genes. (<https://www.york.ac.uk/res/btr/Image%20Library/Wnt%20signalling%20activeinactive.jpg>)

During the active stage of Wnt-signaling, Wnt-ligand binds to the Frizzled receptor (FzL) and the low density lipoprotein receptor-related protein 5 (LRP5) or (LRP6), this leads to activation of DVL (mammalian homologue of *Drosophila Dishevelled*), which inhibits Gsk3 β . Inhibition of Gsk3 β prevents targeted proteosomal degradation, and allows β -catenin to translocate to the nucleus where it interacts with Tcf-7 and Lef-1 resulting in the transcription of Wnt-target genes. Ding et al. reported that TWS119 induced neuronal differentiation in murine embryonic stem cells, by inhibiting Gsk3 β (Ding et al. 2003). Later, Gattinoni et al. showed that activation of the Wnt- β -catenin signaling pathway by treating T cells with TWS119 induced T_{SCM}-like self-renewal capacity in tumor-specific CD8⁺ T cells (Gattinoni et al. 2009).

2.5 mTOR signaling pathway

Mammalian target of rapamycin (mTOR) plays a central role in the regulation of cell growth and metabolism, by sensing nutrient and growth factors availability, which are important for the phosphoinositide-3-kinase (PI3K)-AKT pathway that eventually activates mTOR. There

exist two signaling forms of mTOR, mTOR complex 1 (mTORC1) and mTOR complex 2 (mTORC2), as illustrated in Figure 4.

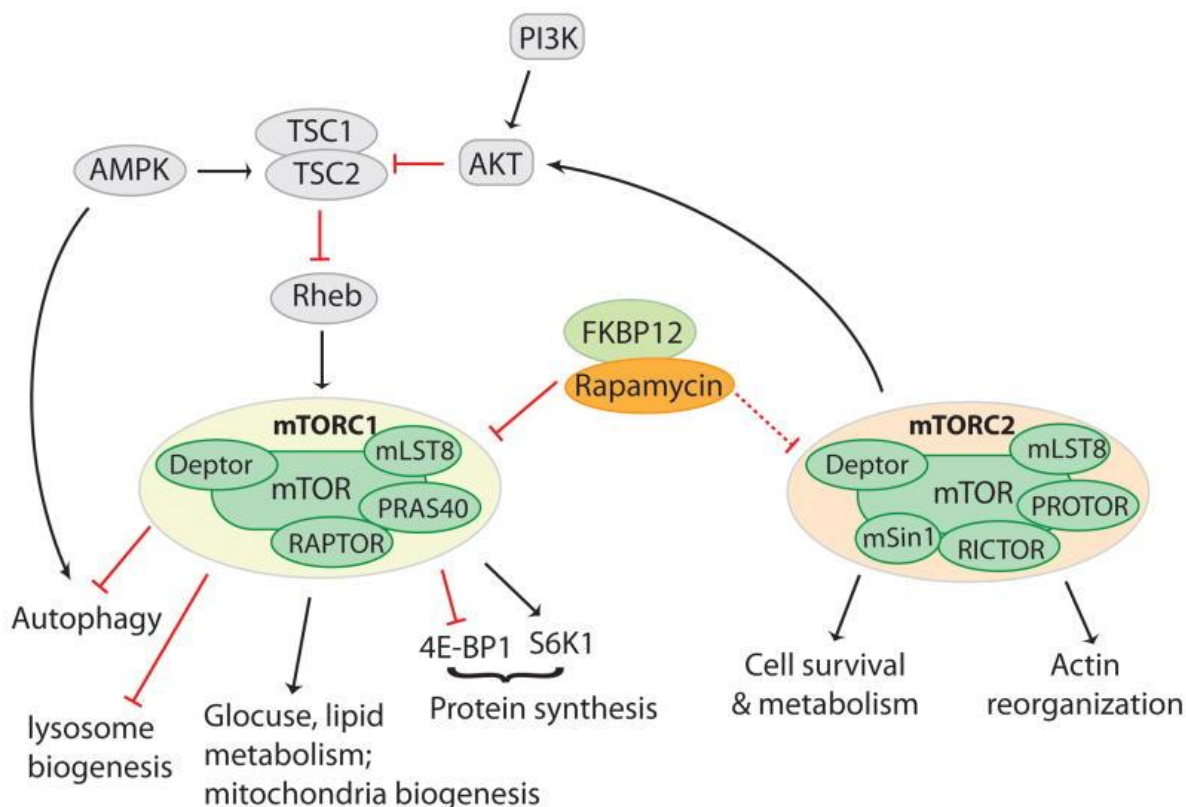


Figure 4: mTOR-signaling cascade. mTOR forms two complexes: mTORC1 and mTORC2. mTORC1 regulates autophagy, protein translation, cell growth and metabolism, while mTORC2 modulates cytoskeleton organisation, cell survival and metabolism. By forming a complex with FKBP12 rapamycin inhibits the kinase activity of mTORC1.

mTORC1 is composed of mTOR and four proteins, including regulatory-associated protein of mTOR (RAPTOR), DEP-containing mTOR-interacting protein (DEPTOR), mammalian lethal with Sec13 protein 8 (mLST8) and the prolin rich Akt substrate 40kDa (PRAS40). mTORC2 consists of mTOR and five proteins, including the scaffold protein raptor-independent companion of TOR (RICTOR), mammalian stress-activated protein kinase interacting protein 1 (mSIN1), DEPTOR, mLST8 and the protein observed with RICTOR (PROTOR) (Laplante & Sabatini 2009).

mTOR is active in a nutrient rich environment and involved in the biosynthesis of proteins, lipids and organelles (Laplante & Sabatini 2009) whereas autophagy is suppressed. mTORC1 is involved in the upregulation of enzymes involved in glycolysis, glutaminolysis and in pentose phosphate pathway (PPP) to increase cell surface expression of glucose transporter Glut-1 and the glutamine transporter SNAT-2 (Düvel et al. 2010); (Buller et al. 2008). When energy resources are limited, mTOR activity declines, resulting in reduced biosynthesis and increased autophagy (Xu et al. 2012).

Memory and effector T cells show drastically different metabolic profiles (see 2.4). While memory T cells utilize oxidative phosphorylation (OXPHOS) and autophagy to generate

energy and substrates for basal levels of biosynthesis, effector T cells mostly employ aerobic glycolysis as a quick way to generate adenosine triphosphate (ATP).

Since mTOR regulates cell growth and metabolism, the inhibition of mTOR signaling pathway might inhibit the induction of glycolysis and concomitantly decelerate the differentiation process in T cells.

It has been shown that the bacterial macrolide rapamycin (RAPA) derived from *Streptomyces hygroscopicus* binds to the 12 kDa FKBP12-protein and therefore inhibits mTORC1 (Abraham & Wiederrecht 1996). Additionally, a prolonged exposure to rapamycin could also inhibit mTORC2 (Sarbassov et al. 2006).

Rapamycin has been used clinically as an immunosuppressive drug to prevent allograft rejection, due to its ability to inhibit IL-2 dependent T cell proliferation (Halloran 2004). However, recent data have shown that the effect of rapamycin is dose dependent.

Araki and colleagues reported that treatment of mice with high doses of rapamycin (600 µg/kg/day) inhibited CD8 T-cell responses during infection with lymphocytic choriomeningitis virus (LCMV). In contrast, lower doses of rapamycin provoked memory CD8⁺ T cell differentiation, whereby added during the expansion and contraction phases, rapamycin improved the quality (expression higher levels of CD62L, CD127 and anti-apoptotic Bcl-2) and quantity of memory T cells after primary immunization (Araki et al. 2009).

Besides the inhibition of T cell proliferation, administration of rapamycin restored fatty acid oxidation (FAO) and memory formation in murine CD8⁺ T cells (Pearce et al. 2009). The study conducted by He et al. showed that antigen-activated CD8⁺ T cells treated with rapamycin gave rise to 5-fold more long-lived murine memory T cells *in vivo* as compared to control cells (He, Kato, Jiang, Daniel R. Wahl, et al. 2011).

2.6 Metabolic profiles of T lymphocytes

T cells change their metabolism during the immune response, displaying distinct metabolic profiles depending on their phase of activation (see Figure 5) (Pearce et al. 2013).

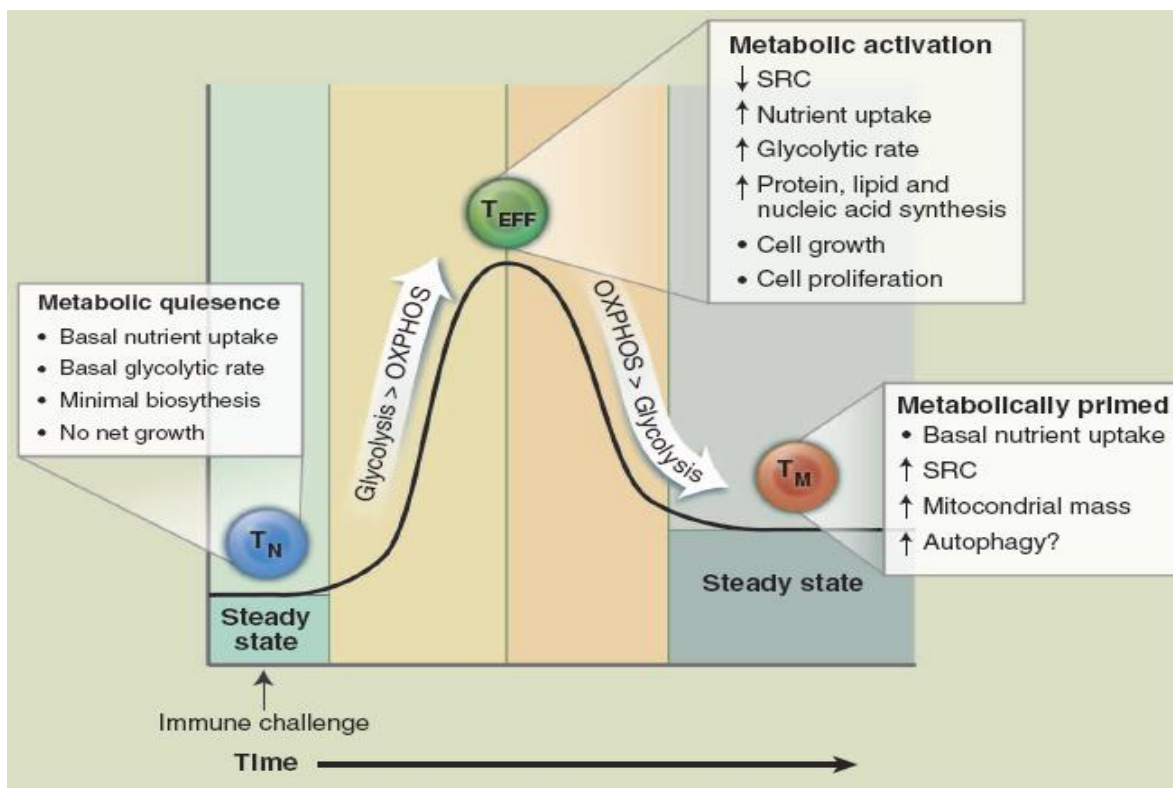


Figure 5: Dynamic of T cell metabolism during an immune response. Naive T cells are metabolically quiescent; adopting a basal level of nutrient uptake as they have reduced their cell growth and proliferation. Upon immune challenge, T cells shift to the stage of metabolic activation, whereby they enhance lipid, protein and nucleic acid synthesis for rapid cell growth and proliferation. They generate the majority of their ATP through aerobic glycolysis. Transition to the memory stage is characterized by quiescent metabolism, with increased reliance on FAO to fuel OXPHOS. Mitochondrial mass and SRC are elevated in memory T cells, suggesting that these cells are metabolically primed to respond upon the reinfection.

Naive T cells are metabolically quiescent, as they do not require high amounts of ATP for ion homeostasis, maintenance of membrane integrity and rearrangement of the actin cytoskeleton for motility. Thus, naive T cells adopt a basal level of nutrient uptake and reduce their cell growth and proliferation. They oxidize glucose-derived pyruvate via oxidative phosphorylation (OXPHOS) as their primary source to produce 96% of ATP, whereas the remaining 4% is produced by glycolysis (Frauwirth & Thompson 2004). OXPHOS is an oxygen dependent process and yields 36 molecules of ATP per glucose molecule (Pearce et al. 2013). Furthermore, naive T cells require extrinsic signals to maintain basal metabolism. IL-4 and IL-7 promote survival of naive T cells, but not the entry into the cell cycle. Thus naive T cells will die even in the presence of extracellular nutrients when cultured without IL-4 and IL-7 (Plas et al. 2002).

Upon immune challenge, quickly generated effector T cells (T_{EFF}) become metabolically active to enhance protein, lipid and nucleic acid synthesis for rapid cell growth and proliferation. In addition, they exhibit an elevated consumption of glucose and glutamine to support the increased cell growth and proliferation. Acutely activated T lymphocytes generate the majority of their ATP similar to cancer cells through aerobic glycolysis (Warburg effect). Consumed glucose molecule is broken down into two molecules of pyruvate, yielding two reduced nicotinamide adenine dinucleotide (NADH) molecules and two net ATP molecules per molecule of glucose. Pyruvate produced this way is fermented into lactate, regenerating NAD^+ for use in glycolysis.

From a bioenergetic perspective, engaging aerobic glycolysis is less efficient than OXPHOS, as it yields only 2 ATP molecules per glucose molecule. However, aerobic glycolysis provides some advantages to actively proliferating T effector cells over oxidative phosphorylation. Firstly, ATP is produced much faster through aerobic glycolysis than through OXPHOS and secondly, glycolysis is not an oxygen dependent process and enables T cell survival in a hypoxic environment, a typical characteristic of many solid malignancies. It is important to remember, that OXPHOS is still utilized by T effector cells, however aerobic glycolysis is the main pathway for ATP production (Mockler et al. 2014).

After pathogens are eliminated most of the T effector cells undergo apoptosis, while memory T cells remain alive to sustain a long-lasting immunity against a particular antigen. This ability poses a unique metabolic profile on these cells. Memory T cells exhibit an elevated spare respiratory capacity (SRC) and enhanced mitochondrial mass as compared to T_{EFF} , which allows for rapid ATP production upon reinfection. Memory T cells adapt a quiescent metabolism and utilize fatty acid oxidation (FAO) to fuel OXPHOS. Oxidation of free fatty acids generates acetyl-coenzyme A which can be metabolized further in the TCA cycle. Likewise, $FADH_2$ and NADH can be used directly by the electron transport chain to generate ATP (Pearce et al. 2013). It has been reported that IL-15 increases SRC by enhancing the expression of carnitine palmitoyltransferase I (CPTI), a key enzyme of FAO (van der Windt et al. 2012).

Interestingly, memory T cells do not consume fatty acids from their micromilieu to increase the rate of fatty acid oxidation as they do not show an increase in the fatty acid uptake. Moreover, memory T cells display reduced expression of CD36 (fatty acid translocase), necessary for fatty acid uptake as compared to T effector cells. Instead, memory T cells drive *de novo* fatty acid synthesis to generate mitochondrial ATP through fatty-acid oxidation (see Figure 6) (Weinberg & Chandel 2014).

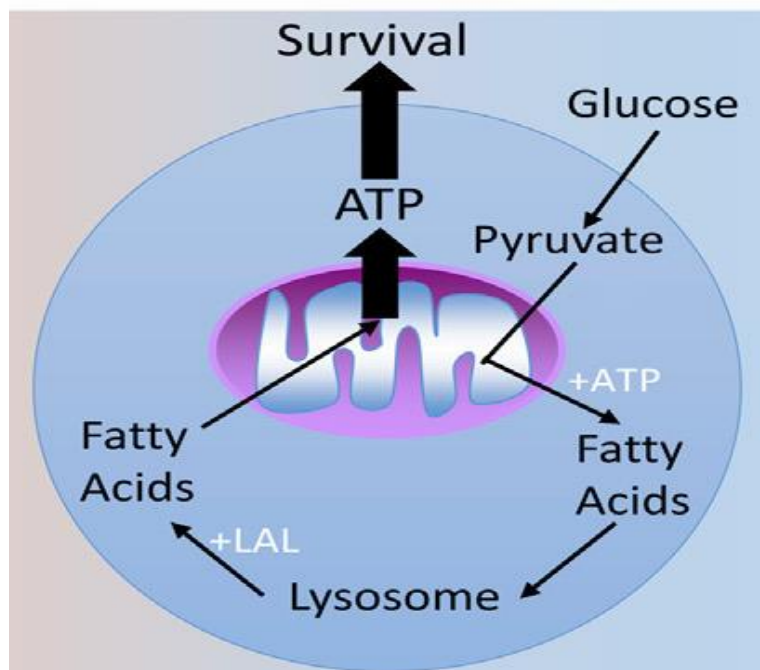


Figure 6: Memory T cells engage in fatty-acid synthesis and oxidation. Memory T cells engage futile cycle of fatty acid synthesis and subsequent fatty acid oxidation. In this cycle, de novo synthesized fatty acids are stored in the lysosome, where they are released by lysosomal acid lipase (LAL) and shuttled into the mitochondria for ATP generation by fatty acid oxidation to sustain a prolonged memory-cell survival

Fatty acids generated in this way are stored in the lysosome and with the help of lysosomal acid lipase (LAL) released and transported into mitochondria for fatty acid oxidation. Engaging the futile cycle of fatty acid synthesis and subsequently fatty acid oxidation must be of advantage for memory T cells. Memory T cells might utilize futile cycle to remain self-sufficient and to reduce reliance on extracellular fatty acids, as the fatty acid levels depends on the tissue where they reside. Lymphoid organs are nutrient- and oxygen-rich areas, but the sites of inflammation and tumor invasion contain highly hypoxic areas with limited nutrient availability. Therefore, T cells must alter their metabolism to adapt to the tumor or infection environment.

As reported by Sukumar and colleagues strong inhibition of glycolysis by 2-deoxy-glucose (2-DG) in tumor-specific murine CD8⁺ T cells promoted the formation of memory CD8⁺ T cells and prevents the complete differentiation into T_{EFF} (Sukumar et al. 2013). 2-DG is a structural analogue of glucose differing at the second carbon atom by the substitution of hydrogen for a hydroxyl group. 2-DG undergoes facilitated diffusion into cells via glucose transporters, where it is phosphorylated by hexokinase to 2-deoxy-D glucose- 6-phosphate (2-DG-6-P). Once formed, 2-DG-6-P is not further metabolized and accumulates in the cell until dephosphorylated by phosphorylase. Thus, prolonged glucose deprivation forces cells to switch to other metabolic pathways e.g. fatty acid oxidation (FAO) for ATP production, which might facilitate generation of T_{SCM} and T_{CM} cells.

2.7 Biology of Epstein-Barr virus infection

The Epstein-Barr virus is one of the eight known human herpes viruses with a large double-stranded DNA genome of 172 kb discovered by Epstein and Barr in 1964 in cultured lymphoblasts from Burkitt's lymphoma (BL) (Epstein, Achong, & Barr, 1964). The first contact with EBV usually happens in the first decade of life and remains lifelong as an asymptomatic latent infection. However, a primary infection by EBV in adulthood evokes an infectious mononucleosis (IM) in 50% of cases.

EBV enters the tonsillar crypts through saliva and crosses a thin layer of epithelium, which is often one cell thick overlying the bed of lymphocytes below (see Figure 7) (Thorley-Lawson 2001). Once inside, EBV infects naive B cells or pre-existing memory cells as a direct route into memory (Young & Rickinson 2004) by binding of the EBV lytic glycoprotein 350 to B-cell CD-21 (Nemerow et al. 1987) and drives them to become blasts through expression of the EBV growth transcription program, which is coordinated by nine latent proteins under the regulation of EBV nuclear antigen 2 (EBNA-2). In addition, for the viral envelope and B-cell membrane to fuse, the EBV virion must possess functional gH, gL, and gp42 spike glycoproteins (Kirschner et al. 2006). After gH-, gL-, gp42-complex have penetrated the B cell membrane, the viral capsid is dissolved, enabling the viral dsDNA genome to enter the cytoplasm. Viral RNA is often packaged in virions in addition to the dsDNA genome. These transduced elements are referred to as tvRNA and include non-coding RNAs and mRNAs. One of these mRNAs, BZLF1 (a transcription factor) helps to activate viral promoters that trigger EBV default transcription program (Jochum et al. 2012). Activated through infection B cells might migrate into the follicles, where they proliferate in germinal centres (GC). At some point EBV-infected blasts switch from the active growth transcription program to the default transcription program by turning off EBNA-2. Expression of latent membrane protein 1 (LMP1) and latent membrane protein 2A (LMP2A) in the absence of EBNA-2 allow the EBV-infected blasts undergo a normal differentiation pathway and become resting memory B cells.

EBV infected resting memory cells leave the follicles and enter the peripheral circulation through the lymphatic vessels. The cells escape from immune recognition by expressing only little or no genetic information. This latency transcription program causing an asymptomatic latent infection is characterized by viral episomal DNA that persists for the lifetime of the host in B cells (Kieff et al.).

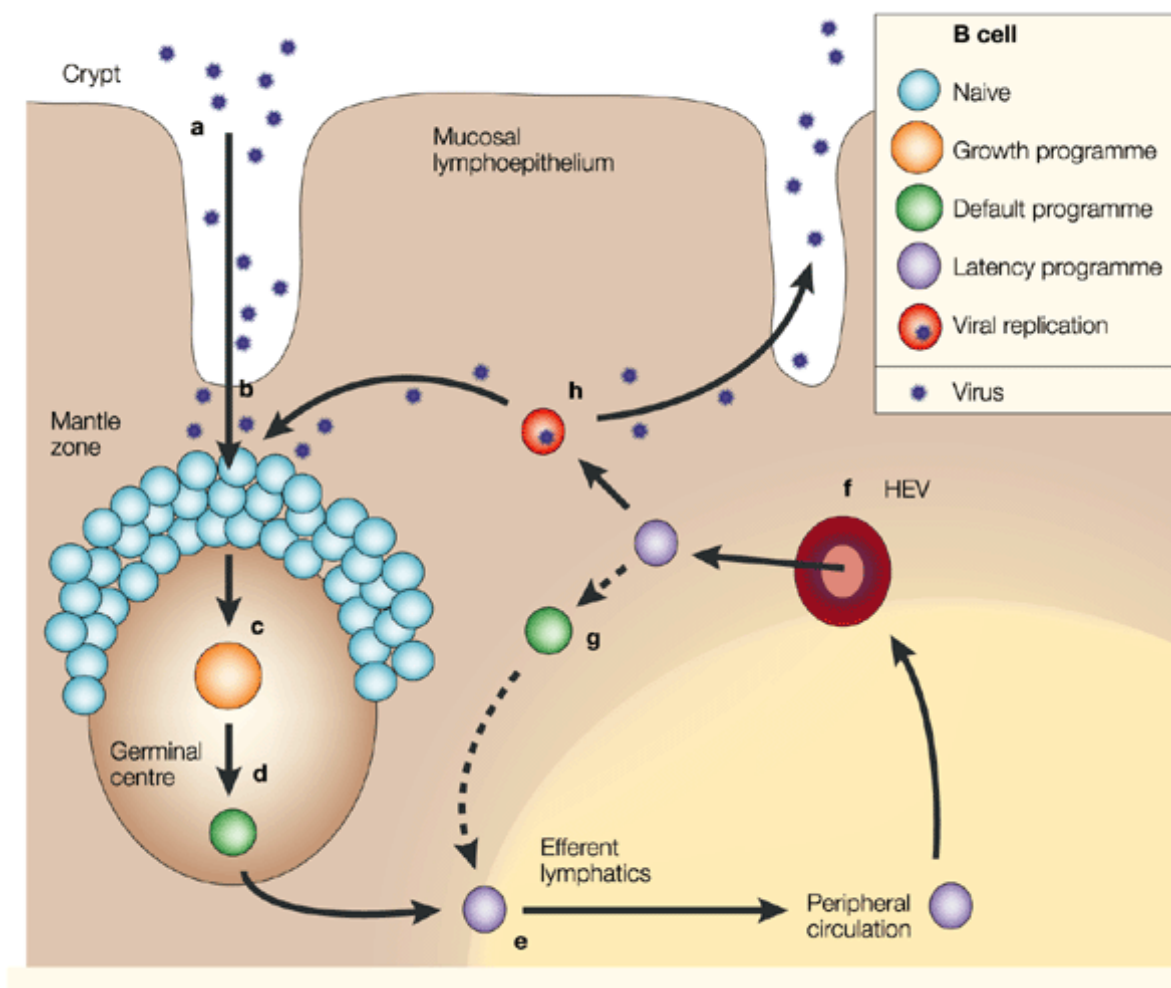


Figure 7: Hypothetical model of EBV persistence in human organism. **A.** EBV enters through saliva into the tonsils. **B.** EBV crosses the epithelial barrier. **C.** EBV converts naive B cells into blasts under the regulation of EBNA2. **D.** EBV-infected blasts switch from the growth programme to the default programme. **E.** EBV latently infected resting memory cells leave the follicles and enter the peripheral circulation through the efferent lymphatics. **F.** Memory cells re-enter the tonsil from the peripheral circulation through high endothelial venules (HEVs). **G.** Survival of antigen-specific memory cells requires an intact BCR. The expression of the default programme might provide the necessary signals for long-term survival of the cells as memory cells. **H.** Occasionally, a fraction of latently infected memory cells initiates replication of the virus to be shed into saliva.

Survival of antigen-specific memory cells requires an intact B cell receptor (BCR). However, LMP2A can replace a survival signal provided usually by BCR (Caldwell et al. 1998). Occasionally, such physiological events as antigen stimulation and delivery of a plasma cell differentiation signal might drive a fraction of latently infected memory cells into a lytic cycle (Thorley-Lawson 2001).

2.7.1 Lytic life cycle

The lytic life cycle of EBV plays a less central role in the maintenance of viral infection but is rather important for the production of virions and their transfer from host to host or from cell to cell. Nevertheless, immunosuppressed patients often show abnormally high levels of virions in their plasma and intracellular transmission of virus may eventually cause a

development of EBV-induced lymphoproliferative disease (LPD) in immunosuppressed patients (Damania & Pipas 2009a). Moreover, early passage B cells immortalized with lytic-defective EBV have a reduced ability to form LPD-like lesions in SCID mice relative to B cells immortalized with wild-type EBV. Infected B cells secrete paracrine factors (cellular IL-6 and vascular endothelial growth factor (VEGF) that may promote the growth of the latently infected B cells in LPD lesions (Hong et al. 2005). For all herpesviruses, the lytic cycle involves the sequential expression of transactivation proteins of viral early gene expression, early proteins, including essential components of the viral DNA replication complex and late proteins many of which are structural proteins of the virion.

To avoid a host's immune response EBV uses its latent replication cycle in which its genome proliferates via clonal replication within dividing host B-cells (Steven et al. 1997). Interestingly, there are differences between herpes virus subfamilies with respect to latent infection.

2.7.2 Latent life cycle

Alpha and beta viruses establish latency by entering a specific cell type and immediately closing down all antigen expression. In contrast, gamma viruses carry a set of latent genes that are crucial for entering the latent cycle. The γ -viruses are divided into two genera, γ -1 and γ -2, with different sets of latent cycle genes. For example, murine γ -herpesvirus 68 (MHV-68) is a classical γ -2 virus, which establishes a latency in B cells but has no independent capacity to drive B cell growth.

By contrast the γ -1 viruses (e.g. EBV), whose members are found only in primates, have acquired direct B cell growth-transforming ability, which depends on the expression of the following latent genes: EBNA-1,-2,-3A,-3B,-3C,-LP, and two latent membrane proteins, LMP1 and LMP2A. EBV infects B cells and forces them to run three different latent gene expression programs in order to escape an immune response (see Table 1) (Thorley-Lawson 2001).

Table 1: Latency transcription programs

Program	Gene expressed	Possible function
Growth program (Latency III)	EBNA1-6 LMP2A-B LMP1	Activates resting B cells to become proliferating lymphoblasts
Default program (Latency II)	EBNA1 LMP1 LMP2A	Provides necessary survival signals for infected lymphoblasts to differentiate into memory and for maintenance of persistently infected memory cells
Latency program (Latency I)	None EBNA1	Allows persistence of the virus in resting recirculating memory cells in a way that is non-pathogenic and not detectable by the immune system

EBV infection establishes typically three distinct latent infection stages: latency type I, II and III. Post-transplant lymphoproliferative disease (PTLD) and *in vitro* EBV infection-mediated establishment of the LCLs show type III latency, Hodgkin's lymphoma (HL) and nasopharyngeal carcinoma (NPC) display type II latency and finally gastric and T and NK lymphomas display I/II types of latency (see Table 2) (Damania & Pipas 2009b).

Table 2: Overview of EBV-associated malignancies

Tumor	Latency	Subtype	Typical Latent Period	EBV Association	EBV Antigen Expression
Burkitts lymphoma	I	Endemic	3-8 years post EBV	100%	EBNA-1
		Sporadic	3-8 years post EBV	15-85%	
		AIDS-associated	3-8 years post HIV	30-40%	
Gastric lymphoma	I/II	UCNT ¹	>30 years post EBV	100%	EBNA-1
		Adenocarcinoma	>30 years post EBV	5-15%	LMP2
Nasopharyngeal carcinoma	I/II	Non-keratinizing	>30 years post EBV	100%	EBNA-1 (LMP1)
		Keratinizing	>30 years post EBV	30-100%	LMP2
T and NK lymphomas	I/II	VAHS ² -associated	1-2 years post EBV	100%	EBNA-1 (LMP1)
		Nasal	>30 years post EBV	100%	LMP2
Hodgkin's lymphoma	II	Mixed cell, lymph.depl.	>10 years post EBV	60-80%	EBNA-1 LMP1
		Nodular sclerosing	>10 years post EBV	20-40%	LMP2
PTLD and similar lesions	III	Immunodeficiency	<3 months post EBV	100 %	EBNA-1,2,3A,
		Post-transplant	<1 year posttranslant	>90 %	3B,3C,-LP
		AIDS ³ associated	>8 years post HIV	>80 %	LMP1 LMP2

Lymphoblastoid B cell lines grown *in vitro* express a restricted set of EBV latent genes: EBNA-1,2,3A-C and LP, LMP1 and LMP2A-B (Taylor et al. 2014).

2.7.3 Association of EBV with malignancies and PTLD

By the age of 30 years almost 95% of the population is infected with EBV (Pariente et al. 2007). Owing to its pathogenic character, EBV is estimated to cause 1% of cancers worldwide, being the fourth most common infectious cause of cancer (Parkin 2006). EBV can

¹ UCNT, undifferentiated carcinomas of the nasopharyngeal type;

² VAHS, virus-associated hemophagocytic syndrome;

³ AIDS, acquired immunodeficiency syndrome;

promote the development of a wide range of human tumors, e.g. Burkitt's lymphoma (BL), Hodgkin's lymphoma (HL), post-transplant lymphoproliferative disease (PTLD), an extra nodal lymphoma of T or natural killer (T/NK) cell origin, undifferentiated nasopharyngeal carcinoma (NPC), a smooth muscle cell sarcoma and a distinct subset of gastric carcinomas (GaCa) (see Table 2) (Taylor et al. 2014).

In contrast to the above mentioned diseases, PTLD occurs as a consequence of a medical intervention. Chemotherapy or radiation following hematopoietic stem cell transplantation (HSCT) or solid organ transplantation (SOT) administered to prevent graft rejection, suppresses the own immune system, giving opportunistic viruses such as e.g. EBV a chance to resurge (Gottschalk et al. 2005).

PTLD encompasses a heterogeneous group of B cell proliferative disorders that occur in the settings of allogenic HSCT or SOT. Three general types of PTLD have been recognized by the WHO (Campo et al. 2011):

- Early lesion (plasmatic hyperplasia and infectious mononucleosis-like PTLD) is characterized by a polyclonal B cell proliferation, preservation of local tissue and absence of malignant transformation. These lesions arise within the first year following a transplant, usually in children or young adults. Early PTLD is likely to respond to a reduction of immunosuppressive therapy.
- Polymorphic lesions are malignant transformations, which cause a destruction of underlying lymphoid architecture. The polymorphic lesion is a very common form of PTLD in both children and adults. It is unlikely to respond to a reduction of immunosuppressive therapy, requiring additional treatment.
- Monomorphic lesions are diffuse, large B cell lymphomas; typically arising after several years of transplantation.

The assessment of the EBV-DNA load is important to identify high-risk recipients. However a detection of an increased EBV load alone is not always enough to predict PTLD, therefore the detection of increased EBV-DNA load in combination with reduced EBV-specific T cells and detection of antibodies against LMP1 or EBNA2 could allow for a better prediction of PTLD development, especially in EBV-seronegative recipients (Mucha et al. 2010). The only known natural host of Epstein-Barr virus is human, however, there were several attempts to create an animal EBV-model.

B-cell lymphomas can be induced in the cotton-top tamarins (*Saguinus oedipus*), that were used in a preclinical study to test an experimental EBV subunit vaccine. Unfortunately, these animals are endangered species and cannot be used for experimental use (Shope et al. 1973).

The owl monkey (*Aotus trivirgatus*) and the common marmoset (*Callithrix jacchus*) can be also infected with EBV; however, they were not characterized good enough to be used as an animal model.

Murine gamma herpesvirus 68 (MHV-68) resembles EBV infection in different aspects, including the ability to induce an MHV68-associated LPD in mice and establish persistent infection in memory B cells. However, a B cell transformation of MHV-68 differs from human EBV, because the genetic homology only exists for the lytic-cycle genes and not for the latent-cycle genes (Barton et al. 2011).

A real revolution in the generation of a small animal model of EBV infection was a development of the C.B-17 severe combined immunodeficiency (SCID) mouse. The SCID mice are unable to generate T and B cells, whereas an erythroid, myeloid and natural killer (NK) cell differentiation is not affected. Thus, lymphomas similar to early PTLD can be induced by infecting SCID mice with EBV and with EBV infected B cells (B-LCL) (Antsiferova et al. 2014; Rowe et al. 1991) or with PBMC isolated from healthy EBV carriers (Fujiwara et al. 2015). In such models PTLD-like tumors arise as a result of an absent T cell response. (*Fields' Virology, Volume 2, 2007*).

2.8 The clinical potential of T stem cell memory cells

T stem cell memory cells (T_{SCM}) are the least differentiated memory T cell subset, which share some phenotypic characteristics with naïve T cells as they express CD45RA, CCR7, CD62L, CD27 and CD28, but differ from naïve T cells by the expression levels of CD95 and CD122. Functionally T stem cell memory cells are more similar to late memory T cells, as they can rapidly generate other antigen-experienced T cells subsets (T_{CM} , T_{EM} and T_{EFF}) and secrete cytokines (TNF- α , IFN- γ and IL-2) upon the reinfection (Gattinoni et al. 2011a). T_{SCM} evoked a therapeutic interest because of their long-lifespan and self-renewal capacity.

The latest study by (Biasco et al. 2015) revealed the longevity of T_{SCM} when transferred into humans. Therefore, two gene-therapy clinical trials to treat severe combined immunodeficiency disease (SCID), using either genetically corrected hematopoietic stem cells or mature lymphocytes were performed. Using high throughput sequencing of retroviral vector integration site (IS) enabled to trace over 1700 individual T cell clones *in vivo* in these studies. Biasco and colleagues could show that T_{SCM} possess the highest percentage of IS as compared to the other populations, indicating the ability to persist whilst retaining a precursor potential for up to 12 years after infusion of retrovirally engineered lymphocytes. Although T_{SCM} displayed lower IFN- γ production than effector T cells, they were able to differentiate into T_{CM} and T_{EM} after anti-CD3/CD28 activation, while maintaining a subset of T_{SCM} . The results of this work suggest that T_{SCM} have the safe, functional, survival and differentiation potential for the development of T cell-based therapies.

The long-lifespan of T_{SCM} plays a positive role in vaccination studies. Fuertes Marraco and colleagues could demonstrate the persistence of yellow fever specific CD8⁺ T_{SCM} for 25 years upon vaccination, which displayed markers and mRNA profiling of T_{SCM} (Fuertes Marraco et al. 2015).

The murine studies conducted by Cieri et al. and Gattinoni et al. demonstrated the ability of T_{SCM} to survive an adoptive transfer and promote anti-tumor regression and cure (Cieri et al. 2012, Gattinoni et al. 2011a).

Cieri and colleagues were able to show the self-renewal capacity of T_{SCM} by mediating a xenogeneic GvHD in serial transplantation experiments. T_{SCM} induced severe GvHD in mice, whereby the majority of circulating cells exhibited a central memory or effector memory phenotype, indicating their ability to differentiate *in vivo*. Additionally, T_{SCM} showed enhanced engraftment and expansion in spleen and bone marrow of infused mice.

One of the potential limitation of using T_{SCM} in immunotherapies is a limited cell number as the T_{SCM} represent only 2-3 % of all circulating CD8⁺ and CD4⁺ T lymphocytes in humans (Gattinoni et al. 2011a). However, Gattinoni and colleagues developed and validated a protocol for the enrichment and expansion of T_{SCM} by activating Wnt-β-catenin signaling in naive CD8⁺ T cells under the impact of TWS119 (Gattinoni et al. 2011a). In addition, Cieri et al. emphasized the role of IL-7 and IL-15 for human T_{SCM} expansion in a clinical setting (Cieri et al. 2012). Finally, Stemberger and colleagues could show in a human study that already small numbers (ca. 5000 cells per kg body weight) of cytomegalovirus (CMV) specific CD8⁺ T cells which contained an extremely low number of T_{SCM} and T_{CM} cells could be very effective (Stemberger et al. 2014).

One limitation of T_{SCM}, however, is observed by the fact that in other diseases, like immunodeficiency virus type 1 (HIV-1), T_{SCM} have not matched the expected therapeutic premises. The studies of (Flynn et al. 2014) and (Buzon et al. 2014) revealed that T_{SCM} can be infected with HIV-1 and become a long-lived reservoir of the virus. Moreover, Nagai et al. demonstrated, that T_{SCM} can be infected with human T cell leukemia virus type 1 (HTLV-1) and give rise to adult T cell leukemia (ATL), acting as ATL-stem cells (Nagai et al. 2015).

An alternative approach to T_{SCM} therapy could be the transfer of tumor-infiltrating lymphocytes (TILs) to treat a range of different cancers, including melanoma (Rosenberg et al. 2011); (Robbins et al. 2013), lung (Djenidi et al. 2015) and human papilloma virus-associated malignancies (Stevanović et al. 2015). Despite the high number of infused TILs it was not possible to reach a complete durable remission in most patients. The reason for that could be a low responsiveness of highly expanded T cells which are unable to warrant an efficient anti-tumor attack. Current researchers seek to develop simpler and faster methods to grow so called “young TILs”, which pass through fewer cell division cycles prior to reinfusion and thereby exhibit a less differentiated phenotype (Itzhaki et al. 2011).

In addition, genetically engineered T cells with chimeric antigen receptors (CAR) targeting CD19 to treat B cell lymphomas (Kochenderfer et al. 2015), chronic lymphocytic leukemia (Kochenderfer et al. 2012); (Brentjens et al. 2011), and acute lymphoblastic B cell leukemia (ALL) (Lee et al. 2014); (Maude et al. 2014) demonstrated remarkable and frequently durable responses. Additionally, a recent study conducted by (Porter et al. 2015) showed, that T cells persisted and remained functional for four years in two chronic lymphocytic leukemia (CLL) patients achieving a complete remission.

Unfortunately, CD19 is also expressed by normal B cells and thus patients usually suffer from B cell aplasia and deficiencies in circulating immunoglobulins. Moreover, many patients exhibit cytokine release syndrome, whereby an exuberant amount of IFN- γ and IL-6 is released. Although, patients can be helped with strong supportive care in combination with immunosuppressants such as steroids or cytokine-specific antibodies, lethal cases occurred at many institutions.

It might thus be an attractive approach to generate or enrich T_{SCM} and T_{CM} cells with high proliferative and engraftment potential and genetically reprogram these cells with T cell receptors (TCR) or CAR by viral gene transfer. T_{SCM} should then ideally give rise to highly lytic effector T cells that will sustain a prolonged immune attack while maintaining a continuous supply of less differentiated T_{SCM} and T_{CM} cells to refresh the pool of cytotoxic T cells over time.

2.9 Aim of this study

The main goal of immunotherapy is to enhance and support the body's own immune response against cancer, virus or bacterial infection. In recent years several different approaches have been introduced to generate and enrich T cells with the potential to eradicate cancer. One of the promising approaches to enhance an immune response might be the application of less differentiated autologous T_{SCM} and T_{CM} cells.

Therefore, the overall aim of this study was to explore innovative strategies to generate human EBV-specific T lymphocytes with stem cell memory and central memory-like properties (CTL_{SCM/CM}) *in vitro* as proof of concept, which could then be applied to treat PTLD in immunosuppressed EBV positive patients or further used for redirecting specificity to tumor or leukemia by viral transfer of TCR- or CAR-encoding genes (Cieri et al. 2012, Sabatino et al. 2016).

Human naive CD8⁺ CD45RA⁺ T cell precursor should be used as a source to generate T_{SCM} and T_{CM}. Since T cells acquire different metabolic profiles during an immune response and glycolysis has been shown to play an important role in T cell differentiation one part of this thesis addressed the question whether CTL_{SCM/CM} cells can be generated and maintained through manipulation of naive T cell metabolism using the glucose analogue 2-deoxyglucose (2-DG) or rapamycin (RAPA). Both modulators strongly reduce glucose consumption and have been shown to decelerate the differentiation process in T cells.

Alternatively, modulating the Wnt-β-catenin signaling pathway using the Gsk3β-inhibitor TWS119 to generate CTL_{SCM/CM} cells should be tested. These studies were based on previous findings reporting that the interaction of β-catenin with transcription factors involved in early gene regulation of T cell differentiation facilitates the generation of CTL_{SCM/CM} cells (Gattinoni et al. 2009).

In this context a comprehensive set of methods including flow cytometry, Seahorse analyses, transmigration assay and functional assays should be used to analyze and characterize phenotype, metabolic characteristics, migration capacity and cytolytic activity of the *in vitro* generated T cells. Moreover, to determine the therapeutic potential of EBV-specific CTL_{SCM/CM} cells *in vivo*, the cells should be adoptively transferred into NOD/SCID/IL2Rcy^{null} (NSG)-mice engrafted with human autologous B-LCL. Finally, persistence of EBV-specific CTL_{SCM/CM} cells will be tested in NSG-mice in the absence of antigen.

3. Methods and Materials

3.1 Materials

3.1.1 Equipment

Autoclave (Varioklav 40-60)	H+P Labortechnik (Oberschleißheim, DE)
Centrifuge (Centrifuge 5810R)	Eppendorf (Hamburg, DE)
Centrifuge (Biofuge Fresco)	Heraeus Centrifuge (Buckinghamshire, UK)
Centrifuge Megafuge 3.0R)	Heraeus Sepatech (Osterode, DE)
CO ₂ -Incubator (Heracell 150i)	Thermo Scientific (Waltham, USA)
Counting chamber (Neubauer)	Sigma-Aldrich (Steinheim, DE)
Cryofreezing container (5100 Cryo 1°C)	Nalgene (Neersje BE)
ELISpot reader S5 Versa Analyzer	C.T.L. (Bonn, DE)
Flow cytometer (FACS Canto II)	BD GmbH (Heidelberg, DE)
Fluorescence and absorption plate reader	Tecan (Männedorf, CH)
Freezer (Herafreeze, -80 °C)	Thermo Scientific (Dreieich, DE)
Gamma-counter Wizard 2	Perkin-Elmer (Rodgau, DE)
Heating block (Thermomixer 5436)	Eppendorf (Hamburg, DE)
Ice machine (UBE 50/35)	Ziegra (Isernhagen, DE)
Irradiator ¹³⁷ Cs cells (Gammacell 2000)	Moolsgard Medical (Gansloe, DK)
MACS multistand	Miltenyi Biotec (Bergisch-Gladbach, DE)
MACS Separator (Mini/Midi)	Miltenyi Biotec (Bergisch-Gladbach, DE)
Microscope (Axiovert 25)	Carl Zeiss AG (Jena, DE)
Microwave	Bosch (Stuttgart, DE)
Multi-channel pipette	Eppendorf (Hamburg, DE)
Nitrogen cryo bank (Espace 331 Gaz)	Air Liquide (Düsseldorf, DE)
Precision scale (EW150-3M)	Kern (Balingen-Frommern, DE)
Real-Time PCR, CFX Connect	Bio Rad (Hercules, CA, USA)
Refrigerator-freezer combo (+4 °C/-20 °C)	Liebherr (Ochsenhausen, DE)
Seahorse Extracellular Flux Analyzer	Seahorse Bioscience (Massachusetts, USA)
Single-channel pipette	Brand (Wertheim, DE)
Sterile work bench (Herasafe HS18)	Heraeus (Hanau, DE)
Spectrophotometer	Nanodrop (Wilmington, USA)
Vortex mixer	VWR (Darmstadt, DE)
Water bath heater (SW22)	Julabo Labortechnik (Seelbach, DE)

3.1.2 Consumables

Cell culture dishes	Greiner (Nürtingen, DE)
96-cell culture microplates	Greiner (Nürtingen, DE)
Cell culture flasks	Greiner (Nürtingen, DE)
Cell culture plates	Greiner (Nürtingen, DE)
Cryotubes	Nunc (Wiesbaden, DE)
FACS tubes	BD Biosciences (Heidelberg, DE)
Falcon tubes	BD Biosciences (Heidelberg, DE)
MACS columns (LD/MS)	Miltenyi Biotec (Bergisch-Gladbach, DE)
Multiscreen HST™ IP 96-well filtration plate	Millipore (Schwalbach, DE)
Needle sharing, (Sterican)	Braun (Melsungen, DE)
Non-skirted low profile 96-well PCR plate	Thermo Scientific (Wilmington, USA)
Pipette tips	Starlab (Ahrensburg, DE)
Reaction tubes	Eppendorf (Hamburg, DE)
Serological pipettes	Greiner (Frickenhausen, DE)
Syringe filter	Millipore (Eschborn, DE)
Syringes	Braun (Melsungen, DE)
Transwellplates	Corning Costar (Amsterdam, NL)

3.1.3 Chemicals

2-deoxy-D-glucose (2-DG)	Sigma-Aldrich (Steinheim, DE)
2,4-dinitrophenol (DNP)	Sigma-Aldrich (Steinheim, DE)
3-amino-9-ethylcarbazole (AEC) tablet	Sigma-Aldrich (Steinheim, DE)
⁵¹ Chromium (Na ₂ ⁵¹ CrO ₄)	Perkin Elmer (Rodgau, DE)
Acetic acid	AppliChem (Darmstadt, DE)
Ammonium chloride (NH ₄ Cl)	Appllichem (Darmstadt, DE)
Calcium chloride (CaCl ₂)	Appllichem (Darmstadt, DE)
Dimethylsulfoxide (DMSO)	Sigma-Aldrich (Steinheim, DE)
Ethanol (>99%, C ₂ H ₅ OH)	Merck (Darmstadt, DE)
Ficoll	PAA Laboratories (Pasching, A)
Folic acid	Sigma-Aldrich (Steinheim, DE)
HEPES	Gibco/Invitrogen (Karlsruhe, DE)
Hydrogen peroxide (30%, H ₂ O ₂)	Sigma-Aldrich (Steinheim, DE)
Isopropyl alcohol	Hedinger (Stuttgart, DE)
L-glutamine	Sigma-Aldrich (Steinheim, DE)
Magnesium sulfate (MgSO ₄)	Roth (Karlsruhe, DE)
Maxima SYBR Green qPCR	Thermo Scientific (Wilmington, USA)
Monopotassium phosphate (KH ₂ PO ₄)	Roth (Karlsruhe, DE)

Oligomycin A	Sigma-Aldrich (Steinheim, DE)
Paraformaldehyde (PFA)	AppliChem (Darmstadt, DE)
Phloretin	Sigma-Aldrich (Steinheim, DE)
Phosphate buffered saline (PBS ^{-/-})	Gibco (Eggenstein, DE)
Phytohaemagglutinin (PHA)	Murex Biotech (Kent, UK)
Potassium bicarbonate (KHCO ₃)	Appllichem (Darmstadt, DE)
Potassium chloride (KCl)	Appllichem (Darmstadt, DE)
Poly-D-lysine (PDL)	Sigma-Aldrich (Steinheim, DE)
Rapamycin	Biozol, (Eching, DE)
Rotenone	Sigma-Aldrich (Steinheim, DE)
Saponin	Sigma-Aldrich (Steinheim, DE)
Sodium acetate (NaOAc)	Roth (Karlsruhe, DE)
Sodium azide (NaN ₂)	Merck (Darmstadt, DE)
Sodium chloride (NaCl)	Appllichem (Darmstadt, DE)
Terralin liquid	Schülke (Hamburg, DE)
TritonX 100	AppliChem (Darmstadt, DE)
Trypan blue	Appllichem (Heidelberg, DE)
Tween20	Appllichem (Heidelberg, DE)
TWS119	Biozol (Eching, DE)

3.1.4 Kits

Glucose Uptake Fluorometric Assay Kit	Biovision (Milpitas, USA)
Lactate Assay Kit	Sigma-Aldrich (Steinheim, DE)
Naive CD8+ T-cell Isolation Kit	Miltenyi Biotec (Bergisch-Gladbach, DE)
Vectastain Elite Kit	Vector Laboratories (Burlingame, USA)
RNeasy Mini Kit	Qiagen (Hilden, DE)
SuperScript III	Invitrogen (Karlsruhe, DE)

3.1.5 Cytokines

CCL21	eBioscience (Darmstadt, DE)
GM-CSF	Berlex (Richmond, CA)
IL-12	R&D Systems (Wiesbaden, DE)
IL-15	R&D Systems (Wiesbaden, DE)
IL-1 β	R&D Systems (Wiesbaden, DE)
IL-2	Novartis (Nürnberg, DE)
IL-21	Biomol (Hamburg, DE)
IL-4	R&D Systems (Wiesbaden, DE)

IL-6	Strathmann (Hamburg, DE)
IL-7	R&D Systems (Wiesbaden, DE)
TNF- α	PromoCell (Heidelberg, DE)

3.1.6 Media and additives

AIM-V medium	Gibco (Karlsruhe, DE)
Bovine serum albumin (BSA)	Sigma-Aldrich (Steinheim, DE)
Cyclosporin A	Novartis (Nürnberg, DE)
DNase I	Roche (Mannheim, DE)
DMEM medium (high Glucose)	Gibco (Karlsruhe, DE)
DMEM medium (low Glucose)	Gibco (Karlsruhe, DE)
DMEM unbuffered medium	Sigma-Aldrich (Steinheim, DE)
EBV peptide pools (LMP2, BZLF-1)	Miltenyi Biotec (Bergisch-Gladbach, DE)
Fetal calf serum (FCS)	Gibco (Karlsruhe, DE)
Human serum	Blood bank (Mainz, DE)
Heparin	Ratiopharm (Ulm, DE)
Human albumin	CSL Behring (Marburg, DE)
Non-essential amino acids (NEAA)	Gibco (Karlsruhe, DE)
Penicillin / Streptomycin	Sigma-Aldrich (Steinheim, DE)
RPMI-1640 medium	Sigma-Aldrich (Steinheim, DE)
X-vivo15 medium	Lonza (Verviers, BE)

3.1.7 Antibodies

CCR7-FITC	Biologend (Eching, DE)
CD19-PE	Beckmann Coulter (Karlsruhe, DE)
CD27-FITC	Biologend (Eching, DE)
CD28-PE	Biologend (Eching, DE)
CD3-APC	Beckmann Coulter (Karlsruhe, DE)
CD3-FITC	Beckmann Coulter (Karlsruhe, DE)
CD3-PE	Beckmann Coulter (Karlsruhe, DE)
CD45RA-APC	BD Pharmigen (Heidelberg, DE)
CD45RO-PE	Beckmann Coulter (Karlsruhe, DE)
CD62L-PE	Beckmann Coulter (Karlsruhe, DE)
CD8-V450	Biologend (Eching, DE)
CD95-FITC	Beckmann Coulter (Karlsruhe, DE)
CD36-APC	Biologend (Eching, DE)
Anti-h IFN- γ -antibody 1-D1K (capture)	Mabtech (Nacka Strand, SWE)
Anti-h IFN- γ -antibody 7-B6-1 (detection)	Mabtech (Nacka Strand, SWE)

3.1.8 Primers

β -Actin**** (fw)	5'-CTGGAACGGTGAAGGTGACA-3'
β -Actin**** (rv)	5'-AAGGGACTTCCTGTAACAATGCA-3'
Tcf-7*** (fw)	5'-TGCAGCTATACCCAGGCTGG-3'
Tcf-7*** (rv)	5'-CCTCGACCGCCTCTTCTTC-3'
Lef-1***(fw)	5'-TGACAGCTGCCTACATCTGAAAC-3'
Lef-1*** (rv)	5'-GCTGCCTTGGCTTTGCAC-3'
Bcl-6***** (fw)	5'- GAGAAGCCATACCCCTGTGA-3'
Bcl-6***** (rv)	5'-TGCACCTTGGTGTGGTGTGAT-3'
EBNA-1* (fw)	5'-GGAGCCTGACCTGTGATCGT-3'
EBNA-1* (rv)	5'-TAGGCCATTTCCAGGTCCTGTA-3'
EBNA-2* (fw)	5'-TTAGAGAGTGGCTGCTACGCATT-3'
EBNA-2* (rv)	5'-AGTGCTGGGTTACTGGCTAAGC-3'
EBNA-3A** (fw)	5'-GCGGCTACGCGCATCGACAC-3'
EBNA-3A** (rv)	5'-GCATTCCAAGCCTGTGCCGT-3'
LMP1* (fw)	5'-ACCCGAAGATGAACAGCACAAT-3'
LMP1* (rv)	5'CCCTTTGTATACTCCTACTGATGATCAC3'
LMP2* (fw)	5'-AAGATCCTTCTGGCAGACTGT-3'
LMP2* (rv)	5'-TGCAGAACAATTGGGTATAAATTCA-3'
BZLF-1* (fw)	5'-CTTAACTTGGCCCGGCATT-3'
BZLF-1* (rv)	5'-ACGCACACGGAAACCACAA-3'

*Primer sequences taken from (Kubota et al. 2008)

** Primer sequences taken from (Touitou et al. 2003)

*** Primer sequences taken from (Willinger et al. 2006a)

**** Primer sequences taken from (Vandesompele et al. 2002)

***** Primer sequences taken from (Alinikula et al. 2011)

All primers were ordered by Sigma-Aldrich.

3.1.9 Cell culture medium and buffer

All cell culture media were prepared under sterile conditions and stored at 4°C. Human serum was isolated from healthy donor blood, pooled, sterile filtrated and heat inactivated for 30 minutes at 56°C.

Medium for generation of CTL_{SCM/CM}

Human serum (HS)	10% (v/v)
+/- TWS119	5 µM
+/- rapamycin	80 mM
in AIM-V medium	
or +/- 2-DG	1 mM
in DMEM medium (low Glc)	

Day 0

IL-21	10 ng/ml
IL-15	5 ng/ml
IL-7	5 ng/ml

Day 7

IL-21	10 ng/ml
IL-15	5 ng/ml
IL-7	5 ng/ml
IL-12	1 ng/ml

Day 14, 21, 28

IL-21	10 ng/ml
IL-15	5 ng/ml
IL-7	5 ng/ml
IL-2	100 IU/ml

Prep medium

Pen/Strep	1% (v/v)
FCS	1% (v/v)
in DMEM medium	

Medium for B-LCL

FCS	10% (v/v)
in RPMI 1640 medium	

Medium for dendritic cells

Day 0 – Day 3

GM-CSF	1000 IU/ml
IL-4	1000 IU/ml

Day 5 (maturation day)

GM-CSF	1000 IU/ml
IL-4	500 IU/ml
IL1-β	10 ng/ml
TNF-α	10 ng/ml

IL-6 1000 IU/ml
in X-vivo15 medium

Freezing medium

DNase I 10 IU/ml
Human albumin 20% (v/v)
DMSO (added prior to use) 10% (v/v)
in RPMI 1640 medium

Thawing medium

DNase I 10 µg/ml
in RPMI 1640 medium

FACS-buffer

BSA 3.0% (v/v)
NaN₂ 1.0% (v/v)
in PBS

FACS fixation buffer

Paraformaldehyde (PFA) 4% (v/v)
in PBS

Permeabilization buffer

Saponin 0.2% (v/v)
in PBS

Blocking buffer

BSA 3.0% (v/v)
TritonX100 0.1% (v/v)
in PBS

Wash-buffer

Tween20 0.1% (v/v)
in PBS

Lysis-buffer

NH₄Cl 8.29 g/l
KHCO₃ 1 g/l
EDTA 0.0372 g/l
in dH₂O, pH 7.29

MACS-buffer

DNase I 0.1% (v/v)
in RPMI 1640 Medium

KRPH-buffer

HEPES	20 mM
MgSO ₄	1 mM
NaCl	136 mM
CaCl ₂	1 mM
KCl	4.7 mM
KH ₂ PO ₄	5 mM
pH 7.4	

AEC-buffer

CH ₃ COOH (0.2N)	1.5% (v/v)
Sodium acetate (0.2N)	2,88 g
in 1l H ₂ O a.d.	

AEC-substrat

AEC tablet (diluted in 25 ml DMF)	10 tablets
AEC buffer	500 ml

Avidin-peroxidase complex (APC)

Reagent A	5 µl
Reagent B	5 µl
in 1 ml PBS (0.1% Tween20)	

3.1.10 Cells**PBMC**

The peripheral blood mononuclear cells (PBMC) were isolated from buffy coats of healthy donors and provided by the Laboratory of the Blood Donation Centre, University Medical Center Mainz. Buffy coat is gained by mechanical separation of 450 ml whole blood product. Buffy coats can be ordered with a desired HLA-haplotype.

Naive and total CD8⁺ T lymphocytes

Naive CD8⁺ T cells and total CD8⁺ T cells were gained from the buffy coats of healthy donors using a “*Naive CD8⁺ T-Cell Isolation Kit*” (Miltenyi Biotec) according to the protocol described in Section 0. EBV-specific CTL_{SCM/CM} cells were generated from naive CD8⁺ T cells under the impact of different inhibitors. Total CD8⁺ T cells include all CD8⁺ subtypes, which carry CD8⁺ marker on their cell surface including both naive CD8⁺ T cells and effector T cells. Total CD8⁺ T cells treated or untreated with inhibitor and untreated naive CD8⁺ T cells were used in this work as negative controls.

B95-8 cells

The EBV-producing marmoset B-cell line (B95-8) was used as a source of EBV virus. B95-8 cells were cultured for several weeks, whereby EBV virus was secreted into the media. EBV supernatants were frozen and used later for transformation of human B cells. Working with these cells is only allowed in the laboratories with a security grade BSL-2.

3.2 Methods**3.2.1 Isolation of peripheral blood mononucleated cells from buffy coats**

T lymphocytes were isolated from eight hours old buffy coat according to Bøyum et al. (Bøyum 1976). The mononuclear cells, granulocytes and erythrocytes were separated by ficoll gradient density centrifugation. Therefore, the buffy coat was diluted with PBS (1:1) and carefully added on top of 15 ml of ficoll solution. After centrifugation at 836 x g for 18 min without breaks to efficiently separate the leucocytes from the erythrocytes, the leucocytes in the interphase were collected, washed with cold PBS and centrifuged afterwards at 677 x g for 10 min. The cells were then pooled and washed several times with cold PBS until the supernatant became clear. Cells were counted, resuspended in freezing medium and frozen with a concentration of 5×10^7 cells/ml.

3.2.2 Isolation of naïve and total CD8⁺ T cells from PBMC

Naive CD8⁺ T cells were isolated by magnetic affinity cell sorting (MACS) in two steps based on the manufacturer's protocol.

In the first step a desired number of PBMC was resuspended in MACS buffer (10^7 cells per 40 μ l MACS buffer) and 10 μ l of naive CD8⁺ T cell Biotin-Antibody cocktail per 10^7 cells was added. After 10 minutes incubation at +4C° another 30 μ l of MACS buffer and 20 μ l of Anti-Biotin Micro-Beads per 1×10^7 cells were added. Cells were mixed well and incubated for 15 minutes at +4C°. Afterwards, cells were washed with 2 ml cold MACS buffer per 10^7 cells and centrifuged at 300 x g for 10 minutes. For depletion a LD-column was placed in the magnetic field and equilibrated with 2 ml MACS buffer. 10^8 cells were resuspended in 500 μ l of MACS buffer and applied onto the column. After the cells passed through, the column was washed with 2 ml MACS buffer. Unlabelled T cells were collected in the effluent, counted and kept on ice. The cells which remained in the column were flushed out immediately by applying a plunger onto the column. They were used as "feeder cells 1" to support the growth of naive T cells *in vitro*. In the second step, a positive selection of naive CD8⁺ T cells was performed. Therefore the eluate of the column (i.e. unlabelled T cells) was resuspended in MACS buffer (10^7 cells per 80 μ l MACS buffer), 40 μ l of CD8⁺ Micro-Beads per 10^7 cells was added, mixed well and incubated for 15 minutes at +4C°. Afterwards, cells were washed with 2 ml of cold MACS buffer per 10^7 cells and centrifuged at 300 x g for 10 minutes. Next, the cell suspension (10^8 cells per 500 μ l of MACS buffer) was applied onto a MS-column, placed

in a magnetic field and equilibrated with 500 μ l MACS buffer. After the cells had passed through, the column was washed with 3x500 μ l of MACS buffer. Naïve CD8⁺ T cells were then flushed out by applying a plunger onto the MS-column, and “feeder cells 2” were collected in the effluent. “Feeder cells 1” and “feeder cells 2” were pooled together and irradiated at 25 Gray. These cells were used to support growth of naïve T cells cultured *in vitro*. Subsequently, purity of isolated cells was assessed by flow cytometric analysis (see 3.2.11) whereby the cells were stained for the surface markers CD3, CD8, CD27, CD28, CD45RO, CD45RA, CD62L, CD95, CCR7.

3.2.3 Generation of mature dendritic cells from PBMC

Dendritic cells (DC) were used for the first stimulation of naive and total CD8⁺ T cells. Therefore, 6x10⁷ PBMC were thawed, washed, resuspended in X-vivo15 medium and seeded in a concentration of 1x10⁷ cells per well in the 6-well plate. The cells were incubated for 2h at 37°C; afterwards all non-adherent cells were washed out with warm PBS. The adherent cells received 3 ml of X-vivo15 medium per well supplemented with IL-4 (1000 UI/ml) and GM-SCF (1000 IU/ml). After three days the cells received the same cytokines again. The final maturation of DC took place on the fifth day after addition of the cytokine cocktail: IL-4, IL1- β , TNF- α , GM-SCF and IL-6 were applied one day before T cell stimulation (see 3.1.9).

3.2.4 Generation of EBV-specific DC

On the day of T cell stimulation DC have to be incubated with EBV-peptides or peptide pools and subsequently given to the T cells as a stimulator. Therefore, mature DC were harvested, washed with AIM-V medium and counted. DC were resuspended in 1 ml AIM-V medium or in 1 ml DMEM (low Glucose) medium, respectively, according to the inhibitor used for generation of CTL_{SCM/CM} cells (see 3.1.9). DC were incubated with three EBV-specific peptides: LMP2 (5.1 μ g/ μ l), BZLF-1 (5.2 μ g/ μ l), BRLF-1 (5.0 μ g/ μ l) in the case of TWS119 treatment and with EBV-peptide pools: LMP2 (5.1 μ g/ μ l) and BZLF-1 (5.2 μ g/ μ l), in the case of 2-DG treatment. After 2h of incubation at 37°C, DC were lethally irradiated by 25 Gray and added to the T cells in an effector:target ratio of (1:10), i.e. 1 DC to 10 T cells.

3.2.5 Generation of EBV-specific PBMC

EBV-specific PBMC were used after first stimulation for further CTL_{SCM/CM} cells expansion. Therefore, the following three EBV-specific peptides were used: LMP2 (5.1 μ g/ μ l), BZLF-1 (5.2 μ g/ μ l), BRLF-1 (5.0 μ g/ μ l) or two EBV-peptide pools: LMP2 (5.1 μ g/ μ l) and BZLF-1 (5.2 μ g/ μ l). Peptides were added to the appropriate quantity of PBMC, incubated for 2h at 37°C and subsequently irradiated at 25 Gray. The lethally irradiated PBMC were added to the T cells in a ratio of (1:1), i.e. one T cell to one PBMC.

3.2.6 Production of EBV transformed B cells

Different EBV transformed lymphoblastoid B cell lines (B-LCL) were used as targets to test EBV-specificity of EBV-specific CTL_{SCM/CM}. Therefore, 0.5 ml of virus particle containing supernatant of B95.8 cells was added to 5×10^6 PBMC. After 2h incubation at 37°C the cells were resuspended in 5 ml RPMI (20% FCS, 1 µg/ml CSA) and transferred into a T25-flask. Cyclosporine A (CSA) was added to inhibit expansion of T cells. Cell growth of B-LCL was observed every week and fresh medium was added if demanded. After 5 weeks infected B cells exhibited a stable cell growth and could be transferred into a T75-flask for further expansion.

3.2.7 Generation of EBV-specific CTL_{SCM/CM}

In order to generate EBV-specific cytotoxic T lymphocytes with stem cell memory and central memory-like properties (CTL_{SCM/CM}), the naive fraction of CD8⁺ T cells was isolated from PBMC (see 0) of EBV negative healthy donors. Total fraction of CD8⁺ T cells was also isolated from PBMC and used as control. CTL_{SCM/CM} cells were generated in different medium, which was supplemented with different cytokines (3.1.9) and was performed, as illustrated in Figure 8:

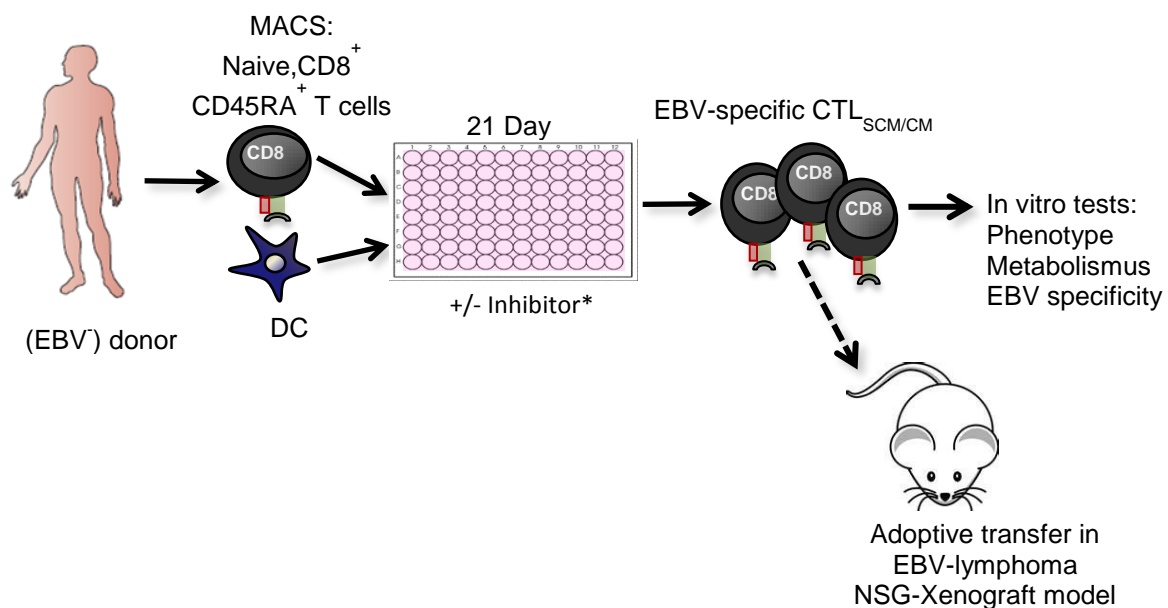


Figure 8: Generation of EBV-specific CTL_{SCM/CM} cells from naive CD8⁺ T cells. Naive CD8⁺ T cells from EBV donors were purified through MACS and primed with EBV-specific DC on day 0. Next, T cells were weekly stimulated with EBV-specific PBMC and supplemented with cytokines: IL-15, IL-21, IL-7, IL-12 (day 7), IL-2 (from day 14). To generate and maintain CTL_{SCM/CM}, T cells were treated with different inhibitors. As Inhibitor* was used TWS119 to modulate Wnt-β-catenin signaling pathway or 2-DG and RAPA to manipulate T cell metabolism. Starting from day 21 *in vitro* assays were performed to characterize the generated cells and subsequently *in vivo* assays to study EBV-specificity and persistence.

For the first stimulation on the day 0, EBV-specific autologous DC and “feeder cells” were lethally irradiated and added to the T cells at a ratio of 1:10:10 (1×10^5 (DC): 1×10^6 (“feeder cells”): 1×10^6 (naïve CD8⁺ T cells / total CD8⁺ T cells)) (see 3.2.4). Discarded non-naïve T cells during MACS separation were used as “feeder cells” to support the cell growth of naïve CD8⁺ T cells. The following stimulations of naïve and total CD8⁺ T cells were boosted by autologous irradiated EBV-specific PBMC (see 3.2.5). The generation and maintenance of CTL_{SCM/CM} was achieved through manipulation of T cell metabolism using 1 mM 2-deoxyglucose (2-DG) and 80 mM RAPA or by activation of Wnt-β-catenin signaling pathway by 5 μM TWS119 (see 3.1.9). All drugs were added weekly upon stimulation. After two weeks of cultivation T cells were transferred into the 48-well plate for further expansion.

3.2.8 Freezing of cells

After centrifugation, the cell pellet was resuspended into freezing medium (see 3.1.9) and 10% of the cryoprotective agent DMSO was added. 1×10^7 cells/ml of T cell suspension or 5×10^7 cells/ml of PBMC were transferred into cryotubes and stored at -80°C overnight. On the next day the frozen cells were transferred to the liquid nitrogen tank (-196°C).

3.2.9 Thawing of cells

Thawing of cells should proceed very quickly. The frozen cells were taken from the nitrogen storage and placed into a 37°C water bath. As soon as cell suspension started to thaw, cells were transferred into 15 ml of thawing medium (see 3.1.9) and centrifuged at 1500 rpm for 5 min. The supernatant was discarded and the cell pellet was resuspended in an appropriate volume of the culture medium and transferred into a culture dish.

3.2.10 Generation of EBV supernatant from B95-8 cells

B95-8 cells were thawed and cultured in RPMI medium for three days. On the third day 1×10^6 cells were transferred into the T60 flask and cultured for 11-12 days by 37 °C. Subsequently the supernatant was removed, centrifuged, sterile filtered and frozen (500 μl per cryotube).

3.2.11 Cell surface marker analysis with flow cytometry

The naïve and total CD8⁺ T cells were stained for the following extracellular cell markers: CD8, CD45RA, CD45RO, CD95, CD27, CD28, CD3, CD62L and CCR7, on the day of isolation and during the expansion. Therefore, cells were washed with FACS-buffer and 2×10^5 cells/100 μl per FACS tube were stained for 15 min by RT with the optimal amount of conjugated antibodies. After incubation, cells were washed with FACS-buffer and fixed with 4 % paraformaldehyde (PFA). All analyses were performed on a BD FACS Canto II flow cytometer. All acquired data were analyzed with BD FACS Diva™ 6.1.3 software.

3.2.12 Analysis of the glucose consumption of *in vitro* generated CTL_{SCM/CM}

One of the main differences between T_{SCM}, T_{CM} and T_{EFF} is a slower proliferation, resulting in less consumption of glucose. To verify this statement, the uptake of 2-deoxy-D-glucose (2-DG) was measured in CTL_{SCM/CM} generated *in vitro* and compared with 2-deoxy-D-glucose (2-DG) uptake of T_{EFF}.

2-DG is a structural analogue of glucose differing at the second carbon atom by the substitution of hydrogen for a hydroxyl group. 2-DG undergoes facilitated diffusion into cells via glucose transporters, where it is phosphorylated by hexokinase to 2-deoxy-D glucose- 6-phosphate (2-DG-6-P). Once formed, 2-DG-6-P is not further metabolized and accumulates in the cell until de-phosphorylated by phosphorylase. Thus, prolonged glucose deprivation forces cells to switch to other metabolic pathways e.g. fatty acid oxidation (FAO) for ATP production.

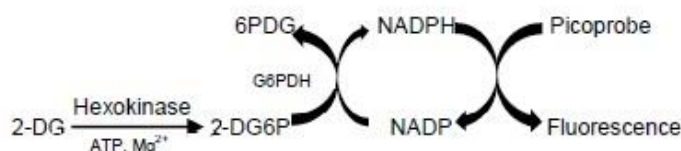


Figure 9: Accumulation of 2-DG6P in the cell. 2-DG is absorbed by the cell through a glucose transporter and inhibits glucose consumption via its interaction with hexokinase. Phosphorylated by hexokinase to 2-DG6P is enzymatically oxidized and coupled to *PicoProbe*, which generates a fluorescence signal in the presence of NADPH*. *<http://www.abcam.com>

The intracellularly accumulated 2-DG6P is directly proportional to the cell absorbed 2-DG. 2-DG6P is enzymatically oxidized and coupled to the *PicoProbe* (developed by *Biovision*) which generates a fluorescence signal in the presence of NADPH. The glucose uptake was measured with a “*Glucose Uptake Fluorometric Assay Kit*” (*Biovision*) according to the manufacturer’s protocol involving some modifications. On day 1, T cells were washed two times with PBS and 1x10⁶ of T cells were resuspended in 1 ml serum free DMEM medium (low Glc) and incubated overnight at 37°C. On day 2, T cells were washed three times with PBS and resuspended in 1 ml KRPH buffer (see 3.1.9) and incubated for 40 min at 37°C. Afterwards, cells were centrifuged and resuspended in 300 µl KRPH buffer in the reaction tube. Next, 100 µl of cell suspension was added into each reaction tube and supplemented with 60 µM phloretin and 10 mM 2-DG according to Table 3.

Table 3: The pipetting schema for glucose uptake assay

Cell group	2-DG	Phloretin	2-DG	Phloretin	2-DG	Phloretin
Naive CD8 ⁺ + 2-DG/+TWS	-	-	+	-	+	+
Naive CD8 ⁺ - 2-DG/-TWS	-	-	+	-	+	+
Total CD8 ⁺ + 2-DG	-	-	+	-	+	+
Total CD8 ⁺ - 2-DG/-TWS	-	-	+	-	+	+

For lysis, T cells were washed three times with PBS to wash out the exogenous 2-DG and 90 μl of extraction buffer (provided in kit) was added per 100 μl of cell suspension. Cells were frozen/thawed once and heated at 85°C for 40 min. Afterwards, cells were cooled for 5 min on ice, 10 μl of neutralization buffer (provided in the kit) and 50 μl of cell suspension per well were pipetted in the flat bottomed 96-well-plate. The final volume was adjusted to 50 μl with assay buffer (provided in the kit). Finally, 50 μl of reaction mix (provided in the kit) was added into each well and the plate was incubated at 37°C for 40 min, protected from light. Fluorescence was measured at Ex/Em = 535/587 nm by a fluorescence plate reader. For the calculation, the 0 pmol standard was subtracted from all standard readings and the 2-DG6P standard curve was plotted. Sample background was corrected by subtracting the value derived from the untreated cells (control i.e. not treated with 2-DG) from all sample readings. To calculate 2-DG concentration of the test samples, which is proportional to accumulated 2-DG6P, the following equation 1 was used:

$$\mathbf{2\text{-DG uptake} = Sa/Sv \text{ (pmol}/\mu\text{l or nmol/ml or } \mu\text{M)} \text{ (1)}}$$

Sa (pmol) represents the amount of 2-DG6P calculated in the sample well according to the standard curve, whereas **Sv (μl)** is a sample volume added into the sample wells.

3.2.13 Analysis of the lactate production of *in vitro* generated CTL_{SCM/CM}

The other evidence of the slow proliferation of T_{SCM} und T_{CM} cells is a reduced production of lactate compared to effector T cells. The lactate production was measured with a “*Lactate Assay Kit*” (Sigma-Aldrich) according to the manufacturer’s protocol involving some modifications. 3×10^5 T cells were resuspended in 300 μl lactate assay buffer (provided in the kit) and homogenized by centrifugation by 13.000 g for 10 min. After, 25 μl of the supernatant and 25 μl of lactate assay buffer (provided in the kit) were added per well in the flat bottomed 96-well plate.

For a lactate standard preparation of 1 nmol/ μl , 10 μl of the 1 nmol/ μl of standard solution was added to 90 μl of lactate assay buffer. Then, 0,2,4,6,8 and 10 μl of 0.1 nmol/ μl standard solution was plated out in a flat bottomed 96-well plate, generating 0 (blank), 0.2, 0.4, 0.6, 0.8 and 1 nmole/well. Finally, lactate assay buffer was added to each well to bring the volume to 50 μl . To start the reaction 50 μl of reaction mix (set up according to Table 4) was added to each well containing 50 μl of sample and mixed. The plate was incubated for 30 min at RT, protected from light. The fluorescence signal was measured at Ex/Em = 535/587 nm by a fluorescence plate reader.

Table 4: Master reaction mix for lactate production assay

Reagent	Master reaction mix x1, μ l
Lactate assay buffer	46
Lactate enzyme mix	2
Lactate probe	2

For the calculation the values obtained from the appropriate lactate standards were used to plot a standard curve. The amount of lactate produced by the cells was determined from the standard curve. Produced lactate concentration was calculated by the equation 2:

$$Sa/Sv = C \quad (2)$$

Sa (nmole) is the amount of lactate acid calculated in the sample from the results obtained from the standard curve, **Sv (ml)** is a sample volume added into the wells, **C (nmole/ml)** is a concentration of lactate acid in the sample. Lactate molecular weight is 89.07 g/mole.

3.2.14 OCR and ECAR measurements of *in vitro* generated CTL_{SCM/CM}

Two important parameters for the assessment of T cells' metabolism are extracellular acidification rate (ECAR) and oxygen consumption rate (OCR). High levels of ECAR indicate, that T cells operate under aerobic glycolysis. OCR exhibits the level of mitochondrial respiration utilized by T cells.

To study the difference of metabolism in CTL_{SCM/CM} and T_{EFF} cells, OCR and ECAR were measured under basal conditions and after pharmacological inhibition of mitochondrial respiration with oligomycin A (5 μ M), rotenone (2.5 μ M) and dinitrophenol (DNP) (250 μ M). OCR and ECAR were measured on a Seahorse XF96 Extracellular Flux Analyzer kindly provided by Dr. Dmitry Namgaladze from the Institute of Biochemistry I of the Goethe-University Frankfurt/Main.

On the day 1, 96XF plate was coated. Therefore, 13 μ l of 50 μ g/ml Poly-D-Lysine (PDL) was added per well to the 96XF plate and incubated at room temperature for 1-2 hrs. Afterwards, the solution was aspirated and the surface rinsed with 500 μ l sterile H₂O and once again aspirated. After the surface of the 96XF plate was dried out, coated plate was stored at room temperature. On the day 2, PDL coated XF96 plate was placed at 37°C without CO₂ and kept at least one hour at 37°C before prior to assay start. The previously restimulated T cells were washed and 100 μ l of cell suspension (final cell density 2x10⁵ cells/well) was pipetted to each well in 96XF plate. The plates were centrifuged by slow acceleration (4 on a scale of 9 for Eppendorf 5810R) without brakes. For this, the 96XF plate was transferred to centrifuge plate carriers and oriented symmetrically. The centrifuge was accelerated up to 450 rpm (about 40 x g) and stopped as soon as 450 rpm was reached. Afterwards, the orientation of the plates was reversed on the plate carriers, the centrifuge was spun up to 650 rpm (about 80 x g) and slowly decelerated. Following centrifugation, cells were kept for 30 min in a 37°C non-CO₂ incubator for better attachment. Next, 100 μ L of assay medium was added to each

well and the cells were incubated for 1h prior the XF assay. Prior starting the assay measurement, rotenone (2.5 μ M), DNP (250 μ M) and oligomycin A (5 μ M) were pipetted into the lid of the XF96 plate.

3.2.15 Polymerase chain reaction (PCR)

The total RNA was isolated from 1×10^6 T cells or B-LCL using the *RNeasy Mini Kit* according to the manufacturer's protocol. RNA concentrations were determined photometrically at 260 nm using spectrophotometer. Samples were stored at -80 °C.

1 μ g of total RNA was used for cDNA synthesis. The DNA synthesis was performed by using the *SuperScript III TM First-Strand Synthesis System* according to the manufacturer's protocol. cDNA concentrations were determined photometrically at 260 nm using a spectrophotometer. Samples were stored at -20 °C.

For the amplification of cDNA, the following reaction mix was prepared:

- 1 μ l Forward Primer (10 μ M)
- 1 μ l Reverse Primer (10 μ M)
- 1 μ l cDNA (50 ng)
- 9.5 μ l Water, PCR-grade
- 12.5 μ l Maxima SYBR Green qPCR Master Mix (2x)

24 μ l of the reaction mix was pipetted into each well of a PCR plate and subsequently 1 μ l (50 ng) of cDNA was added. The PCR plate was sealed, centrifuged and loaded into the thermal cycler (Real-Time PCR detection system). All primers were tested in advance to determine an optimal annealing temperature. The expression of EBV latent and lytic genes in B-LCL was analyzed using the following settings:

- **10 min 95 °C (initial denaturation and polymerase activation)**
- **15 s 95 °C (denaturation) 50x**
- **1 min 60 °C (annealing/extension) 50x**

The expression of Wnt-signaling transcription factors Tcf-7, Lef-1 was accessed in T lymphocytes using the following settings:

- **10 min 95 °C (initial denaturation and polymerase activation)**
- **15 s 95 °C (denaturation) 40x**
- **1 min 60 °C (annealing/extension) 40x**

3.2.16 IFN- γ ELISpot assay

In order to measure the cytolytic activity of EBV-specific CTL_{SCM/CM} cells *in vitro* the IFN- γ secreting T cells were quantified in an ELISpot assay. Upon seeding of effector and target cells (B-LCL) into each well EBV-specific T cells become activated and start to release cytokine IFN- γ that is secreted and bound by capture antibodies immobilized to a membrane

in each well 96-well of a ELISpot plate. After the co-incubation, cells are washed away and the released cytokines that are captured are detected by a secondary antibody. This detection antibody can be coupled to the avidin/horse radish peroxidase (HRP)-complex, which converts substrate (AEC) and induces coloured spots on the membrane surface. Each spot corresponds to one activated, cytokine producing T cell. The ELISpot assay was performed in two days.

On day 1, a 96-well plate was coated with 20 μ l of 35% C₂H₅OH per well, washed 3 times with 150 μ l PBS per well and subsequently coated with 10 μ g/ml of mAb 1-D1K (anti-IFN- γ) per well. After 2h incubation at 37°C, the plate was washed 3 times with PBS and the unspecific binding sites were blocked with 100 μ l of RPMI (10% FCS) per well. After, the plate was incubated for 1h at 37°C and afterwards seeded with 2.5x10⁴ T cells and 2.5x10⁴ of EBV-specific PBMC/or 1x10⁴ B-LCL per well with the end volume of 200 μ l. T cells were tested either on day 4 or 5 after restimulation. 2.5x10⁴ PBMC/ 1x10⁴ B-LCL per well were seeded as negative control and 2.5x10⁴ to 5x10⁴ T cells per well supplemented with phytohaemagglutinin (PHA) (10 μ g/ml) were used as positive control. Subsequently, the 96-well plate was incubated overnight at 37°C with 5% CO₂.

On day 2, the 96-well plate was washed six times with 150 μ l of PBS (0.05 % Tween) and coated with 2 μ g/ml of biotinylated anti-IFN- γ (7-B6-1) per well. After 2h incubation at 37°C, the plate was again washed six times with PBS (0.05% Tween) and 60 μ l of APC complex (see 3.1.9) was added per well. The plate was incubated for 1h at RT protected from light and washed 3 times with PBS (0.05% Tween) and then 3 times with PBS. Afterwards, 60 μ l of ACE buffer (see 3.1.9) was added per well and the plate was incubated for 10 min at RT. Subsequently, the plate was washed with tap water to stop the reaction and left for two days to dry. Finally, the spots were counted with an ELISpot reader S5 Versa Analyzer.

3.2.17 The transmigration assay

The chemotactic capacity of *in vitro* generated EBV-specific CTL_{SCM/CM} cells was assessed by transmigration assay. Therefore, 5x10⁵ T cells/100 μ l were placed on the upper layer of the cell permeable membrane and 600 μ l RPMI medium containing 1 μ g/ml CCL21, which is a ligand for CCR7, was placed below the cell permeable membrane.

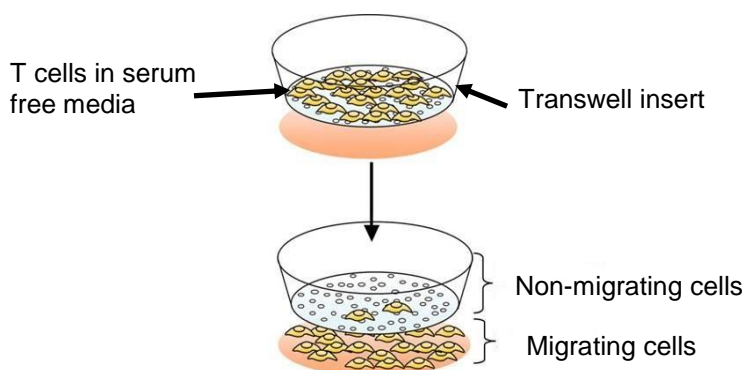


Figure 10: Transmigration assay. Cells were placed on the upper layer of the cell permeable membrane in the transwell insert and medium containing CCL21 was placed below the cell permeable membrane. After 5h incubation, migrated cell were harvested and counted.

Following an incubation period of 5h, the cells that have migrated through the membrane were harvested, stained with trypan blue and counted. The transmigration assay was performed in duplicates, as illustrated in Table 5.

Table 5: The pipetting schema for transwell assay

Time	Naïve CD8 ⁺ +2-DG/+TWS		Naïve CD8 ⁺ -2-DG/-TWS		Total CD8 ⁺ +2-DG/+TWS		Total CD8 ⁺ + 2-DG/+TWS	
	+CCL21	-CCL21	+CCL21	-CCL21	+CCL21	-CCL21	+CCL21	-CCL21
5h	+CCL21	-CCL21	+CCL21	-CCL21	+CCL21	-CCL21	+CCL21	-CCL21
5h	+CCL21	-CCL21	+CCL21	-CCL21	+CCL21	-CCL21	+CCL21	-CCL21

3.2.18 Chromium-51 release assay

Chromium-51 (⁵¹Cr) release assay was used to determine the cytolytic activity of EBV-specific CTL_{SCM/CM} generated *in vitro*. Target cells (B-LCL) were labelled with the radioactive ⁵¹Cr isotope and then incubated with the T cells. If the target cells are lysed by the T cells, radioactive ⁵¹Cr is released into the supernatant and can be detected.

For the labelling, 5x10⁵ B-LCL (target cells) were incubated with 50 µCi Chromium in 25 µL FCS at 37 °C for 1.5h. Target cells were then washed three times and adjusted to their final working concentration in AIM-V medium. 1.5x10³ B-LCL per well were seeded in a total volume of 80 µL in 96-well V-bottom plates. T cells were added as duplicates in a serial dilution (Effector:Target 1/2/7/20/60) in a final volume of 80 µL and incubated at 37°C for 5 h. The supernatant was then harvested by centrifugation at 282 x g for 5 min with zero breaking. 80 µL of the supernatant was transferred into the cytotox tubes and measured in the Gamma-counter Wizard 2.

Controls for a minimum and maximum lysis of target cells were performed in at least four replicates. For minimum lysis, the labelled target cells were incubated with a plain medium.

For maximum lysis, the labelled target cells were incubated with PBS containing 1% Triton X. Specific lysis was calculated according to Equation 3.

$$\text{Specific lysis (\%)} = (\text{exp} - \text{min}) / (\text{max} - \text{min}) \times 100 \quad (3)$$

(Exp) is an experimental value, **(max)** represents maximum lysis and **(min)** applies for minimum lysis.

3.2.19 *In vivo* analysis on survival of CTL_{SCM/CM} in the absence of antigen

The long-term persistence of EBV-specific CTL_{SCM/CM} cells was analyzed in NOD/SCID/IL2R γ ^{null} (NSG)-mice in the absence of antigen. These mice have a severe combined immune deficiency mutation (SCID) and a common gamma chain (γ) receptor knockout which leads to a lack of mature T cells and B cells, functional NK cells due to a deficient cytokine signaling of the cytokines IL-2, -4, -7, -9, -15, and -21 which all use γ as part of their high affinity cytokine receptor. Stock breeding, maintenance, and manipulation of mice were carried out in the Translational Animal Research Center (TARC) of the Johannes Gutenberg-University Mainz under specific pathogen free (SPF) conditions. The autoclaved drinking water was supplemented with 0.08 mg/ml Borgal (sulafadoxinum, trimethoprimum). All animal studies were approved by the German state authorities and were performed according to guidelines of the European Union and national German law.

NSG-mice were intravenously (*i.v.*) injected with 1×10^6 2-DG treated, EBV-specific CTL_{SCM/CM} cells or 5×10^6 TWS119 treated EBV-specific CTL_{SCM/CM} cells in 200 μ L PBS supplemented with 0.5% FCS per mouse. The injected T cells were selected based on their level of IFN- γ secretion *in vitro* and by flow cytometric analysis. Additionally, 66 μ g of human ILR13⁺-Fc (IL-15 with extended half-life, generously provided by A. Mades, a PhD student in our lab) was weekly injected into NSG-mice to improve the local cytokine milieu for the T cells. Peripheral blood from mice injected with 2-DG treated EBV-specific CTL_{SCM/CM} cells was drawn weekly and analyzed for the frequency of CD45/CD3 cells as compared to control groups that had not been supplemented with ILR13⁺-Fc. The analyses were performed weekly, because of the small number of injected T cells, as illustrated in Figure 10A.

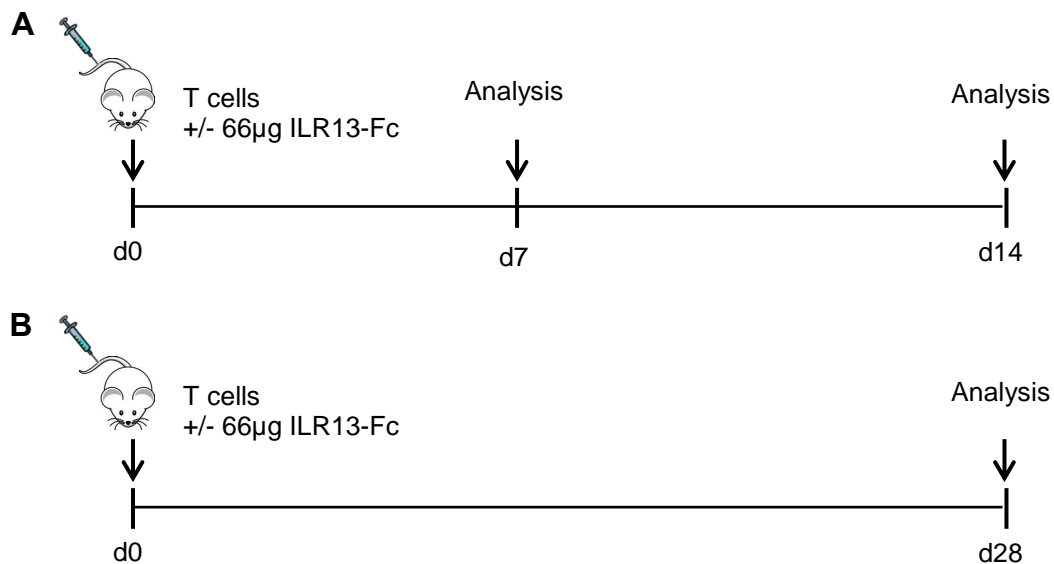


Figure 11: EBV-specific CTL_{SCM/CM} transfer into NSG-mice. A. NSG-mice were (*i.v.*) injected with 1×10^6 2-DG treated EBV-specific CTL_{SCM/CM}. 66 µg of human ILR13⁺-Fc was weekly injected into mice to improve environment for the T cells. Peripheral blood from mice was drawn weekly and analyzed for the expression of CD45/CD3 cells. B. Mice injected with TWS119 treated EBV-specific CTL_{SCM/CM} were sacrificed after 4 weeks and murine bone marrow, spleen, and peripheral blood were analyzed for expression of CD45/CD3 cells. 66 µg of human ILR13⁺-Fc was weekly injected into mice to improve environment for the T cells.

Mice injected with TWS119 treated EBV-specific CTL_{SCM/CM} cells were sacrificed after 4 weeks and murine bone marrow, spleen, and peripheral blood were analyzed for expression of CD45/CD3 cells and compared to control groups that were not supplemented with ILR13-Fc (see Figure 11B).

3.2.20 Adoptive T cell transfer in EBV-engrafted mice

To generate a therapeutic mouse model, NSG-mice were transferred (*i.v.*) with 5×10^5 B-LCL in 200 µL PBS supplemented with 0.5% FCS per mouse. When B-LCL were successfully engrafted to an extent of 1% to 3% blasts in murine bone marrow, T cells were adoptively transferred into the mice. Adoptive transfer of EBV-specific CTL_{SCM/CM} cells was performed on day three after stimulation of the T cells to provide optimal conditions for T cell growth and antigen recognition in mice. Either 1.5×10^6 EBV-specific CTL_{SCM/CM} cells generated under the impact of TWS119 or 1×10^6 EBV-specific CTL_{SCM/CM} cells generated using 2-DG were (*i.v.*) transferred in 200 µL PBS supplemented with 0.5% FCS into each mouse. 66 µg ILR13-Fc was added to increase the persistence of 2-DG treated T cells. On the day before transfer, T cell reactivity towards B-LCL was confirmed by IFN-γ ELISpot assay. The phenotype of transferred T cells was determined using flow cytometric analysis.

3.2.21 Isolation and preparation of peripheral blood and organs from NSG-mice

To determine the level of B-LCL, analysis of bone marrow, spleen, kidney and peripheral blood of the mice was performed. After cervical dislocation, 50 µL blood was taken from the

pericardium and diluted with 20 μ L heparin to prevent coagulation. The spleen and kidney were removed and shredded through a 100 μ m cell strainer. The bone marrow was flushed out of excised femur with prep medium and filtered through a 100 μ m cell strainer. Kidney, spleen and bone marrow samples were centrifuged and cell pellets were incubated with 2 ml lysis buffer for 2 minutes. Subsequently, cells were washed with prep medium and resuspended in FACS-buffer. 100 μ L of cell suspension and 50 μ L of blood were then stained for flow cytometry using CD3 and CD45 antibodies to identify human T cells and CD20, CD19 and CD45 to determine human B-LCL. Blood samples were incubated with 300 μ L lysis buffer (see 3.1.9) for 2 minutes. Afterwards, blood and organ samples were washed with FACS-buffer (see 3.1.9) and resuspended in 300 μ L FACS fixation buffer (see 3.1.9).

4. Results

4.1 Phenotype of *in vitro* generated EBV-CTL_{SCM/CM} using RAPA

In this work three different approaches were tested to generate EBV-specific cytotoxic T lymphocytes with stem cell- and central memory-like characteristics (EBV-CTL_{SCM/CM}). In the first approach naive CD8⁺ T cells were treated with RAPA to limit the glucose consumption and concomitantly decelerate the differentiation process in T cells. Freshly purified naive CD8⁺ T cells were analyzed for the expression of typical T_{SCM} and T_{CM} surface markers as previously published (Gattinoni et al. 2011b) on the day of isolation and after 21 days of RAPA treatment.

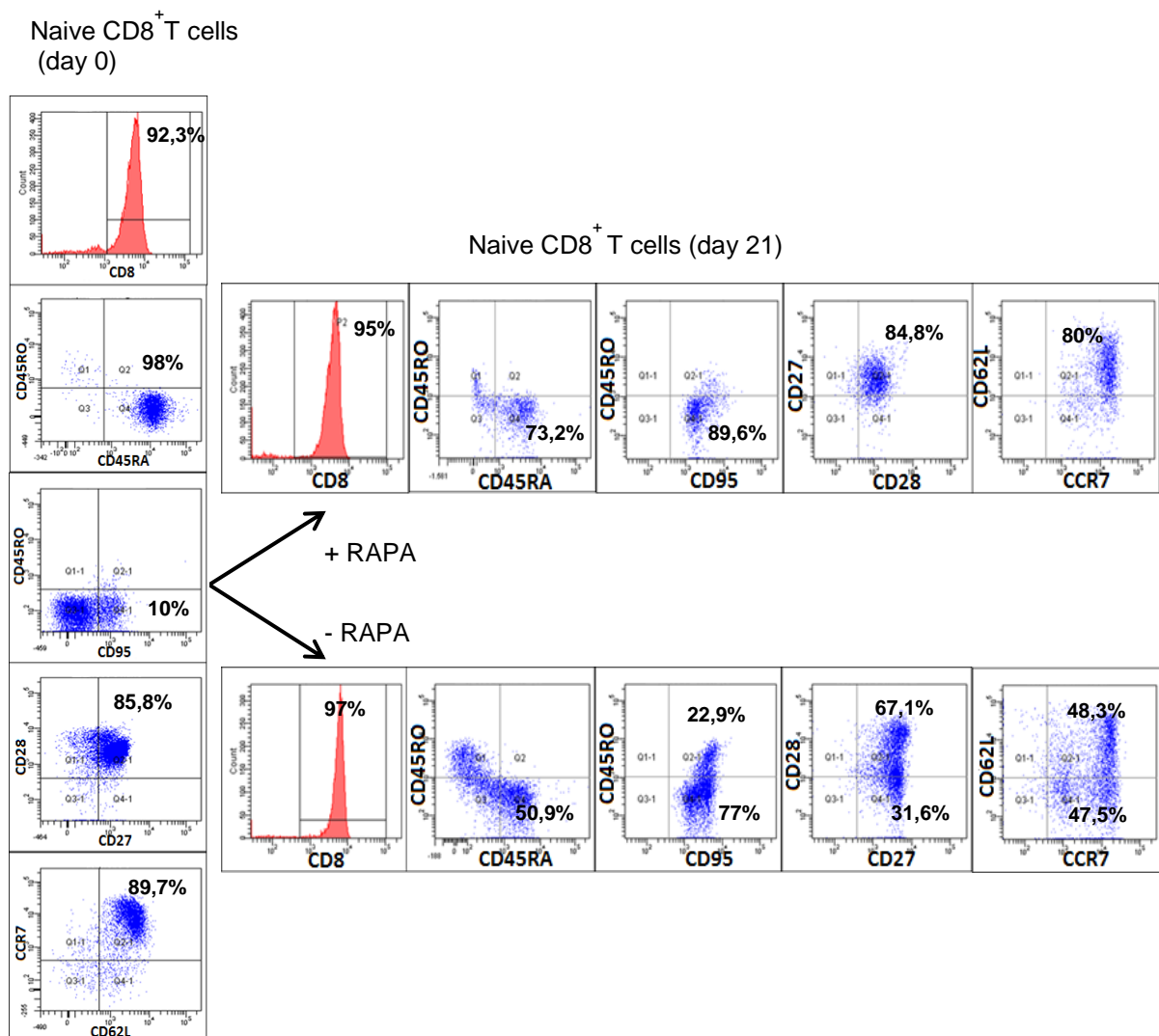


Figure 12: Phenotype of naive CD8⁺ T cells examined on day of isolation and on day 21 after RAPA treatment. Shown are representative analyses of naive CD8⁺ T cells isolated from different donors. T cells were gated in the FSC/SSC channel and out of this population CD8⁺ T cells were further gated. The expression of CD45RA, CD45RO, CD27, CD28, CCR7 and CD62L on the surface of CD8⁺ T cells is illustrated.

Naive T cells exhibited a naive-like phenotype: CD45RA⁺ CD45RO⁻ CD27⁺ CD28⁺ CD95⁻ CCR7⁺ CD62L⁺ (see Figure 12left). After rapamycin treatment naive CD8⁺ T cells expressed high levels of CD45RA (73.2%), CD95 (89.6%), CD28/CD27 (84.8%) and both homing markers CCR7/CD62L (80%), similar to the conventional memory T cells, and were therefore identified as human CTL_{SCM/CM} cells. In the absence of mTORC1 inhibition, T cells uniformly upregulated the late memory marker CD45RO and exhibited only 50.9% of CD45RA (see Figure 12). The total population of CD8⁺ T cells, which consisted of different CD8⁺ T cell subsets including all stages of CD8⁺ T cell memory development, was used as a control to analyze phenotype rapamycin treated CD8⁺ T cells.

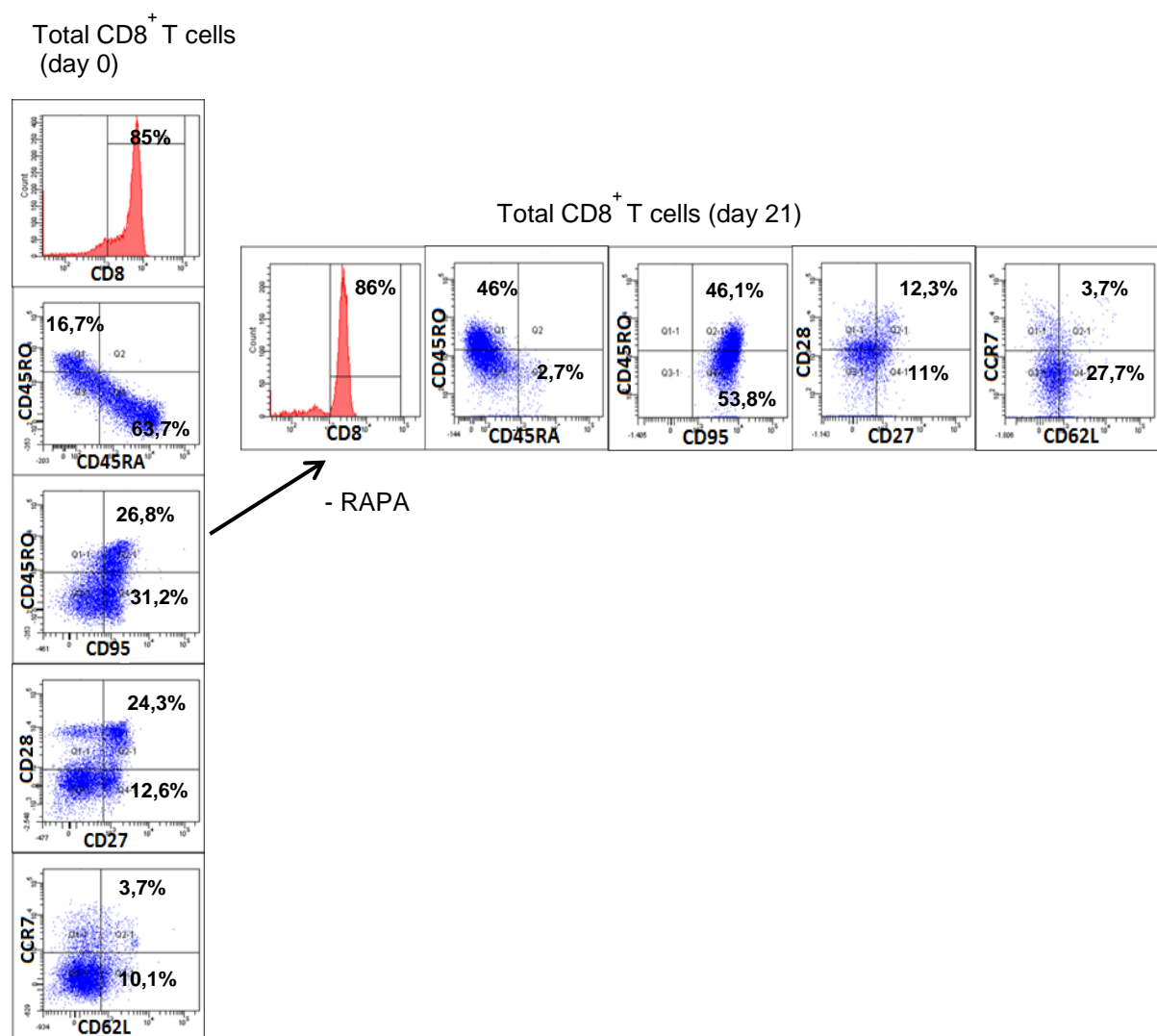


Figure 13: Phenotype of total CD8⁺ T cells examined on day of isolation and on day 21 in the culture. Shown are representative analyses of total CD8⁺ T cells isolated from different donors. T cells were gated in FSC/SSC channel and out of this population CD8⁺ T cells were further gated. The expression of CD45RA, CD45RO, CD27, CD28, CCR7 and CD62L on the surface of CD8⁺ T cells is illustrated.

The phenotype of the total population of CD8⁺ T cells was analyzed on the day of isolation at which 63.7 % of the cells expressed CD45RA and 16,7 % CD45RO, indicating that this T cell population consists of all CD8⁺ T cell subsets (see Figure 13). At day 21 of culture, total CD8⁺ T cells upregulated the expression of CD45RO (46%) and homing markers CCR7 and CD62L (3.7%), thus showing an effector T cell-like phenotype.

4.2 Phenotype of *in vitro* generated EBV-CTL_{SCM/CM} using 2-DG

In the second approach the generation of EBV-specific CTLs with stem cell- and central memory-like characteristics was enforced by the inhibition of glucose consumption using 2-DG. 2-DG is a glucose analogue, which is absorbed by the cell through a glucose transporter and inhibits glycolysis via its interaction with hexokinase. 2-DG treated cells become metabolically quiescent and utilize fatty acid oxidation (FAO) to fuel OXPHOS. 2-DG was added to the cells upon every stimulation. T cells were analyzed after the isolation to check the purity of naïve population and after 21 days of 2-DG treatment, for the expression of T_{SCM} and T_{CM} typical cell surface markers (see Figure 14).

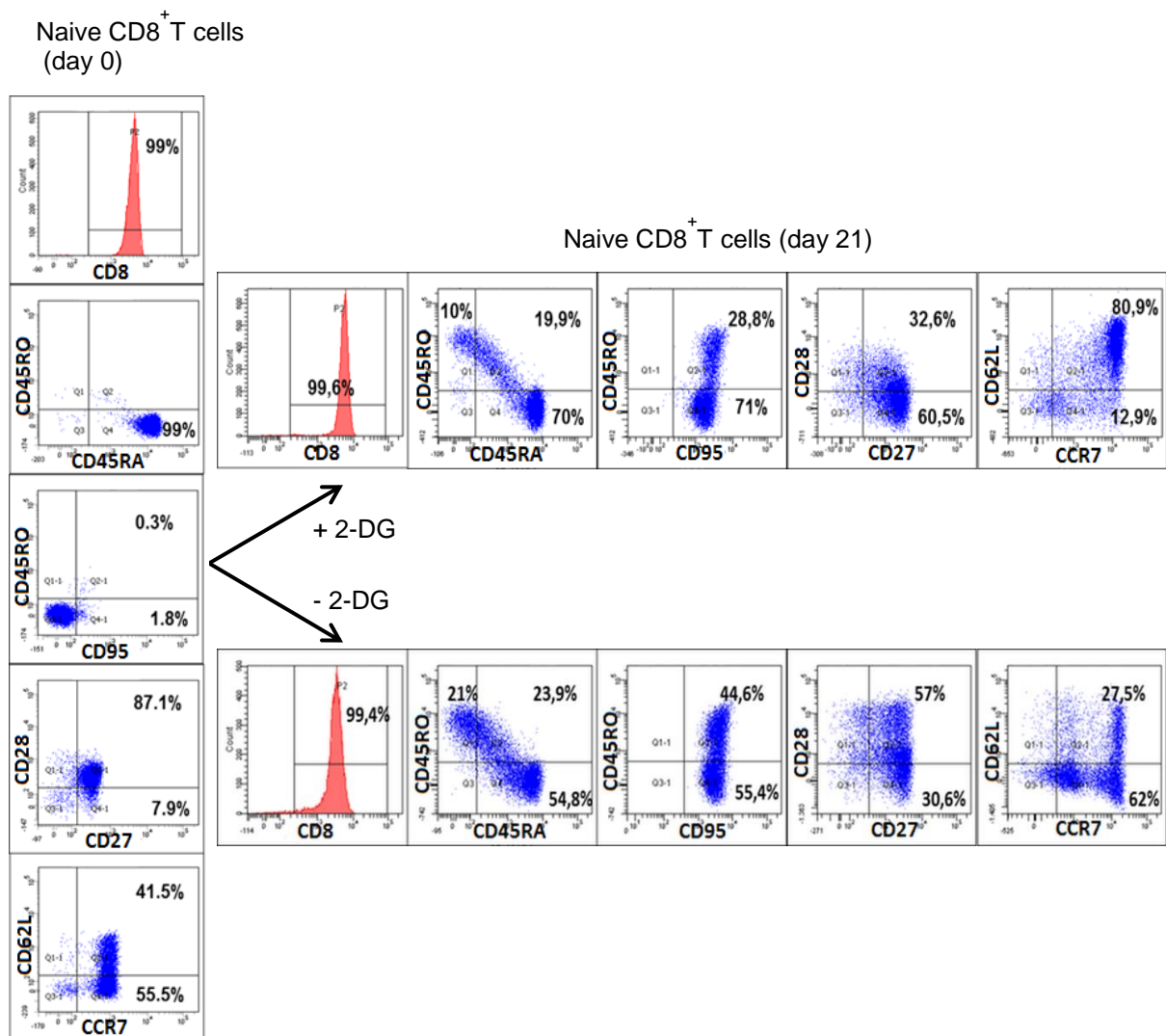
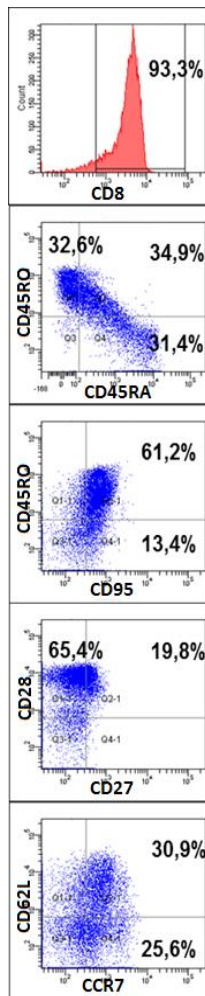


Figure 14: Phenotype of naïve CD8⁺ T cells examined on day of isolation and on day 21 after 2-DG treatment. Shown are representative analyses of naïve CD8⁺ T cells isolated from different donors. T cells were gated in FSC/SSC channel and out of this population CD8⁺T cells were further gated. The expression of CD45RA, CD45RO, CD27, CD28, CCR7 and CD62L on the surface of CD8⁺T cells is illustrated.

The addition of 2-DG could arrest the differentiation process, thus 70% of T cells remained CD45RA positive after three weeks in culture. Additionally, these T cells showed 80.9% expression of homing markers (CCR7 and CD62L) and 71% of CD95 expression. In contrast, T cells which were not treated with 2-DG underwent a differentiation process: 54.8% of T cells were positive for CD45RA and only 27.5% showed expression of homing markers. These results showed that 2-DG can efficiently be used to preserve T cells in an early memory stage and is able to slow down differentiation into terminated effector T cells.

Total CD8⁺T cells
(day 0)



Total CD8⁺T cells (day 21)

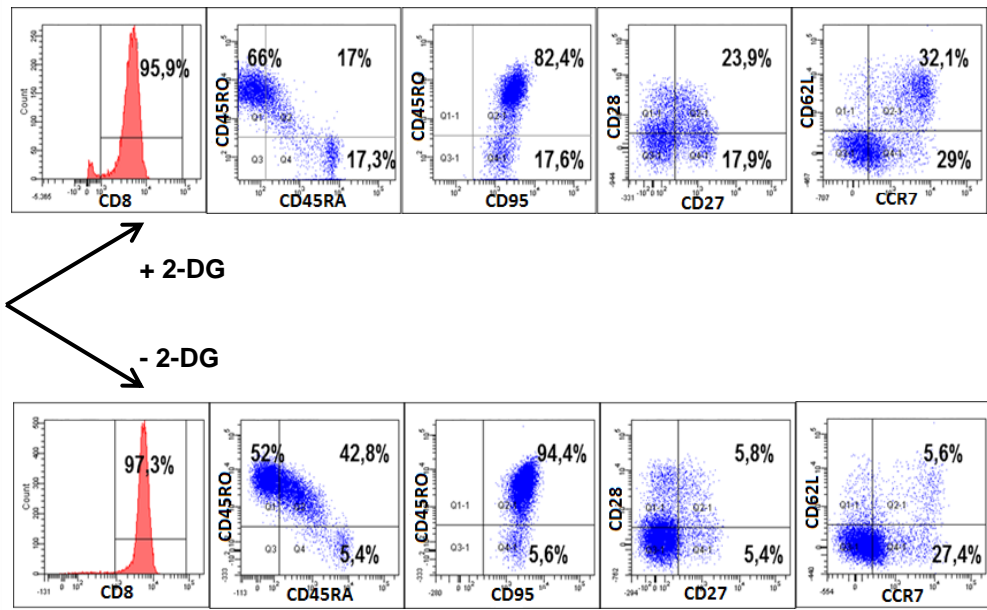


Figure 15: Phenotype of total CD8⁺T cells examined on day of isolation and on day 21 after 2-DG treatment. Shown are representative analyses of total CD8⁺ T cells isolated from different donors. T cells were gated in FSC/SSC channel and out of this population CD8⁺T cells were further gated. The expression of CD45RA, CD45RO, CD27, CD28, CCR7 and CD62L on the surface of CD8⁺T cells is illustrated.

In comparative experiments total CD8⁺ T cells were again cultured in the presence of 2-DG. At day 21 of culture, the T cells upregulated expression of CD45RO and reduced expression of homing markers (CCR7 and CD62L), thus showing an effector T cell-like phenotype. The results exhibited in Figure 15 indicate that 2-DG was not able to equally slow down the differentiation process in mature T cells.

4.3 Phenotype of *in vitro* generated EBV-CTL_{SCM/CM} using TWS119

In the third approach, naïve T cells were treated with TWS119 to activate the Wnt- β -catenin signaling that subsequently prevents differentiation into effector T cells. Therefore, the naïve T cells were isolated, checked for the expression of a naïve-like phenotype and kept in cell culture. At day 21 of culture, T cells were analyzed for the expression of T_{SCM} and T_{CM}-like phenotype. After TWS119 treatment, more than a half of T cells remained CD45RA positive (61.8%), 50.8% were double positive for homing markers (CCR7 and CD62L) and 87% were CD95 positive. In contrast, naïve T cells left untreated showed 45.2% of CD45RA expression and only 8.7% expressed the homing markers CD62L and CCR7 (see Figure 16).

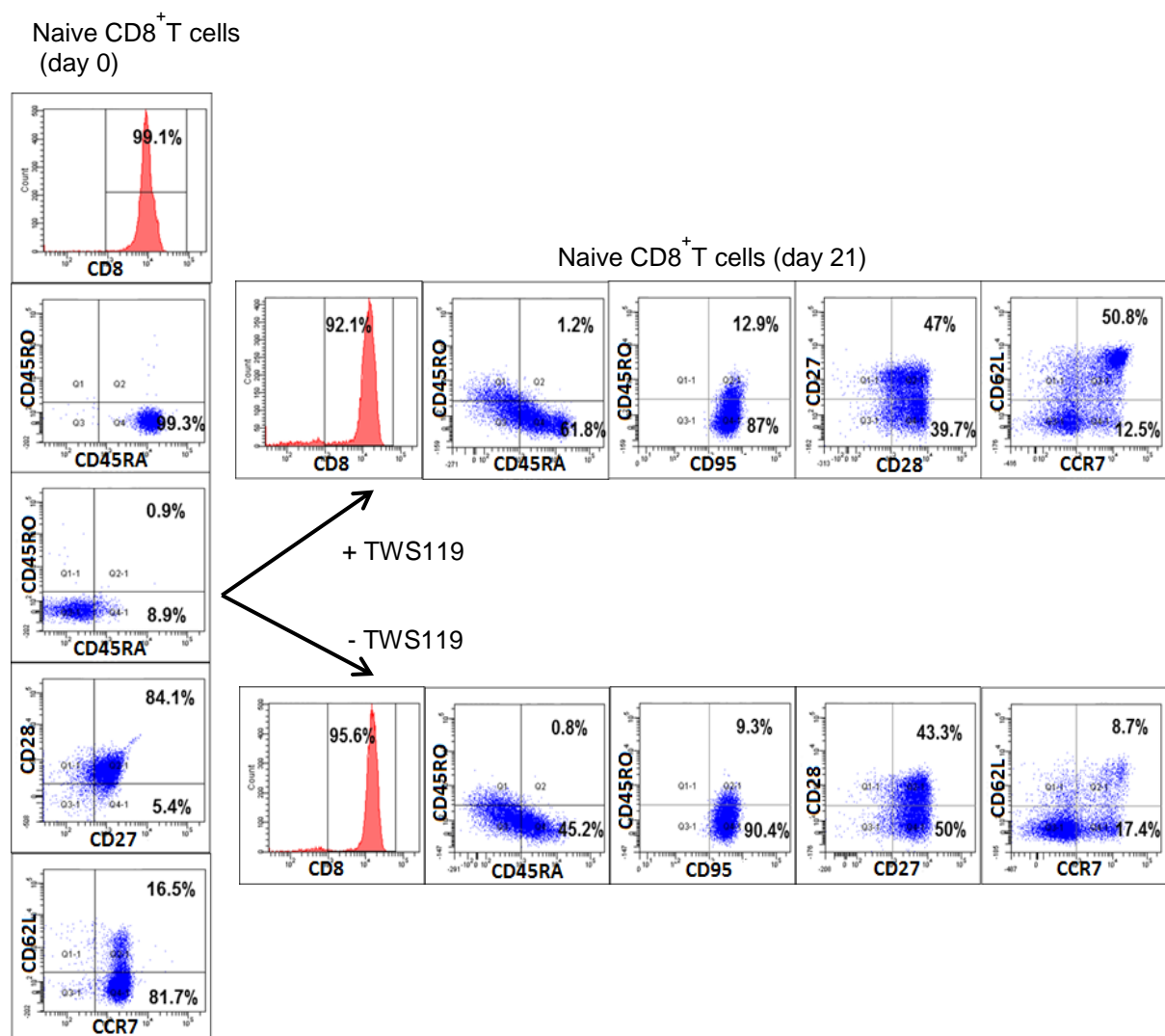


Figure 16: Phenotype of naïve CD8⁺ T cells examined on day of isolation and on day 21 after TWS119 treatment. Shown are representative analyses of naïve CD8⁺ T cells isolated from different donors. T cells were gated in FSC/SSC channel and out of this population CD8⁺ T cells were further gated. The expression of CD45RA, CD45RO, CD27, CD28, CCR7 and CD62L on the surface of CD8⁺ T cells is illustrated.

In comparison, untreated total CD8⁺ T cells upregulated the expression of CD45RO (51.2%) and expression of homing markers CCR7 and CD62L (2.5%), thus showing an effector T cell-like phenotype (see Figure 17).

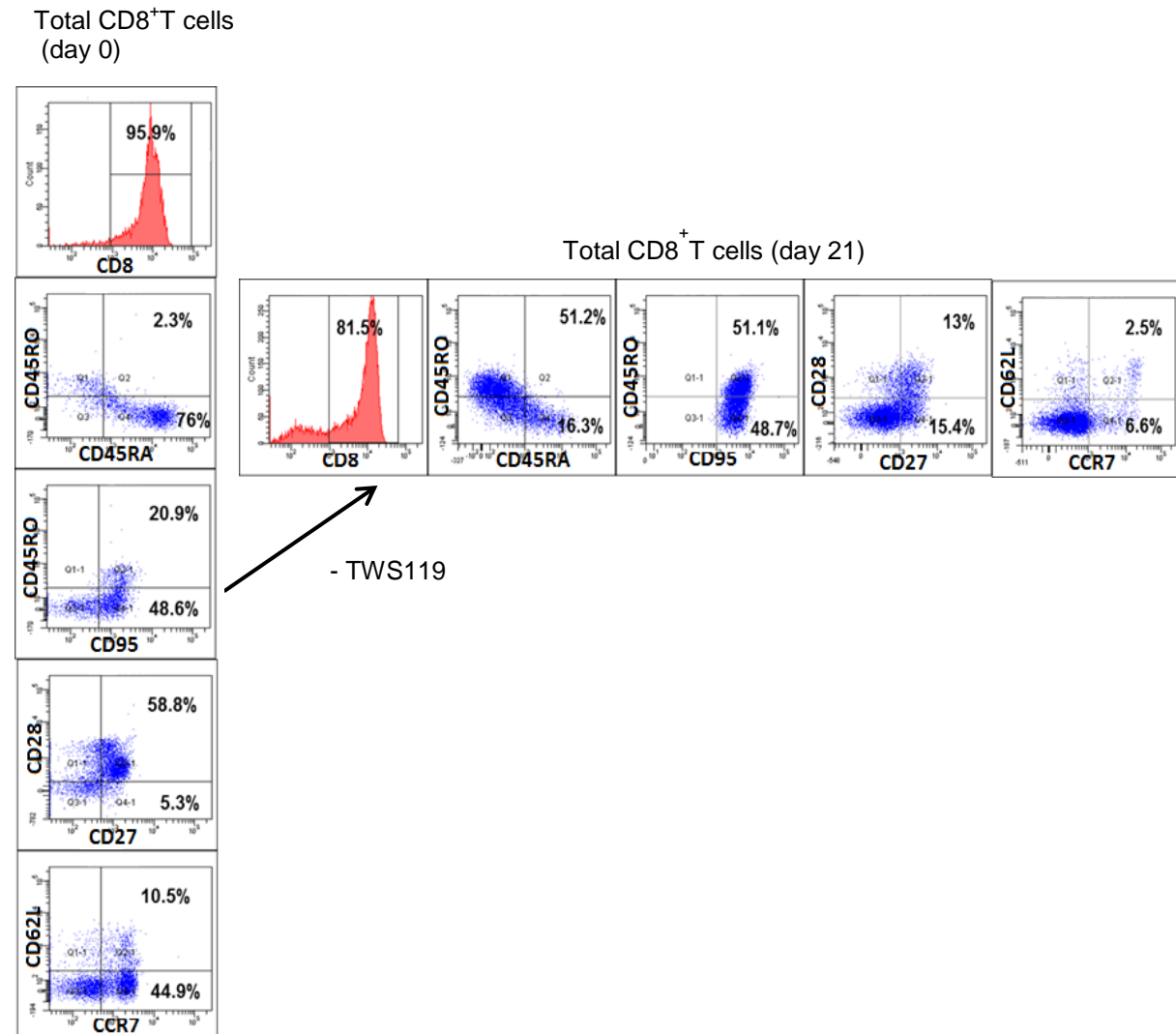


Figure 17: Phenotype of total CD8⁺ T cells examined on day of isolation and on day 21 in the culture. Shown are representative analyses of total CD8⁺ T cells isolated from different donors. T cells were gated in FSC/SSC channel and out of this population CD8⁺T cells were further gated. The expression of CD45RA, CD45RO, CD27, CD28, CCR7 and CD62L on the surface of CD8⁺ T cells is illustrated.

These results indicate that TWS119 could successfully slow down the differentiation process in more than 50% of treated T cells. In comparison, the untreated total CD8⁺ T cell population upregulated expression of CD45RO (51.2%), thus showing an effector T cell-like phenotype (see Figure 17). In all phenotype analyses performed, naïve CD8⁺ T cells treated either with RAPA, 2-DG or TWS119 showed a T_{SCM} and T_{CM}-like phenotype and were identified as CTL_{SCM/CM} cells. Untreated naïve and total CD8⁺ T cells were identified as effector memory and effector T cells.

4.4 Proliferative capacity of EBV-CTL_{SCM/CM}

While naive CD8⁺ T cells treated with RAPA, 2-DG and TWS119 displayed a T_{SCM} and T_{CM}⁻ like phenotype to a comparable degree after 3 weeks, the *in vitro* generated subsets demonstrated very different proliferative capacities. The proliferation rate of EBV-CTL_{SCM/CM} cells was also variable among the different naive CD45RA precursors isolated from donor PBMC. We observed that RAPA treatment dramatically inhibited cell growth in T cells, so that after 21 days of culture it was only possible to generate about 2x10⁶ EBV-CTL_{SCM/CM} cells/96-well plate starting with 1x10⁶ naive CD8⁺ T cells /96-well plate (see Figure 18).

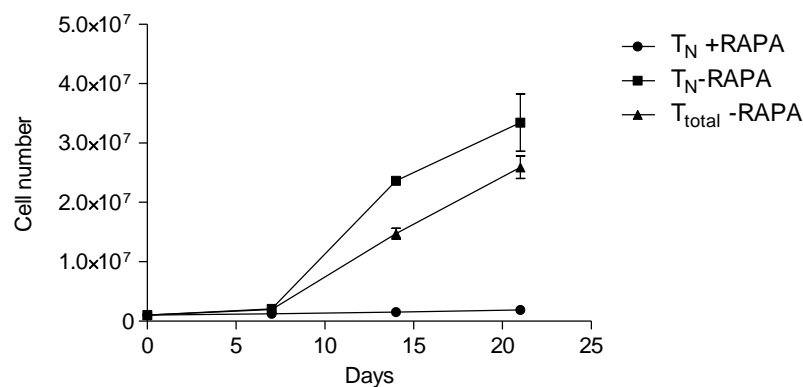


Figure 18: *In vitro* proliferation of EBV-CTL_{SCM/CM} cells after RAPA treatment. Proliferation of rapamycin treated EBV-CTL_{SCM/CM} cells in response to weekly stimulation with autologous EBV preloaded PBMC was measured after 3 weeks culture. Mean values of two donors are shown.

In response to weekly stimulation with irradiated autologous EBV preloaded PBMC, a good proliferation of 2-DG treated EBV-CTL_{SCM/CM} cells was observed as shown for two representative donors in Figure 19, where expansion from 1x10⁶ naive CD8⁺ T cells to 5-6x10⁶ EBV-CTL_{SCM/CM} cells occurred over 3 weeks.

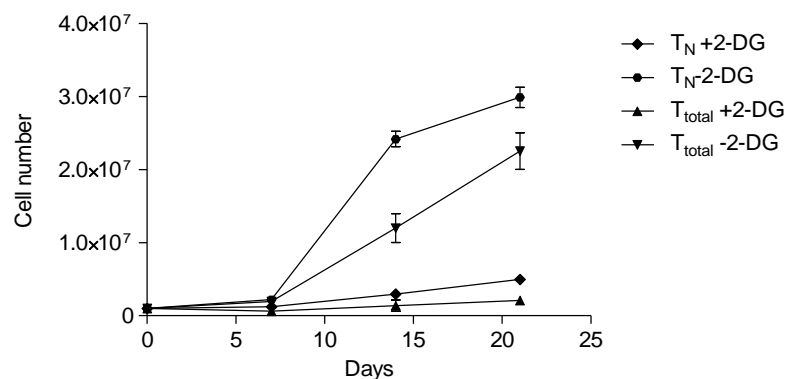


Figure 19: *In vitro* proliferation of EBV-CTL_{SCM/CM} cells after 2-DG treatment. Proliferation of 2-DG treated EBV-CTL_{SCM/CM} cells in response to weekly stimulation with autologous EBV preloaded PBMC was measured after 3 weeks culture. Mean values of two donors are shown.

2-DG treatment slightly inhibited the proliferation of T cells; however, sufficient cell number to perform functional assays could be generated following 3 weeks culture.

The proliferation capacity of EBV-CTL_{SCM/CM} cells treated with TWS119 was at least affected. Starting initially with 1×10^6 naive CD8⁺ T cells it was possible to yield about $10\text{-}15 \times 10^6$ CD8⁺CD45RA⁺CCR7⁺CD62L⁺ T cells within 3 weeks of culture (see Figure 20).

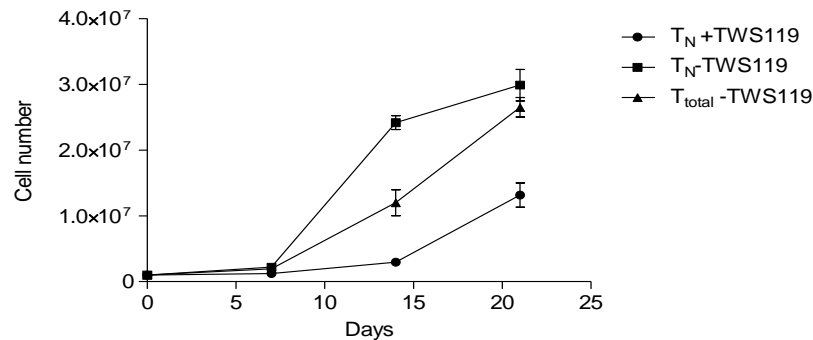


Figure 20: *In vitro* proliferation of EBV-CTL_{SCM/CM} cells after TWS119 treatment. Proliferation of TWS119 treated EBV-CTL_{SCM/CM} cells in response to weekly stimulation with autologous EBV preloaded PBMC was measured after 3 weeks culture. Mean values of two donors are shown.

4.5 Phenotypic characterization of *in vitro* generated B-LCL

Lymphomas similar to early PTLD can be established by engrafting NSG-mice with EBV-immortalized B lymphoblastoid cell lines (B-LCL). As we intended to use these mice as a xenograft model to study *in vivo* EBV reactivity of *in vitro* generated EBV-CTL_{SCM/CM} cells, we first analyzed the expression pattern of EBV proteins in EBV-infected B cells both *in vitro* and *in vivo*.

Moreover, to allow accurate planning of subsequent experiments, reliable and consistent engraftment of lymphomas at a defined time point is desirable. Therefore, B-LCL from three different donors were generated *in vitro* (see 3.2.6) and examined for their ability to produce lymphomas in NSG-mice. Mice were sacrificed between 24-27 days after initial intravenous B-LCL transfer and showed consistent tumor growth in kidney, spleen and bone marrow. Ex vivo isolated B-LCL clearly expressed the latent proteins EBNA2, LMP1 and LMP2, which indicate that the viral growth transcription program (Latency III) was active (see Figure 21).

Moreover, as it has been reported that EBV infected B cells can switch from latent to lytic cycle at some point (Thorley-Lawson 2001), expression of BZLF-1 known to be the most abundant lytic protein, was analyzed (see Figure 21).

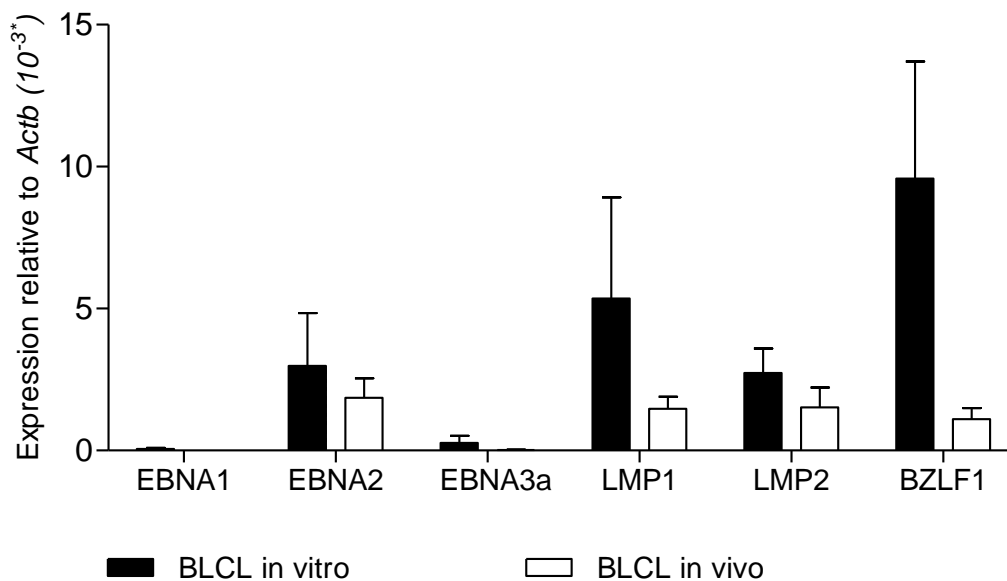


Figure 21: Expression pattern of EBV encoded proteins in B-LCL. The expression of EBV latent and lytic genes in B-LCL was analyzed using qRT-PCR. *In vitro* generated B-LCL were analyzed after 4 weeks culture. Four weeks old B-LCL were injected in mice, isolated after 25 days and analyzed (B-LCL *in vivo*). Mean values of three donors are shown. *Because the reference gene showed very high threshold cycle and the genes of interest showed a much lower threshold cycle the data were presented $\times 10^{-3}$.

Expression of the analyzed EBV proteins appeared to be higher *in vitro* than *in vivo*. Based on these results, LMP2 and BZLF-1 peptide pools were used to stimulate CD8⁺ T cells weekly to generate EBV-specific CTL_{SCM/CM} cells.

4.6 *In vitro* EBV reactivity of EBV-CTL_{SCM/CM} cells

Memory T cells can be also distinguished by their ability to rapidly acquire effector functions upon antigen exposure. Thus, to examine the EBV-specificity *in vitro* generated CTL_{SCM/CM} cells were either cultured with autologous B-LCL or with EBV-preloaded PBMC for 24 hours and subsequently tested for their IFN- γ production by ELISpot-assay. The results, presented in Figure 22 illustrate that EBV reactivity of rapamycin treated naive CD8⁺ T cells was diminished when compared to the naive and total untreated CD8⁺ T cells. Thus, rapamycin treatment has a negative impact on the antigen reactivity of *in vitro* generated CTL_{SCM/CM} cells.

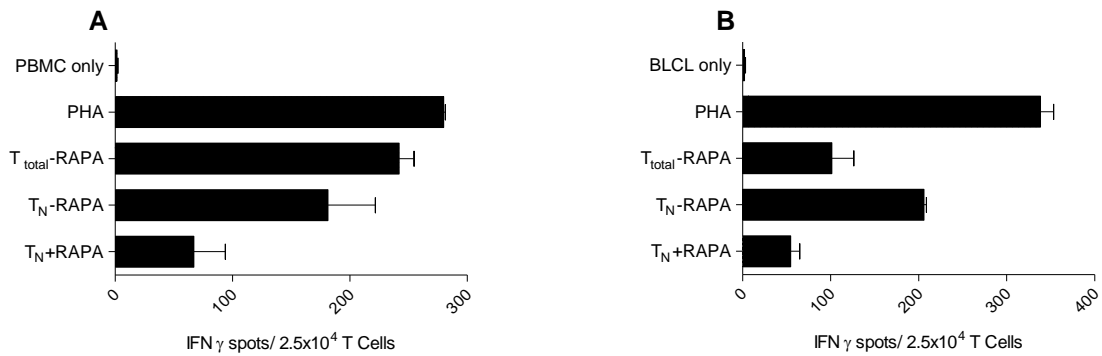


Figure 22: IFN- γ secretion from rapamycin treated CTL_{SCM/CM} cells. **A.** IFN- γ secretion was measured in an ELISpot assay using 2.5×10^4 T cells / well and 2.5×10^4 EBV-preloaded PBMC / well. **B.** IFN- γ secretion was measured in an ELISpot assay using 2.5×10^4 T cells / well and 1×10^4 B-LCL / well. One representative donor of three is shown.

Since we had also observed a very weak proliferative capacity of rapamycin treated T cells, T_{SCM} and T_{CM} cells obtained by this approach could not be expanded to sufficient cell numbers and characterized in detail (see Figure 19). We therefore decided not to further follow up the *in vitro* generation of T_{SCM} and T_{CM} cells by rapamycin.

In contrast, 2-DG and TWS119 treatment did not impair EBV reactivity of T cells. Thus, 2-DG treated T cells elicited comparable EBV reactivity *in vitro*, when compared to untreated naive and total T cells, which exhibited mostly an effector phenotype (see Figure 23A). In fact, the *in vitro* EBV reactivity of TWS119 treated T cells was even slightly higher as compared to T cells with an effector-like phenotype (naive and total T cells untreated with TWS119, see Figure 23B).

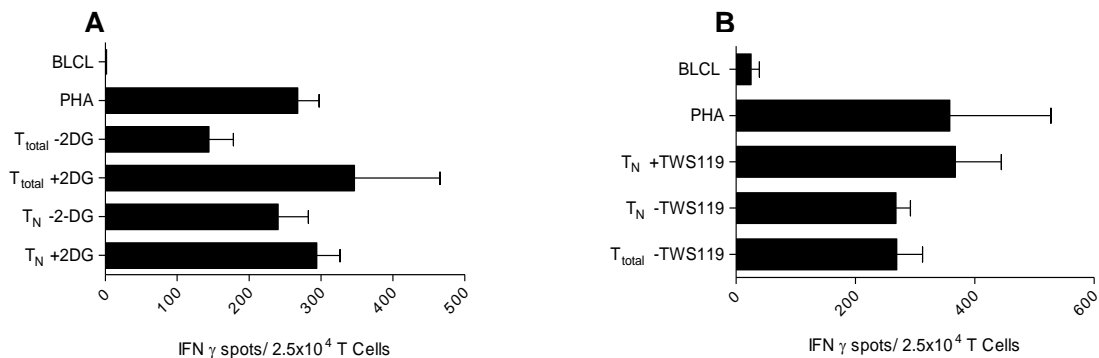


Figure 23: IFN- γ secretion from 2-DG and TWS119 treated CTL_{SCM/CM} cells. **A.** IFN- γ secretion was measured in an ELISpot assay using 2.5×10^4 2-DG treated T cells / well and 1×10^4 B-LCL / well. **B.** IFN- γ secretion was measured in an ELISpot assay using 2.5×10^4 TWS119 treated T cells / well and 1×10^4 B-LCL / well. One representative donor of three is shown.

The results presented in Figure 23 indicate that neither 2-DG nor TWS119 impaired the *in vitro* EBV reactivity of CTL_{SCM/CM} cells determined by IFN- γ secretion. In addition, to also confirm the cytolytic reactivity of EBV-specific CTL_{SCM/CM} cells *in vitro* we performed chromium-51 release cytotoxic assays using autologous B-LCL as target cells following 2-DG (see Figure 24) and TWS119 (see Figure 25) treatment.

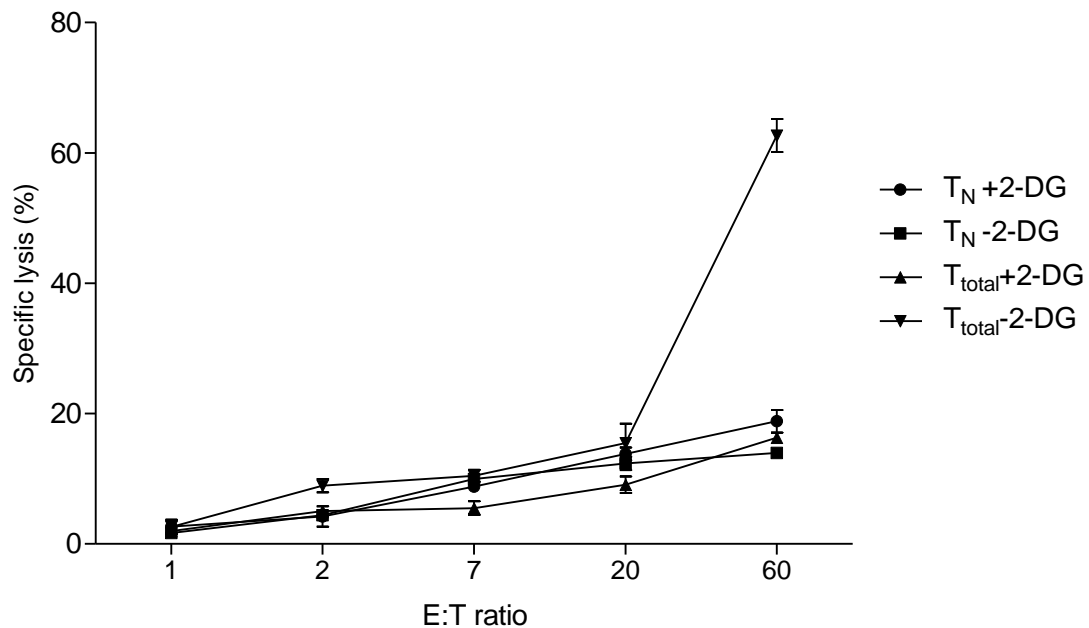


Figure 24: Lytic activity of 2-DG treated CTL_{SCM/CM} cells. Weekly restimulated EBV-specific CTL_{SCM/CM} cells were analyzed regarding their lytic capacity in 4h chromium-51 release assay. Cytotoxicity was tested towards *in vitro* generated autologous B-LCL. Effector to target (E:T).

The results of the chromium-51 release assays demonstrated that 2-DG treated EBV-specific CTL_{SCM/CM} cells could only exert 20% lysis of *in vitro* generated autologous B-LCL. In comparison, T cells with an effector-like phenotype (e.g. total T cells without 2-DG treatment) showed superior, i.e. more than 60%. lysis of B-LCL. Interestingly, the other T cells with effector-like phenotype (naive T cells without 2-DG treatment and total T cells with 2-DG treatment) showed ca.15% lysis of B-LCL. These results questioned the use of 2-DG to generate truly cytolytic EBV-specific CTL_{SCM/CM} cells and may rather suggest that 2-DG has a negative impact on exerting cytolytic effector functions.

In contrast, naive T cells treated with TWS119 elicited a stronger cytotoxicity against B-LCL (ca.40% lysis at a 60:1 E:T ratio) as compared to the cytotoxic capacity of naive T cells propagated without TWS119 treatment, which was slightly lower (about 30% at a 6:1 E:T ratio). In addition, total T cells without TWS119 treatment were only capable of inducing about 20% cytolytic reactivity at a 60:1 E:T ratio (see Figure 25).

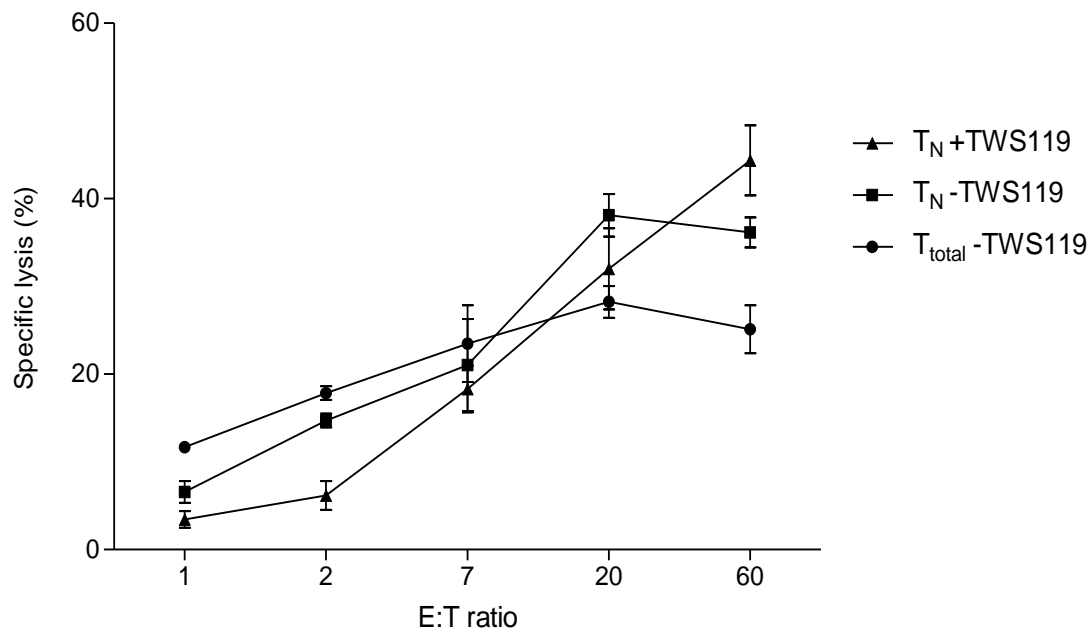


Figure 25: Lytic activity of TWS119 treated CTL_{SCM/CM} cells. Weekly restimulated EBV-specific CTL_{SCM/CM} cells were analyzed regarding their lytic capacity in 4h chromium-51 release assay. Cytotoxicity was tested towards *in vitro* generated autologous B-LCL.

These results indicate that TWS119 treatment could not only generate T cells with T_{SCM}⁻ and T_{CM}⁻ like phenotype, but also preserved their EBV reactivity *in vitro*.

4.7 Manipulation of T cell metabolism

2-DG treatment of naive T cells was applied successfully to restrain the differentiation of naive T cells into effector T cells as shown in Figure 14. Hence, we investigated additional possibilities of modulating T cell metabolic pathways in order to generate T_{SCM} and T_{CM} out of naive T cells. It has been shown, that in contrast to T_{EFF}, memory T cells utilize mostly fatty acid oxidation (FAO) instead of glycolysis to produce ATP for a long term survival (van der Windt et al. 2012). Therefore, glucose was withdrawn from the culture medium and replaced by other energy suppliers such as oleic acid (monounsaturated fatty acid, which is very abundant in the body) and galactose to enforce OXPHOS in T cells. Upon weekly stimulation, T cells received 5 μ M of oleic acid (see Figure 26A) or 10 mM galactose (see Figure 26B) instead of glucose to initiate fatty acid oxidation and subsequently to induce oxidative phosphorylation.

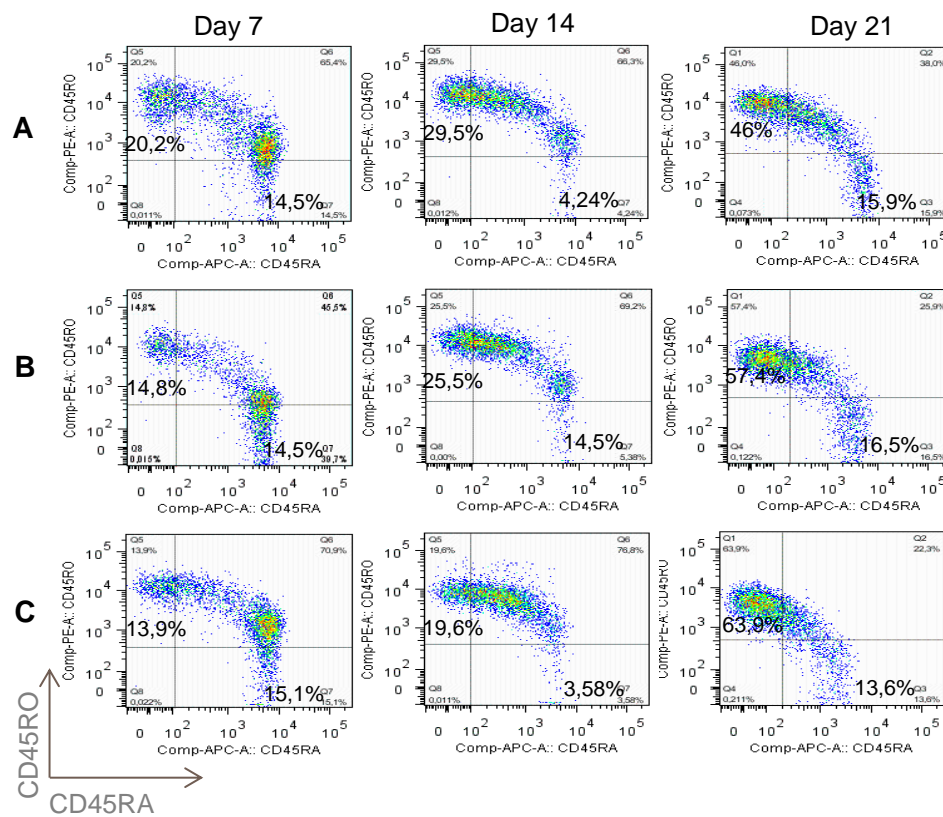


Figure 26: Manipulation of naïve CD8⁺ T cell metabolism. **A.** Naïve T cells cultured in the presence of 5 μ M oleic acid. **B.** Naïve T cells were treated with 10 mM galactose. **C.** Naïve T cells were cultured with 25 mM glucose to accelerate the differentiation process in T cells (positive control).

However, the addition of oleic acid and galactose did not prevent cells from undergoing differentiation process, thus T cells upregulated CD45RO indicating differentiation into effector T cell subset. As expected, the fraction of naïve T cells cultured in high glucose medium (25 mM) upregulated CD45RO and thus showed effector T cell phenotype (see Figure 26C).

Thus, the data illustrated in Figure 26 indicate that the majority of naïve CD8⁺ T cells, treated with oleic acid differentiated mostly into T_{EM/EFF} within 3 weeks presumably due to their incapability to incorporate fatty acids from the external environment. Since it has been described that memory T cells are incapable of incorporating fatty acids from the external environment as a result of decreased surface expression of fatty acid translocase (CD36) (van der Windt et al. 2012) we compared CD36 expression levels of T_N with T_{EFF} cells. As also in our experiments naïve T cells displayed a diminished level of CD36 expression compared with T_{EFF} cells (see Figure 27).

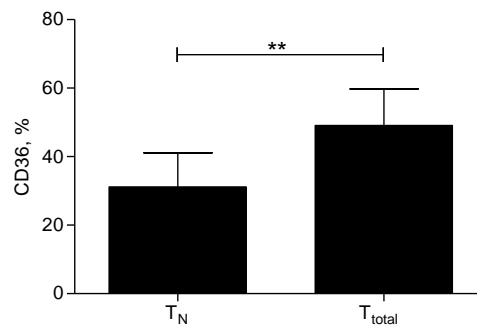


Figure 27: CD36 expression in naïve and total CD8⁺ T cell populations. Naïve and total CD8⁺ T cells were freshly isolated and dyed for the expression of CD36. Data are mean \pm SD of 3 measurements, $p < 0.05$ (2-tailed, paired Student's t test).

Treatment of total CD8⁺ T cell population with oleic acid and galactose as shown in Figure 28A and 28B, did not have any impact on the differentiation process of T cells. In 3 weeks T cells showed an upregulated CD45RO expression comparable with T cells that had been cultured in high glucose medium (see Figure 28C).

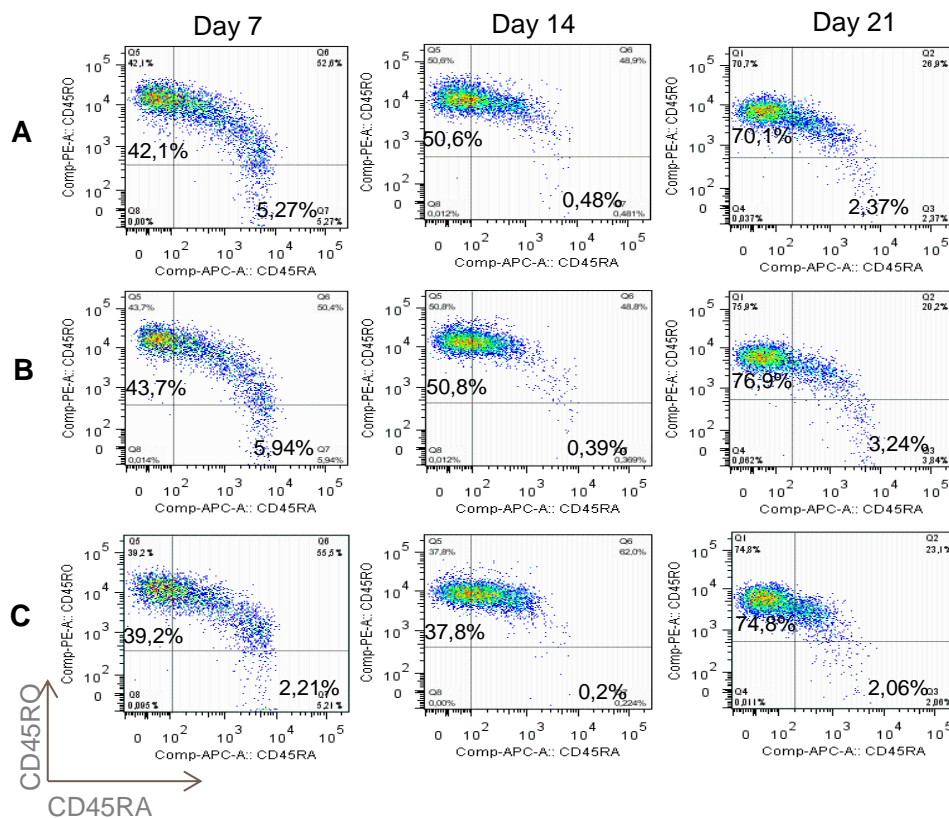


Figure 28: Manipulation of total CD8⁺ T cell metabolism. **A.** Total CD8⁺ T cells cultured in the presence of 5 μ M oleic acid. **B.** Total CD8⁺ T cells treated with 10 mM galactose. **C.** Total CD8⁺ T cells were cultured with 25 mM glucose to accelerate the differentiation process in T cells (positive control).

4.8 Metabolic features of EBV-CTL_{SCM/CM} cells cultured with 2-DG and TWS119

In order to extend the analyses on metabolic characteristics of *in vitro* generated EBV-specific CTL_{SCM/CM}, we measured their glucose uptake as well as oxidative consumption and extracellular acidification. T_{SCM} and T_{CM} have been found to consume less glucose, as they have a quiescent metabolism and utilize mostly fatty acid oxidation (FAO) to fuel OXPHOS. Thus reduced glucose and lactate production might indicate the generation of T_{SCM} and T_{CM}, whereas the cells with effector phenotype should show enhanced glucose consumption and lactate production.

In line with the previous findings reported 2-DG treated naïve CD8⁺ T cells showed reduced glucose uptake (see Figure 29A) and concomitantly produced less lactate (see Figure 30A) when compared to naïve and total CD8⁺ T cells which were not treated with 2-DG as well as total CD8⁺ T cells, cultured with 2-DG.

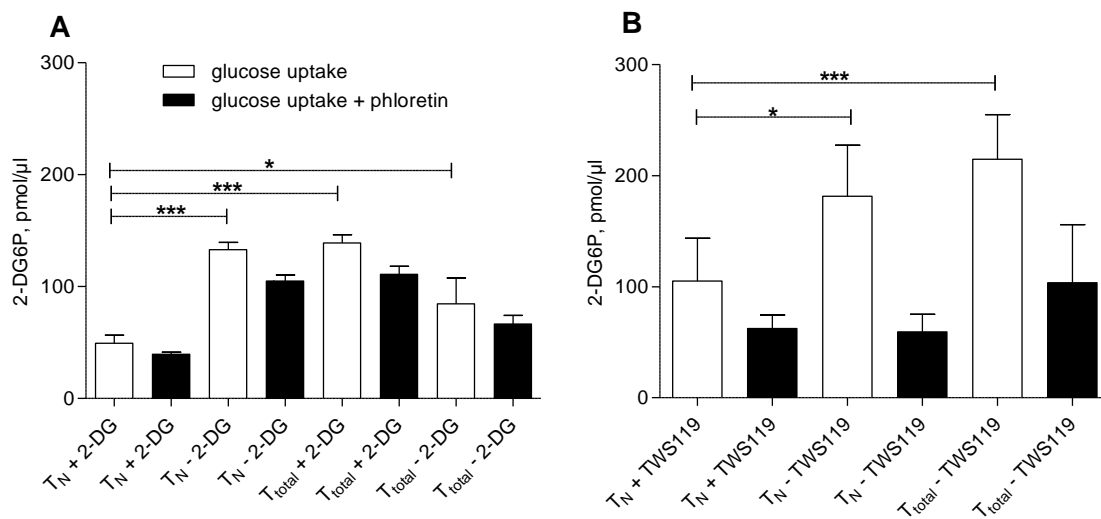


Figure 29: Glucose uptake measured in 2-DG and TWS119 treated T cells. A. Glucose uptake of 2-DG treated naïve and total CD8⁺ T cells. **B.** Glucose uptake of TWS119 treated naïve and total CD8⁺ T cells. Phloretin, an inhibitor of GLUT1 and GLUT2, was used as positive control. Data are mean ± SD of three measurements.

Moreover, TWS119 treated naïve CD8⁺ T cells also showed reduced glucose consumption (see Figure 29B) and lactate production (see Figure 30B), when compared to naïve and total CD8⁺ T cells following culture in the absence of TWS119.

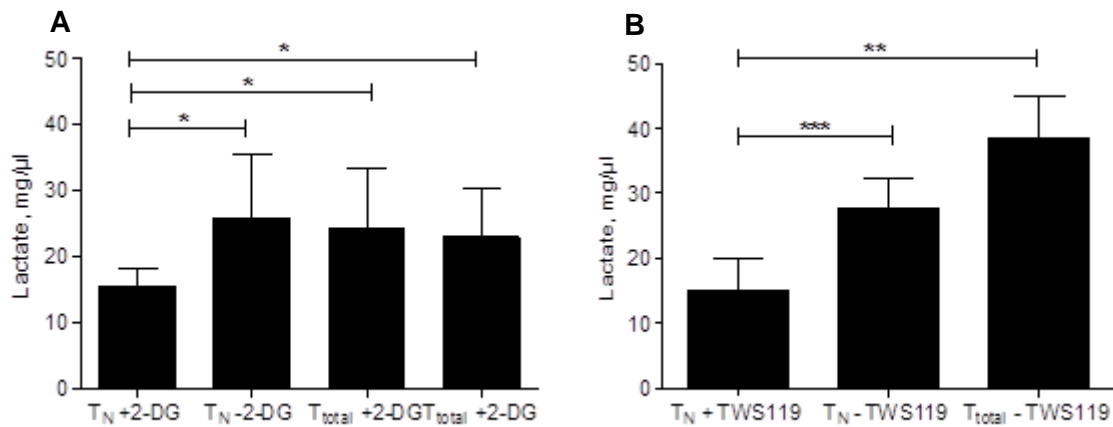


Figure 30: Lactate production measured in 2-DG and TWS119 treated T cells. A. Lactate production of 2-DG treated naive and total CD8⁺ T cells. **B.** Lactate production of TWS119 treated naive and total CD8⁺ T cells. Data are mean \pm SD of three measurements.

Moreover, as metabolically quiescent T_{SCM} and T_{CM} mainly use OXPHOS to produce ATP, mitochondrial respiration and aerobic glycolysis was determined under basal conditions and after pharmacological inhibition of mitochondrial respiration with oligomycin (ATP synthase blocker), DNP (mitochondrial uncoupler) and rotenone (complex I inhibitor). Oxygen consumption rate (OCR), an indicator of OXPHOS was similar between 2-DG treated CTL_{SCM/CM} cells and T effector cells (see Figure 31A and B) under basal conditions and after pharmacological inhibition. The extracellular acidification rate (ECAR), a marker of aerobic glycolysis was higher in T effector cells when compared with 2-DG treated CTL_{SCM/CM} under basal conditions and after perturbation of mitochondrial respiration with oligomycin, DNP and rotenone (see Figure 31C and D).

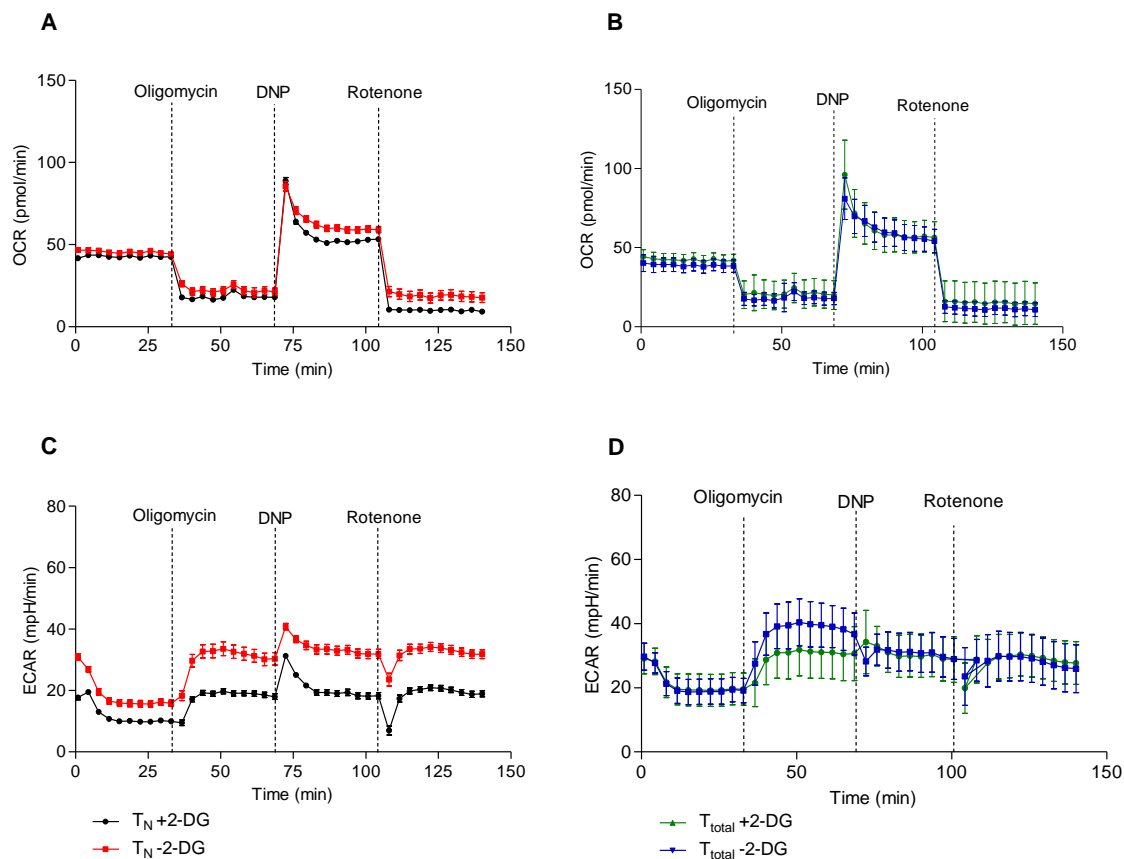


Figure 31: OCR and ECAR measured in 2-DG treated T cells. **A.** O₂ consumption rates (OCR) were measured in 2-DG treated and untreated naive CD8⁺ T cells under basal conditions and in response to indicated mitochondrial inhibitors (oligomycin, DNP and rotenone). **B.** OCR rates were measured in 2-DG treated and untreated total CD8⁺ T cells under basal conditions and in response to indicated mitochondrial inhibitors. **C.** ECAR rates were measured in 2-DG treated and untreated naive CD8⁺ T cells under basal conditions and in response to indicated mitochondrial inhibitors. **D.** ECAR rates were measured in 2-DG treated and untreated total CD8⁺ T cells under basal conditions and in response to indicated mitochondrial inhibitors. Data are representative of two independent experiments.

Mitochondrial respiration was also analyzed in TWS119 treated T cells to verify that TWS119 CTL_{SCM/CM} utilize mainly OXPHOS to generate ATP. Oxygen consumption rate (OCR), an indicator of OXPHOS was slightly higher in T effector cells as compared to TWS119 treated naive CD8⁺ T cells (see Figure 32A and B) under basal conditions and after pharmacological inhibition.

The extracellular acidification rate was higher in T effector cells when compared to TWS119 treated CTL_{SCM/CM} under basal conditions and after perturbation of mitochondrial respiration (see Figure 32C and D).

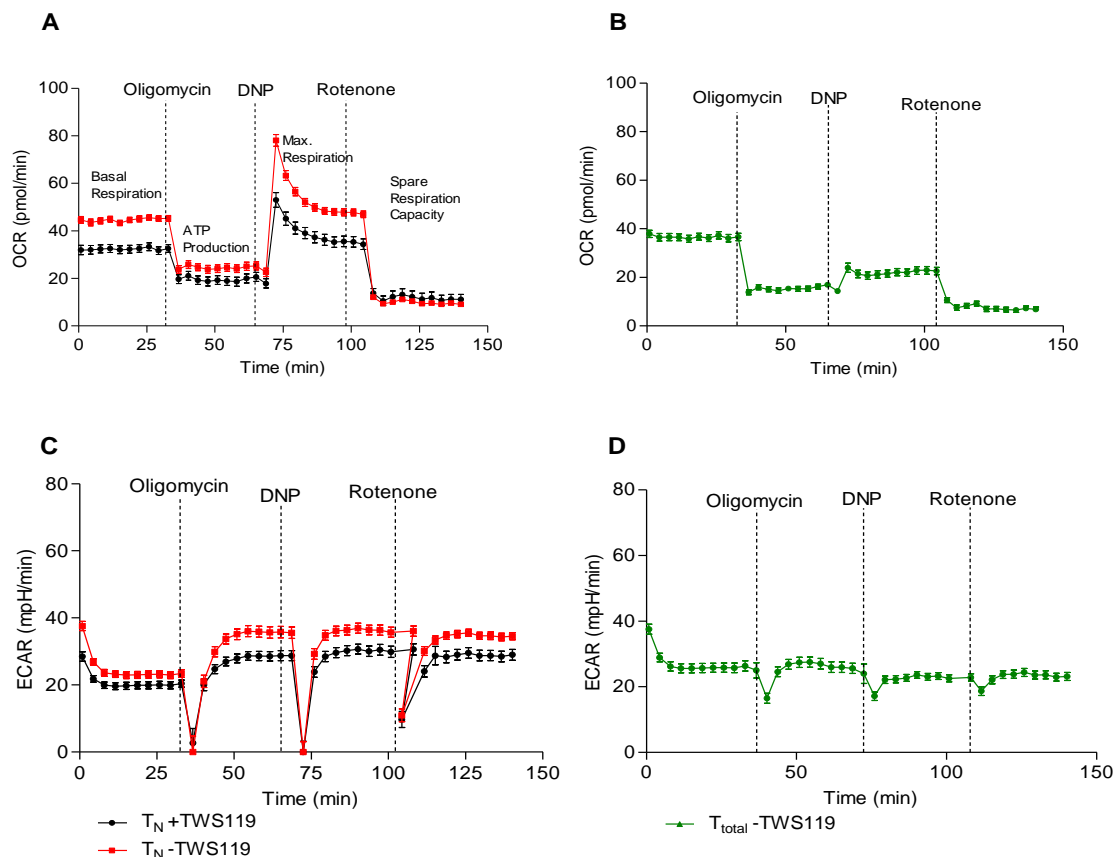


Figure 32: OCR and ECAR measured in TWS119 treated T cells. **A.** O_2 consumption rates (OCR) were measured in TWS119 treated and untreated naive $CD8^+$ T cells under basal conditions and in response to indicated mitochondrial inhibitors (oligomycin, DNP and rotenone). **B.** OCR rates were measured in TWS119 untreated total $CD8^+$ T cells under basal conditions and in response to indicated mitochondrial inhibitors. **C.** ECAR rates were measured in TWS119 treated and untreated naive $CD8^+$ T cells under basal conditions and in response to indicated mitochondrial inhibitors. **D.** ECAR rates were measured in TWS119 untreated total $CD8^+$ T cells under basal conditions and in response to indicated mitochondrial inhibitors. Data are representative of two independent experiments.

These data indicated that activation and effector differentiation of $CD8^+$ T cells was associated with dramatic increases in glycolysis and lactate production.

Therefore, taken together, these results suggest that $CTL_{SCM/CM}$ cells generated under the impact of 2-DG and TWS119 utilize mostly OXPHOS, whereas T effector cells use both OXPHOS and aerobic glycolysis.

4.9 Expression of Lef-1 and Tcf-7 in 2-DG/TWS119 treated EBV- $CTL_{SCM/CM}$

As reported earlier the Wnt- β -catenin signaling transducers transcription factor 7 (Tcf-7), lymphoid enhancer factor 1 (Lef-1), and B cell CLL/lymphoma 6 (Bcl-6) promote memory $CD8^+$ T cell formation (Gattinoni et al. 2009); (Ichii et al. 2002); (Zhou et al. 2010). To verify this finding in our T cell subsets, T cells treated with 2-DG and TWS119 were analyzed with qRT-PCR for the expression of Lef-1, Tcf-7 and Bcl-6.

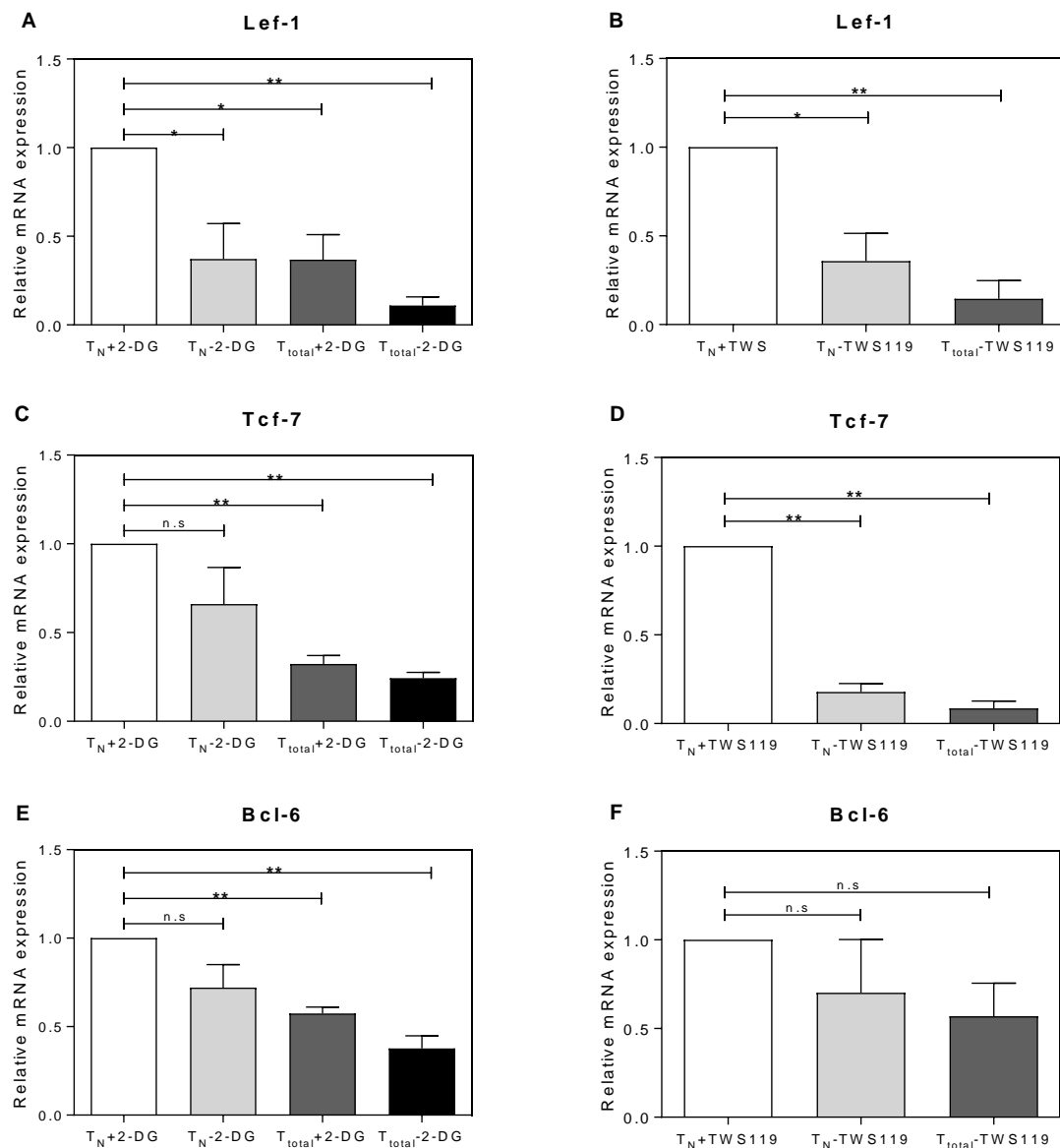


Figure 33: Lef-1, Tcf-7 and Bcl-6 expression in 2-DG and TWS119 treated T cells. Quantitative RT-PCR analysis of the expression of Wnt- β -catenin signaling transcription factors (Lef-1 and Tcf-7) and B cell CLL/lymphoma 6. Inhibition of glycolysis and activation of Wnt- β -catenin signaling triggers the expression of Lef-1, Tcf-7 and Bcl-6. **A.** Expression of Lef-1 in 2-DG treated T cells. **B.** Expression of Lef-1 in TWS119 treated T cells. **C.** Expression of Tcf-7 in 2-DG treated T cells. **D.** Expression of Tcf-7 in TWS119 treated T cells. **E.** Expression of Bcl-6 in 2-DG treated T cells. **F.** Expression of Bcl-6 in TWS119 treated T cells. Results are presented relative to Actb. Data are mean \pm SD of 3 measurements, $p < 0.05$ (1-tailed, paired Student's t-test).

The results presented in Figure 33 demonstrate that TWS119 treatment induced the expression of Wnt- β -catenin signaling transducers and B cell CLL/lymphoma 6 in naive CD8⁺ T cells. Moreover, a direct inhibition of glycolysis using 2-DG was also associated with enhanced expression of the transcription factors (Tcf-7 and Lef-1) and B cell CLL/lymphoma 6, which regulate memory versus effector differentiation in CD8⁺ T cells. These data support

the previously found link between metabolism and transcriptional regulation of cell fate determination.

4.10 *In vitro* transmigration capacity of 2-DG/TWS119 treated EBV-CTL_{SCM/CM}

As CCR7 and CD62L are essential for lymphocyte migration to lymph nodes (Butcher & Picker 1996), the co-expression of these receptors distinguishes the lymph node homing CTL_{SCM/CM} cells from T_{EM} and effector T cells. Using a transmigration assay CTL_{SCM/CM} cells generated *in vitro* under the impact of 2-DG (see Figure 34A) and TWS119 (see Figure 34B) were analyzed for their ability to migrate in the direction of CCL21 (ligand of CCR7) across a cell permeable membrane.

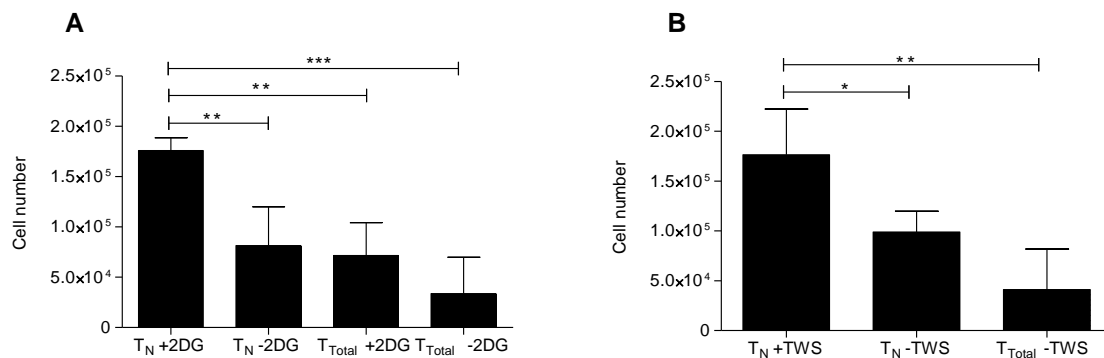


Figure 34: Transmigration potential of 2-DG and TWS119 treated CTL_{SCM/CM} cells *in vitro*. Cells were placed on the upper layer of permeable membrane and RPMI medium containing 1µg/ml CCL21 was placed below the cell permeable membrane. Following 5h incubation, the migrated cells were stained and counted. Data are mean ± SD of 4 measurements, $p < 0.05$ (1-tailed, paired Student's t-test).

Due to the enhanced expression of CCR7, EBV-specific CTL_{SCM/CM} treated with 2-DG and TWS119 displayed a superior transmigration capacity across the cell permeable membrane *in vitro*. About 1.5x10⁵ T_N+2-DG or T_N+TWS119 cells could be detected after 5h chemotaxis in direction to CCL21. In contrast, all T cell populations with a more differentiated phenotype (T_N w/o 2-DG, ca. 7.5x10⁴ cells; T_{Total} plus 2-DG, ca. 6x10⁴ cells; T_{Total} w/o 2-DG ca. 4x10⁴ cells; T_N w/o TWS119, ca. 8x10⁴ cells and T_{Total} w/o TWS119, ca. 4.5x10⁴ cells) showed only poor migration across the membrane. These results indicate that both prolonged reduction of glycolytic activity and sustained activation of Wnt-β-signaling could reprogram T cells to preferentially migrate to lymphoid tissues.

4.11 *In vivo* survival of EBV-CTL_{SCM/CM} cells cultured with 2-DG and TWS119

Having determined the T_{SCM}⁺ and T_{CM}⁺ like phenotype, metabolism characteristics and *in vitro* functional properties, it was finally of pivotal interest to examine whether the EBV-CTL_{SCM/CM} cells were capable of showing at least some degree of homeostatic proliferation and effector functions under *in vivo* conditions.

To first determine the persistence of 2-DG and TWS119 treated CD8⁺ T cells upon adoptive transfer, the cells were (*i.v.*) injected into NOD/SCID/IL2R γ ^{null} (NSG)-mice in the absence of antigen. In addition, human ILR13-Fc (an IL-15-Fc fusion protein with extended half-life produced in our lab) was weekly injected to improve the IL-15 mediated homeostatic cytokine micromilieu for T cells. Peripheral blood from mice drawn weekly after injection of 1x10⁶ 2-DG treated CD8⁺ T cells was analyzed for the expression of CD45/CD3 cells (see Figure 35).

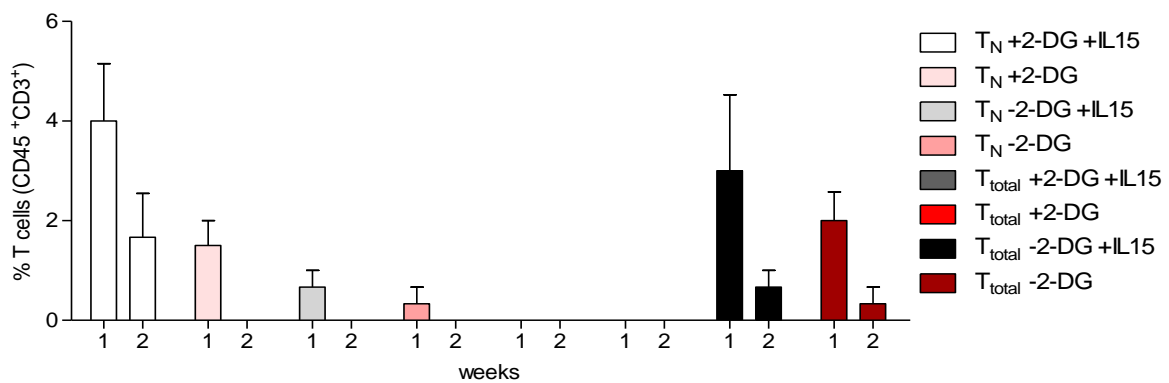


Figure 35: *In vivo* persistence of 2-DG treated EBV-specific CTL_{SCM/CM} cells in NSG-mice. 1x10⁶ T cells were injected (*i.v.*) into NOD/SCID/IL2R γ ^{null} (NSG)-mice and partly supplemented with ILR13-Fc (IL-15 with extended half-life). Peripheral blood was drawn weekly and analyzed for the expression of CD45 and CD3. Data are mean \pm SD. N=3.

After one week 4% of 2-DG treated CTL_{SCM/CM} cells supplemented with IL-15 and 1.8% of CTL_{SCM/CM} cells without IL-15 were detected in the peripheral blood. Moreover, after 2 weeks only 1.8% CTL_{SCM/CM} cells supplemented with IL-15 and 0.4% of CTL_{SCM/CM} cells without IL-15 could be detected. These data indicate that the number of transferred CTL_{SCM/CM} cells treated with 2-DG declined profoundly *in vivo* within two weeks.

Surprisingly, total CD8⁺ effector T cells showed a similar declining pattern as only 2% - 2.5% of non 2-DG treated cells could be detected in peripheral blood after 1 week irrespective of IL-15 supplementation. These frequencies declined further to 0.2 - 0.3% after 2 weeks.

Thus, the data illustrated in Figure 35 clearly showed that 2-DG treated CTL_{SCM/CM} cells could not survive and persist for a long time *in vivo* in the absence of antigen. Despite the short-term persistence of the transferred CTL_{SCM/CM} cells the effect of IL-15 could be confirmed. However, the comparable decline of effector T cells also strongly suggests that highly

immunodeficient NSG mice provide a very limited homeostasis promoting lymphoid infrastructure and cytokine milieu and may not be a valid model to examine the homeostatic features of these T cell subsets.

In addition to the analyses described above peripheral blood, bone marrow and spleen were harvested from mice injected with 5×10^6 TWS119 treated $CD8^+$ T cells after 28 days and checked for the expression of CD45/CD3 cells (see Figure 36).

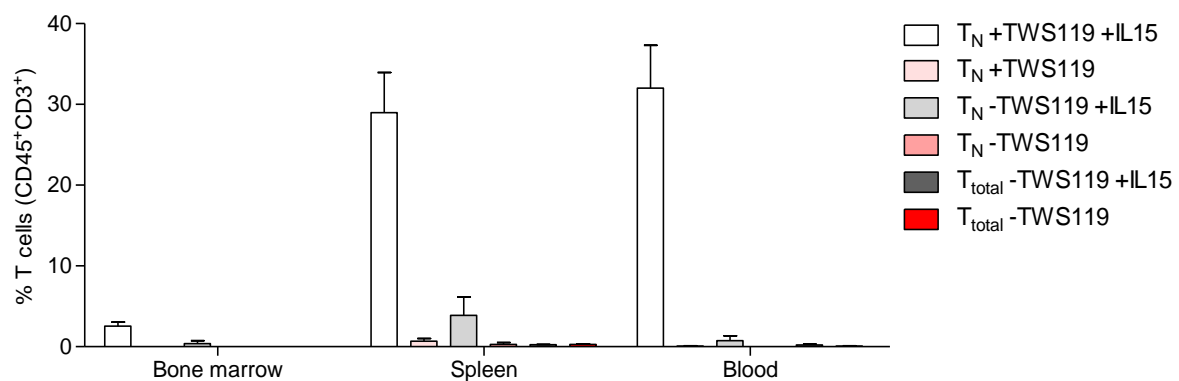


Figure 36: *In vivo* persistence of TWS119 treated EBV-specific CTL_{SCM/CM} in NSG-mice. 5×10^6 T cells were injected (*i.v.*) into NOD/SCID/IL2R γ null (NSG)-mice and partly supplemented with ILR13-Fc (IL-15 with extended half-life). Peripheral blood, spleen and bone marrow were harvested after 28 days and analyzed for the expression of CD45 and CD3. Data are mean \pm SD.

As depicted in Figure 36 and in clear contrast to the results obtained with 2-DG, around 30% of TWS119 treated CTL_{SCM/CM} cells were detected in spleen and blood, whereas less than 0.5% of T cells were found in bone marrow. On the contrary, only 0.3% of effector T cells ($T_N - TWS119 + IL15$) could be identified in spleen, bone marrow and blood. The results displayed in the Figure 36 clearly confirm the positive effect of IL-15 on the long-term survival of TWS119 treated naïve $CD8^+$ T cells. EBV-CTL_{SCM/CM} cells treated with TWS119 showed longer *in vivo* persistence compared to the differentiated T cells and compared to the 2-DG treated EBV-CTL_{SCM/CM} cells.

4.12 *In vivo* EBV reactivity of EBV-CTL_{SCM/CM} cultured with 2-DG

In addition to analyzing persistence we wanted to examine whether *intravenous* (*i.v.*) injection of 2-DG treated EBV-CTL_{SCM/CM} cells resulted in regression of B-LCL tumors *in vivo*. First, the engraftment of 5×10^5 B-LCL/mouse injected into 15 NSG-mice was tested 11 days after injection. Therefore, peripheral blood of two mice was drawn and analyzed for the expression of CD45/CD19/CD20/CD3 surface markers. We detected 2-5% of CD45⁺CD19⁺CD20⁺CD3⁻ cells in the murine blood indicating that B-LCL had successfully engrafted in bone marrow and spleen of recipient mice. Subsequently, each mouse received 1×10^6 T cells supplemented with ILR13-Fc (IL-15 with extended half-life). The control group

did not receive any T cells. Mice were macroscopically inspected daily and sacrificed on day 23-25. Inspection of intact organs revealed macroscopically visible tumor lesions. Of note, the majority of human B-LCL analyzed *ex vivo* had downregulated the expression of CD19 (data not shown). Therefore B-LCL found in the different organs depicted in Figure 37 were quantified by the expression of CD20 as CD3⁻CD45⁺CD20⁺ cells.

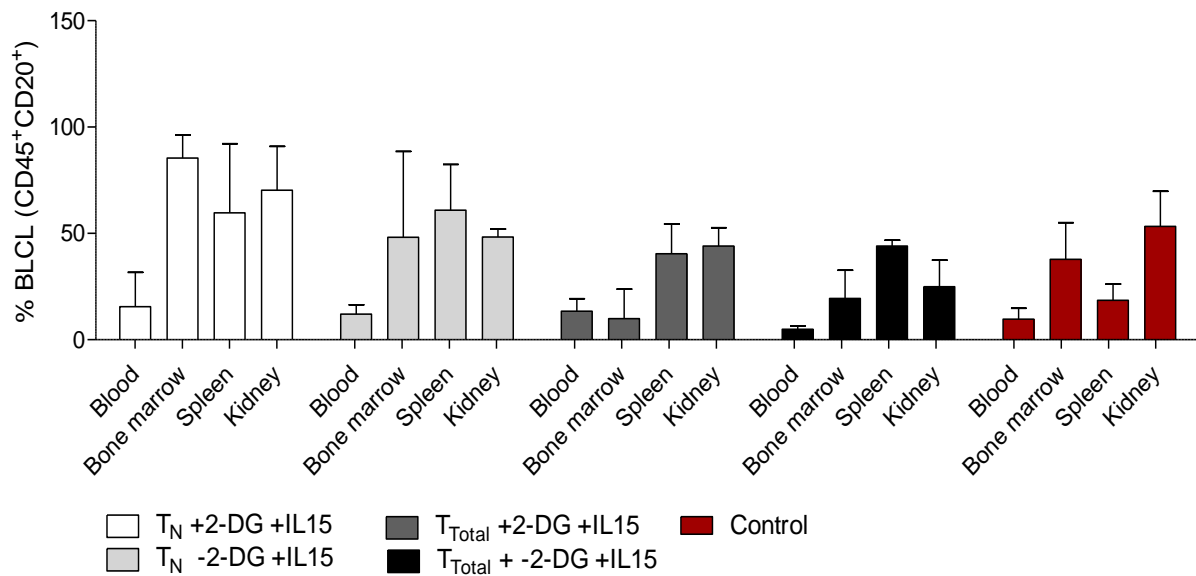


Figure 37: *In vivo* EBV-reactivity of 2-DG treated EBV-CTL_{SCM/CM} cells. 1×10^6 T cells were injected (*i.v.*) into NOD/SCID/IL2Rc^γnull (NSG)-mice and supplemented with ILR13-F_C on day 11 after B-LCL engraftment. After 7 days peripheral blood, spleen, kidney and bone marrow were harvested and analyzed for the expression of CD45/CD3/CD19/CD20. Data are mean \pm SD. N=3

T cells found in the different organs depicted in Figure 38 were quantified by the expression of CD45 and CD3. The analyzed data suggest very poor survival of transferred T cells *in vivo*, even though, the antigen (B-LCL) was present in the system. Interestingly, that most of T cells, indicated by CD45/CD3 expression, were found in mice, who received EBV-CTL_{SCM/CM} cells (T_N-2-DG+IL-15) (see Figure 38).

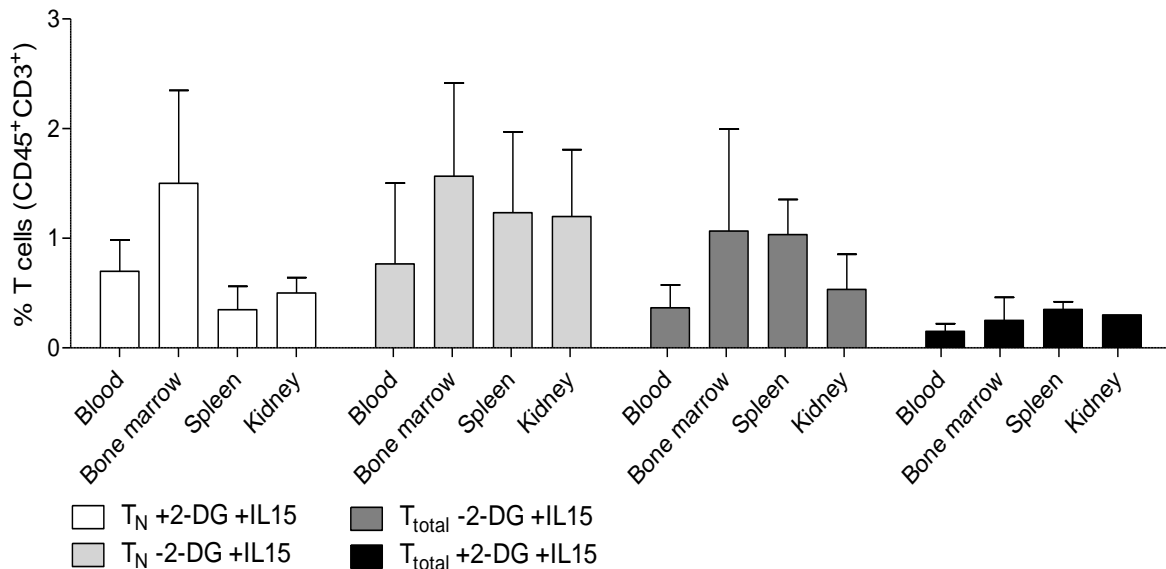


Figure 38: Survival of 2-DG treated EBV-CTL_{SCM/CM} and T_{EFF} cells *in vivo*. 1×10^6 T cells were injected (*i.v.*) into NOD/SCID/IL2Rcnull (NSG)-mice and supplemented with ILR13-F_C (IL-15 with extended half-life) on day 11 of B-LCL engraftment. After 7 days peripheral blood, spleen and bone marrow were harvested and analyzed for the expression of CD45/CD3. Data are mean \pm SD. N=3

Unfortunately, tumor development was equally rapid in control mice and in mice, who received T cells (see Figure 37). Neither 2-deoxy-glucose treated T cells nor ILR13-Fc supplementation could promote T cells to inhibit or at least control tumor regression.

4.13 *In vivo* EBV reactivity of TWS119 treated EBV-CTL_{SCM/CM} cells

Having shown a better long-term survival *in vivo* without antigen as compared to the 2-DG treated EBV-CTL_{SCM/CM} cells (see Figure 36) additional experiments were carried out to examine whether (*i.v.*) injection of TWS119 treated EBV-CTL_{SCM/CM} cells resulted in regression of B-LCL tumors *in vivo*. The engraftment of 5×10^5 B-LCL injected into NSG-mice was verified on day ten. Subsequently, each mice group received 1.5×10^6 EBV-CTL_{SCM/CM} cells derived from T_N plus TWS119, 1.5×10^6 EBV-T_{EFF} cells derived from T_N w/o TWS119 and T_{Total} w/o TWS119, respectively. 1.5×10^6 Melan-A-T_{EFF} cells derived from T_{Total} w/o TWS119 treatment. Mice, who did not receive any T cells or Melan-A specific T cells were analyzed as negative and specificity controls. Control mice lived for ca. 35-38 days whereas the EBV-T_{EFF} cells lived approximately 10 days longer (see Figure 39). All sacrificed control mice contained tumor cells. In contrast, mice treated with TWS119 treated EBV-CTL_{SCM/CM} cells survived up to 80 days. Some sacrificed mice contained residual tumor cells as well, but the clearly extended survival of mice suggests that the *in vitro* TWS119 treatment of naive CD8⁺ T cells significantly augmented their activity towards EBV-peptide antigens, resulting in controlled tumor regression.

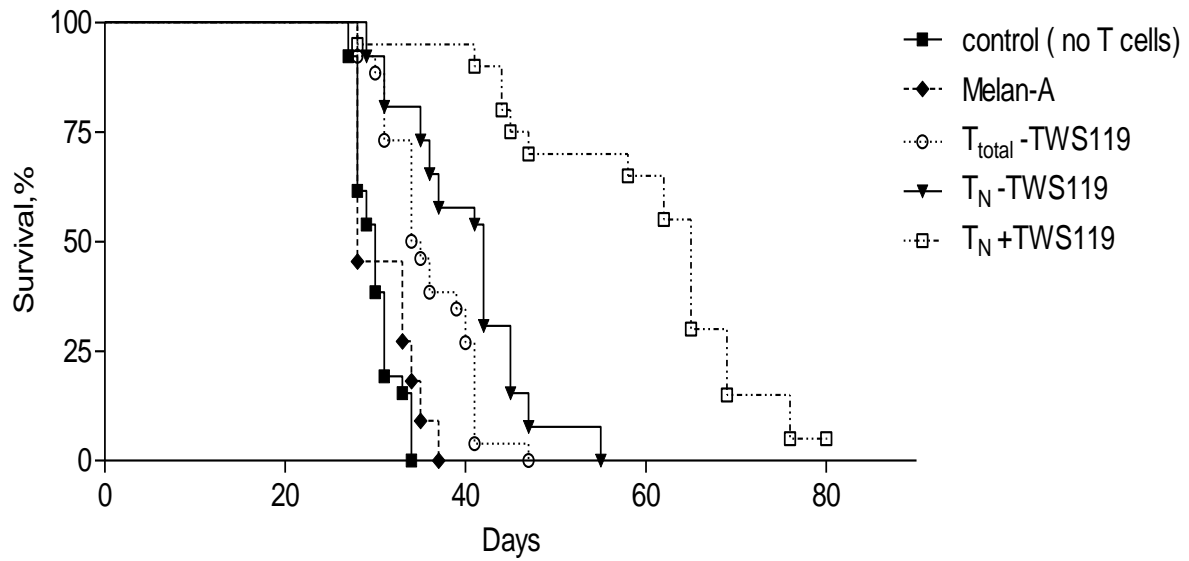
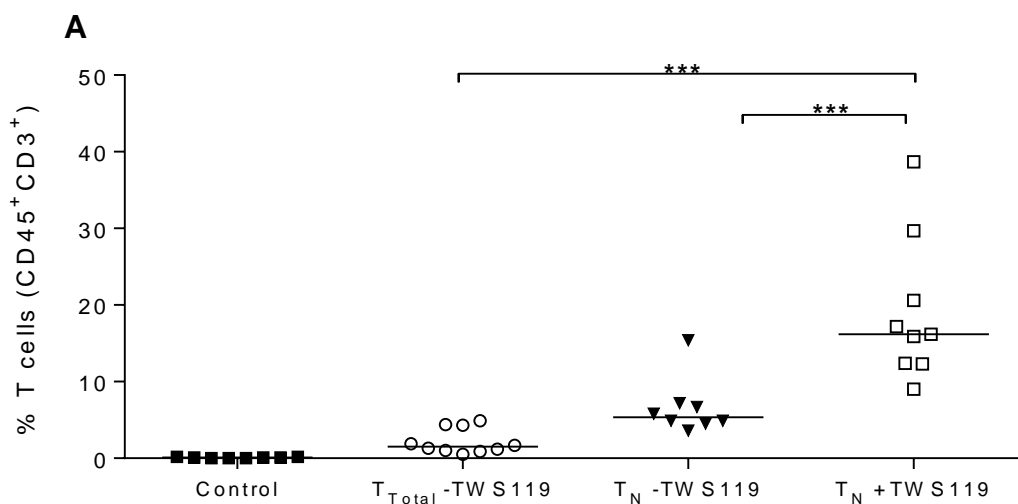


Figure 39: Prolonged survival of mice post transfer of TWS119 treated EBV-CTL_{SCM/CM}. 1.5×10^6 T cells were injected (*i.v.*) into NOD/SCID/IL2Rcynull (NSG)-mice on day 10 following B-LCL engraftment. N = 8-10 mice/group

T cells found in the spleen and bone marrow depicted in Figure 40 were quantified by expression of CD45 and CD3. The analyzed data suggest a very good survival of transferred T cells *in vivo*, thus about 40% of T_N plus TWS119 cells were found in bone marrow and ca.85% in spleen of mice sacrificed on day 14. These data were generated in collaboration with Dr. Yan Xu (AG Hartwig).



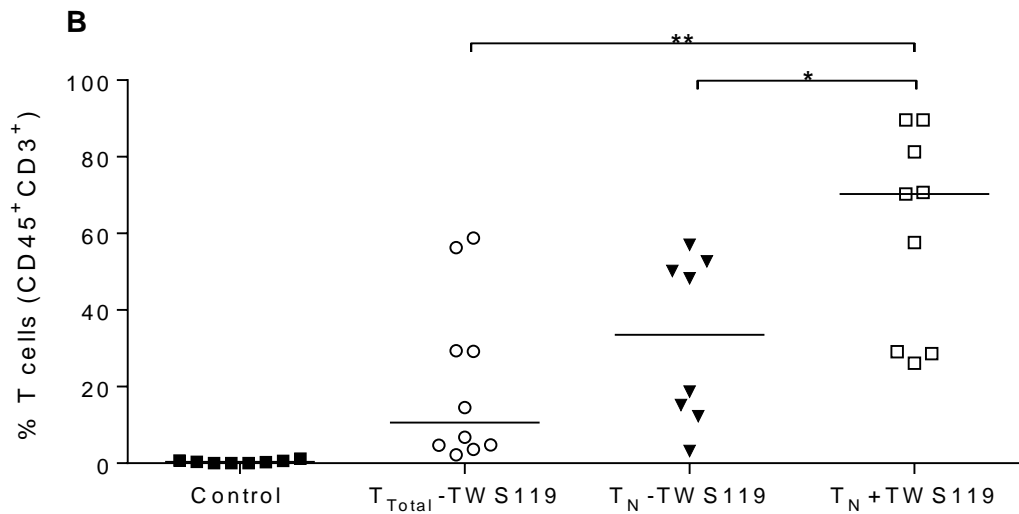


Figure 40: Increased engraftment of TWS119 treated EBV-CTL_{SCM/CM} cells. 1.5×10^6 T cells were injected (*i.v.*) into NOD/SCID/IL2R γ null (NSG)-mice on day 10 following B-LCL engraftment. **A.** On day 14, bone marrow was harvested and analyzed for the expression of CD45/CD3. **B.** On day 14, spleen was harvested and analyzed for the expression of CD45/CD3. N= 8-10 mice/group. 1-Way ANOVA was used for statistical analysis.

5. Discussion

The focus of this study was to find the best approach to generate long-lasting stem cell memory T cells (T_{SCM}) and central memory T cells (T_{CM}) directed against Epstein Bar virus from naive $CD8^+$ T cells *in vitro*. According to the “linear” or “developmental” model proposed by Restifo et al. naive T cells give rise to all memory subsets (T_{SCM} , T_{CM} , T_{EM} and T_{EFF}) in both the human and mouse organism (Restifo 2014). Therefore, for the generation of EBV-reactive $CTL_{SCM/CM}$ cells, naive $CD8^+$ T cells were isolated from healthy donors and were initially stimulated with autologous, irradiated DC derived from the non T cell PBMC fraction and preloaded with EBV-peptide pools for antigen presentation in the presence of a defined cytokine cocktail comprised of IL-7, IL-15 and IL-21. Effective expansion and stimulation was supported by the homeostatic cytokines IL-7 and IL-15 (Surh & Sprent 2008); (Lugli et al. 2013) while IL-21 was added to promote the development of antigen-specific $CD8^+$ T cells from the naive subset (Li et al. 2005). Alternatively, T cells were stimulated with autologous irradiated and peptide loaded PBMC in the presence of the cytokines listed above and IL-12 to compensate for IL-12 mediated DC priming (Heufler et al. 1996). On day 7 of culture (second stimulation), T cells were restimulated with EBV-preloaded autologous PBMC and IL-12 to further promote proliferation and survival during a primary response (Obar & Lefrançois 2010). From day 14 (third stimulation) onward, IL-12 was exchanged to IL-2 for optimal memory function and to enhance proliferation and survival (Cheng et al. 2002). Memory T cells are unique cells and display distinct metabolic profiles, phenotype, migration capacity and antigen reactivity as compared to T effector cells.

5.1 Phenotype and *in vitro* reactivity of EBV-specific $CTL_{SCM/CM}$ cells generated under the impact of RAPA

Ahmed et al. reported that mTOR (mammalian target of rapamycin) is a major regulator of memory $CD8^+$ T cell differentiation, cell growth and metabolism. Therefore, rapamycin promotes the generation of memory $CD8^+$ T cells by inhibiting mTOR Complex I (Araki et al. 2010). Furthermore, it was observed that rapamycin treatment prevented the downregulation of CCR7 and CD62L in $CD8^+$ T cells, which reveals that mTOR plays a role in T cell migration (Sinclair et al. 2008).

Thus, as a first approach, naive $CD8^+$ T cells were co-cultured with rapamycin to facilitate the generation of early memory T cells. Rapamycin was added on the day 0 and upon all further stimulations. We observed that rapamycin has a negative impact on the T cell growth. Different concentrations of rapamycin have been tested to generate $CTL_{SCM/CM}$ cells (data not shown). A concentration of 80 mM was chosen to induce a typical $CTL_{SCM/CM}$ cells' phenotype (see Figure 12), and this concentration gave rise to just enough T cells for the further *in vitro* analysis. However, in comparison to the 2-DG treatment which resulted in $5-6 \times 10^6$ EBV-

CTL_{SCM/CM} cells over 3 weeks (see Figure 19) or about $10\text{-}15 \times 10^6$ EBV-CTL_{SCM/CM} cells obtained following TWS119 treatment (see Figure 20), the use of rapamycin dramatically inhibited cell growth in T cells. As a final result, it was only possible to generate about 2×10^6 EBV-CTL_{SCM/CM} cells within 21 days of culture (see Figure 18).

In addition, RAPA treatment had a negative impact on the EBV-reactivity of generated CTL_{SCM/CM} cells as tested *in vitro* (see Figure 22). Because of the weak proliferative capacity and diminished EBV-reactivity *in vitro* of the rapamycin treated T cells, T_{SCM} and T_{CM} cells obtained by this approach were not further analyzed in this work.

5.2 Phenotype and *in vitro* reactivity of EBV-specific CTL_{SCM/CM} cells generated in presence of 2-DG

T cells undergo changes in metabolism during the immune response, displaying distinct metabolic profiles depending on their phase of activation (Pearce et al. 2013). Thus, generation and maintenance of CTL_{SCM/CM} cells by manipulation of naive T cell metabolism in presence of 2-deoxy-glucose (2-DG) was examined as a second approach. 2-DG prevents naive T cells from excessive glucose consumption, whereby T cells adapt early memory-like metabolism (OXPHOS) and remain largely undifferentiated.

Added on day 0 and upon all further stimulations 2-DG slightly inhibited the proliferation of T cells, however, a sufficient cell number of $5\text{-}6 \times 10^6$ EBV-CTL_{SCM/CM} cells (see Figure 19) could be generated after 3 weeks culture to perform further analysis.

The inhibition of glycolysis by 2-DG preserved T cells in an early memory stage as 70% of T cells remained CD45RA positive while 80.9% expressed the homing markers CCR7 and CD62L, and 71% of the CD45RA⁺ T cells were CD95⁺ (see Figure 14). In contrast, naive CD8⁺ T cells which were not treated with 2-DG underwent a differentiation process: 54.8% of T cells were positive for CD45RA, 55.4% were positive for CD95 and only 27.5% showed the expression of homing markers (see Figure 15). Noticeably, T_N+2-DG cells which displayed a less differentiated phenotype when compared to the T_N-2-DG, T_{Total}+2-DG and T_{Total}-2-DG cells, were CD95 positive too. The expression of CD95 in T cells is attributed to the dual function of CD95L-CD95 interaction. The outcome of CD95L-CD95 interaction depends on the cellular microenvironment and the state of activation of the T cell. Low levels of CD95 on APC in combination with CD27 and CD28 costimulate naive T cells and support their expansion (Paulsen & Janssen 2011). Thus, 2-DG treatment could promote the proliferation and survival of CTL_{SCM/CM} cells and activate apoptosis in much more differentiated T_{EFF} cells. Nevertheless, it has been shown that 2-DG treatment could be used to slow down the differentiation process in naive CD8⁺ T cells and therefore induce generation of CTL_{SCM/CM} cells.

In contrast to rapamycin, the addition of 2-DG did not impair IFN- γ production of T cells as measured by ELISpot-assay. Thus, 2-DG treated naive CD8⁺ T cells showed a comparable IFN- γ production *in vitro* when compared to untreated naive and total T cells, which mostly exhibited effector phenotype (see Figure 23A). However, 2-DG treated EBV-specific CTL_{SCM/CM} cells could only promote 20% lysis of *in vitro* generated autologous B-LCL, whereby T cells with effector-like phenotype (T_{total}-2-DG) showed superior, i.e. more than 60% lysis of B-LCL as shown by chromium-51 release assay (see Figure 24). Biasco et al. reported that T_{SCM} and T_{CM} cells need more time than T effector memory cells to differentiate into T effector cells and thus do not secrete large amounts of cytokines upon stimulation (Biasco et al. 2015). This could be one possible reason for not lysing B-LCL in chromium-51 release assays, which lasted only 4h. These results challenge the ability of 2-DG to generate cytolytic EBV-specific CTL_{SCM/CM} cells *in vitro*. To address this question, the cells were tested *in vivo* over longer period of time to verify their ability to recognize B-LCL in murine models (see 5.7).

5.3 Phenotype and *in vitro* reactivity of EBV-specific CTL_{SCM/CM} cells generated in presence of TWS119

Gattinoni and colleagues reported that inhibition of Gsk3 β by TWS119, arrest CD8⁺ T cell differentiation into effector T cells (Gattinoni et al. 2009). Thus, in the last approach of this work naive CD8⁺ T cells were treated with TWS119 to facilitate Wnt- β -catenin signaling pathway and promote the generation of CTL_{SCM/CM} cells. The proliferative capacity of EBV-CTL_{SCM/CM} cells treated with TWS119 on day 0 and upon all further stimulations was at least affected when compared to rapamycin and 2-DG. Starting initially with 1x10⁶ naive CD8⁺ T cells it was possible to yield about 10 to 15x10⁶ EBV-CTL_{SCM/CM} cells after 3 weeks (see Figure 20).

As a result of TWS119 treatment, more than a half of the naive CD8⁺ T cells remained CD45RA positive (61.8%), double positive for the homing markers CCR7 and CD62L (50.8%) and highly positive for CD95 (87%). These data indicate that TWS119 could successfully slow down the differentiation process in more than 50% of naive CD8⁺ T cells. In contrast, naive CD8⁺ T cells that were not treated with TWS119 showed 45.2% of CD45RA expression, only 8.7% showed the expression of the homing markers and 90.4% were positive for CD95 (see Figure 16). These results suggest that TWS119 is a potentially successful agent to generate T_{SCM}⁻ and T_{CM}⁻ like cells *in vitro*.

In addition, TWS119 treated T cells elicited slightly higher EBV reactivity *in vitro* as compared to T cells with effector-like phenotype (T_N-TWS119 and T_{total}-TWS119 cells) (see Figure 23B).

Moreover, naive CD8⁺ T cells treated with TWS119 elicited a stronger cytotoxicity against B-LCL (ca.40% lysis at 60:1 E:T ratio) as compared to the cytotoxic capacity of naive T cells propagated without TWS119 treatment, which was slightly lower (about 30% at 6:1 E:T ratio). In contrast, T_{total}⁻TWS119 cells demonstrated about 20% cytolytic reactivity at a 60:1 E:T ratio (see Figure 25). EBV-CTL_{SCM/CM} cells treated with TWS119 didn't show very high cytotoxicity against B-LCL *in vitro*, but their EBV-reactivity was much higher than of the EBV-CTL_{SCM/CM} cells treated with 2-DG. Therefore, TWS119 treated T cells were also tested *in vivo* over longer period of time to verify their ability to recognize B-LCL in mice models (see 5.7).

5.4 Similar phenotype but different functionality of EBV-specific CTL_{SCM/CM} cells generated by three different inhibitors

Although EBV-CTL_{SCM/CM} cells generated by rapamycin treatment were phenotypically similar to T_{SCM} and T_{CM} cells generated by TWS119, they were incapable to recognize an antigen *in vitro* (see Figure 22A und B). This is in contrast to the data published by Araki and colleagues who did not only show an increased generation of memory CD8⁺ T cells in rapamycin treated mice as compared to control mice but also an improved homeostatic proliferation and responses upon re-exposure to antigen (Araki et al. 2009).

Since we obtained a very low number of EBV-CTL_{SCM/CM} cells under rapamycin treatment *in vitro* (see Figure 18), these cells were not further characterized. Interestingly, He and colleagues claimed to generate 5-fold more long-lived memory T cells in rapamycin treated mice than in untreated controls (He, Kato, Jiang, Daniel R. Wahl, et al. 2011). Pearce et al. published data proving that rapamycin application resulted in strikingly increased T memory cell development of murine OTI-TRAF6-ΔT⁴ and OTI-TRAF6-WT CD8⁺ T cells (Pearce et al. 2009). Thus, the rapamycin data presented in this work are controversial to the published data, which could be possibly explained by the origin of treated T cells (murine vs. human). Obviously, rapamycin treatment could induce the successful generation of T memory cells in the mouse but not in human *in vitro* systems. Moreover, the antigen specificity of generated memory T cells *in vivo* was not impaired.

EBV-specific CTL_{SCM/CM} cells, generated by manipulating the metabolism of naive CD8⁺ T cells with 2-DG exhibited a T_{SCM}⁻ and T_{CM}⁻ like phenotype (see Figure 14). These cells were capable of secreting IFN-γ *in vitro* in the presence of EBV infected B cells (B-LCL) but unfortunately failed to lyse the same targets in chromium-51 release assay (20% lysis). Regardless of the somewhat inconsistent *in vitro* functionality of 2-DG treated EBV-specific CTL_{SCM/CM} cells, they were further characterized in this work and subsequently tested *in vivo*.

⁴ OTI-TRAF6-ΔT cells are murine T cells, lacking TRAF6, which display defective AMPK-activation and mitochondrial fatty acid oxidation (FAO) in response to growth factor withdrawal (Pearce et al. 2009)

Finally, the induction of Wnt- β -catenin signaling pathway in naive CD8⁺ T cells by TWS119 resulted not only in the generation of phenotypically T_{SCM}⁻ and T_{CM}⁻ like cells (see Figure 16), but these cells also showed superior IFN- γ production *in vitro* and 40% cytotoxicity towards B-LCL in chromium-51 release assay. To note, naive T cells treated with 2-DG or TWS119 showed less differentiated phenotype but to different extents. After 3 weeks of 2-DG treatment, ca.70% of cells remained CD45RA positive, whereas T cells treated with TWS119 expressed about 60% of CD45RA. This slight difference in the phenotype of TWS119 and 2-DG treated EBV-CTL_{SCM/CM} cell was reproducibly observed in all experiments performed. Better proliferative capacity and exhibition of a more differentiated phenotype, thus containing more effector memory T cells, could partly explain a better cytolytic activity of the TWS119 treated T cells as compared to the 2-DG treated naive T cells.

5.5 Metabolism profiles and migration potential of 2-DG treated CTL_{SCM/CM}

One of the hallmarks of memory T cells is their unique metabolic profile, which allows them to maintain a resting stage by utilizing OXPHOS in the absence of antigen, but to proliferate rapidly after antigen encounter upon switching to aerobic glycolysis (Pearce et al. 2009). 2-DG treated EBV-CTL_{SCM/CM} cells were analyzed for glucose consumption and lactate production on the same day as they were tested in functional assays, which was between two stimulations. As to be expected T cells with T_{SCM}⁻ and T_{CM}⁻ like phenotype consumed less glucose and produced less lactate (see Figure 29A and Figure 30A) when compared to T effector cells. This finding suggests that 2-DG treated CTL_{SCM/CM} cells do not primarily utilize glycolysis to generate ATP, whereas T effector cells do.

Furthermore, it was of interest to examine whether EBV-CTL_{SCM/CM} and T_{EFF} cells utilize OXPHOS. Therefore, cells were analyzed with an extracellular flux analyzer to measure oxygen consumption rate (OCR) and extracellular acidification rate (ECAR) under basal conditions and after pharmacological inhibition of mitochondrial respiration with oligomycin A, rotenone and DNP. These drugs inhibit oxidative phosphorylation in different ways: oligomycin A inhibits ATP synthase by blocking its proton channel, which is necessary for oxidative phosphorylation of ADP to ATP; however, electron flow is not completely stopped due to a process known as proton leak. By inhibiting the Complex I, rotenone obstructs electrons to pass off further; therefore the electrons are hold back within the mitochondrial matrix. DNP is a proton ionophore, an agent that binds the protons (hydrogen cations) and shuttles them across a biological membrane where it releases them. It defeats the proton gradient across mitochondria and instead of producing ATP; the energy of the proton gradient is lost as "heat".

Measuring OCR revealed that EBV-CTL_{SCM/CM} and EBV-T_{EFF} cells utilize OXPHOS to generate ATP, as they both showed a similar response to the inhibition of mitochondrial respiration (see Figure 31A and B). After the mitochondrial respiration was perturbed by the drugs (oligomycin A, DNP and rotenone), T effector cells could switch to aerobic glycolysis and thus showed a higher level of ECAR compared to the CTL_{SCM/CM} cells.

Collectively, these data indicate that, T effector cells use mainly aerobic glycolysis, but also OXPHOS to generate ATP, whereas CTL_{SCM/CM} cells use mainly OXPHOS.

Van der Windt and colleagues showed that memory T cells display high levels of fatty-acid oxidation by mitochondria to fuel OXPHOS and subsequently produce ATP as compared to T effector cells (van der Windt et al. 2012). Interestingly, memory T cells do not acquire fatty acids from the environment to increase the rate of fatty acid oxidation since they display reduced expression of CD36 (fatty acid translocase), which is necessary for fatty acid uptake in T effector cells (Weinberg & Chandel 2014). Instead, memory T cells drive *de novo* fatty acid synthesis to generate mitochondrial ATP through fatty-acid oxidation (see Figure 6). The naive CD8⁺ T cells used to generate EBV-CTL_{SCM/CM} cells exhibited a reduced level of CD36 expression when compared with T_{EFF} cells (see Figure 27). The feature of T memory cells to engage a “futile cycle” of fatty acid synthesis explains why T cells failed to consume oleic acid from culture media and upregulated CD45RO expression (see Figure 26A). Glucose is the typical sugar in T cell media and, T cells activated in glucose adopt aerobic glycolysis. In contrast, cells grown in galactose are forced to utilize OXPHOS and do not use aerobic glycolysis (Bustamante & Pedersen 1977); (Rossignol et al. 2004). Nevertheless, in our settings, naive CD8⁺ T cells cultured with galactose, instead of glucose, initiated a differentiation process, by upregulating CD45RO.

The next feature of the T_{SCM} and T_{CM} cells is the ability to home to secondary lymphoid organs, where they quickly respond to the presence of cognate antigen by APCs (Klebanoff et al. 2012). Therefore, the cells must co-express the lymphoid homing marker L-selectin (CD62L) and CC-chemokine receptor 7 (CCR7). 2-DG treated EBV-CTL_{SCM/CM} cells showed an increased expression of both homing markers as compared to T_{EFF} cells, which strongly downregulate the expression of CD62L and CCR7 and therefore preferentially reside in peripheral tissues (see Figure 14) and (see Figure 15).

To determine whether modulation of glucose metabolism could regulate such lymphoid homing behavior, cells were analyzed in the transmigration assay for their ability to migrate towards CCL21. CCL21 is expressed by vascular high endothelial cells and the stromal cells of lymphoid tissues, and binds to the chemokine receptor CCR7 on naive T cells, T_{SCM} and T_{CM} cells. Naive CD8⁺ T cells treated with 2-DG exhibited greater migration capacity when compared with control cells (see Figure 34A and B). These results indicate that sustained

(reduced) glycolytic activity is required to reprogram T cells to preferentially migrate to lymphoid tissues.

Moreover, the direct inhibition of glycolysis using 2-DG was also associated with enhanced expression of the transcription factors Tcf-7 and Lef-1 (see Figure 33A and C), which regulate memory versus effector differentiation in CD8⁺ T cells. This fact provides a link between metabolism and transcriptional regulation of cell fate determination.

In addition, Bcl-6 was also implicated to promote memory cell formation in CD8⁺ T cells (Ichii et al. 2002) by inhibiting the expression of Blimp-1, a transcriptional regulatory protein required for the terminal differentiation of effector cell populations (Crotty et al. 2010). Along this line, the qRT-PCR data revealed an increased expression of B cell CLL/lymphoma 6 (Bcl-6) in 2-DG treated EBV-CTL_{SCM/CM} cells (see Figure 33E).

5.6 Metabolism profiles and migration potential of TWS119 treated CTL_{SCM/CM}

Although the generation of EBV-CTL_{SCM/CM} cells under the impact of TWS119 did not directly involve the modulation of metabolism in naive CD8⁺ T cells, the metabolism of memory T cells generated by this mode was examined. TWS119 treated EBV-CTL_{SCM/CM} cells were analyzed in the same way as 2-DG treated T cells for the glucose consumption and lactate production on the same day they were tested in functional assays, which is between two stimulations. Again, as to be expected, T cells which expressed a T_{SCM}⁻ and T_{CM}⁻ like phenotype consumed less glucose and produced less lactate (see Figure 29B and Figure 30B) when compared to T effector cells. This finding suggests that TWS119 treated CTL_{SCM/CM} cells do not primarily utilize glycolysis to generate ATP whereas T effector cells do. Measuring OCR revealed that TWS119 treated EBV-CTL_{SCM/CM} and EBV-T_{EFF} cells utilize OXPHOS to generate ATP as they both showed a similar response to the inhibition of mitochondrial respiration (see Figure 31A and B). After the mitochondrial respiration was perturbed by oligomycin A, DNP and rotenone, T effector cells could switch to aerobic glycolysis and thus showed a higher level of ECAR as compared to the CTL_{SCM/CM} cells. These data indicate that T effector cells use mainly aerobic glycolysis but also OXPHOS to generate ATP, whereas CTL_{SCM/CM} cells use mainly OXPHOS. All the metabolic analysis proved that TWS119 had an indirect impact on the metabolism of naive CD8⁺ T cells.

In order to generate EBV-CTL_{SCM/CM} cells, naive CD8⁺ T cells were treated with TWS119 which activates Wnt-β-catenin signaling (Gattinoni et al. 2009). Therefore, the TWS119 treated EBV-CTL_{SCM/CM} cells showed an increased expression of transcription factor 7 (Tcf-7) and lymphoid enhancer factor 1 (Lef-1) (see Figure 33B and 33D).

In addition, the qRT-PCR data revealed an increased expression of B cell CLL/lymphoma 6 (Bcl-6) in TWS119 treated EBV-CTL_{SCM/CM} cells (see Figure 33F).

In vitro generated T_{SCM} and T_{CM} cells under the impact of TWS119 showed an increased expression of both homing markers CD62L and CCR7 as compared to T_{EFF} cells which strongly downregulated the expression of CD62L and CCR7 (see Figure 16 and Figure 17). To determine whether activation of Wnt- β -catenin-signaling could regulate lymphoid homing behavior, cells were analyzed in the transmigration assay for their ability to migrate towards CCL21. Naive CD8⁺ T cells treated with TWS119 exhibited greater migration capacity when compared with control cells (see Figure 34B). These results indicate that activation of Wnt- β -signaling in CD8⁺ T cells could reprogram T cells to preferentially migrate to lymphoid tissues.

5.7 Adoptive transfer of 2-DG and TWS119 treated EBV-specific CTL_{SCM/CM} cells into B-LCL engrafted NSG-mice

After adoptive transfer into immunosuppressive patients CTLs with stem cell memory and central memory properties are expected to survive, migrate to the secondary lymphoid organs, recognize an antigen and give a rise to T effector cells with strong lytic functions. Therefore, cells must express homing molecules (e.g. CD62L, CCR7) to migrate to lymph nodes, co-stimulatory molecules (CD27, CD28) which enable activation and proliferation, and early memory marker CD45RA which indicate their self-renewal capacity to give a rise to highly lytic T effector cells.

Furthermore, the ability of T cells to proliferate and persist in the long term after transfer correlates with effective antigen responses in mice and humans receiving adoptive T cell based therapies (Gattinoni et al. 2009); (Rosenberg et al. 2011); (Gattinoni et al. 2011a).

In this work it was shown that “early memory” (stem cell memory/central memory) differentiation markers were expressed by EBV-CTL_{SCM/CM} cells generated in presence of 2-DG or TWS119, and functional *in vitro* assays revealed a potential EBV reactivity of the generated T cells. Thus, it was of importance to evaluate if *ex vivo* generated EBV-CTL_{SCM/CM} cells could show a long-term survival *in vivo* and eliminate B-LCL in the murine model.

To comply with naturally occurring T_{SCM} and T_{CM} cells, *in vitro* generated EBV-CTL_{SCM/CM} cells should have a long-lifespan which is supported by their quiescent metabolism. To test this assumption, 2-DG treated EBV-CTL_{SCM/CM} cells were transferred in NOD/SCID/IL2R γ ^{null} (NSG)-mice supplemented with human IL13-Fc (IL-15 with extended half-life produced in our lab) to test their long-term survival in absence of antigen. It has been reported that IL-15 supports the generation of T_{SCM} cells (Cieri et al. 2012). Unfortunately, 2-DG treated EBV-CTL_{SCM/CM} cells could not survive and persist for a long time *in vivo* in the absence of antigen.

Despite the short-term persistence of the transferred EBV-CTL_{SCM/CM} cells the effect of IL-15 could still be confirmed, as the mice injected with IL-15 yielded more T cells as compared to untreated mice. In contrast, TWS119 treated naive CD8⁺ T cells supplemented with human ILR13-Fc survived *in vivo* in the absence of antigen (B-LCL targets) for 28 days.

Next, to determine the therapeutic potential of EBV-specific CTL_{SCM/CM} cells, adoptive transfer studies in NSG-mice engrafted with human B-LCL were performed. NSG-mice have a severe combined immune deficiency mutation (SCID) and an IL-2 receptor gamma chain knockout which leads to a lack of mature T cells and B cells, functional NK cells, and a deficiency in cytokine signaling (Shultz et al. 2005). SCID mice showed a reliable engraftment of EBV infected B cells (Rowe et al. 1991), whereby lymphomas similar to early PTLD can be induced as a result of an absent immune response. As previously mentioned, the ability of T cells to proliferate and persist long-term after transfer correlates with effective antigen responses. The study published by Sukumar and colleagues revealed that inhibition of glycolysis by 2-DG in tumor-specific murine CD8⁺ T cells not only promoted the formation of memory CD8⁺ T cells but also enhanced their antitumor function in mice with large vascularized tumors (Sukumar et al. 2013). Unfortunately, just like in chromium-51 release assay, 2-DG treated EBV-specific CTL_{SCM/CM} cells could not lyse B-LCL and thus failed to inhibit or at least control tumor development in mice (see Figure 37).

2-DG treatment has resulted in the generation of more T cells with T_{SCM}⁻ and T_{CM}⁻ like phenotype and quiescent metabolism than TWS119 treatment, but might not be very effective in inducing a therapeutic effect *in vivo* (see Figure 37). Less differentiated 2-DG treated naive CD8⁺ T cells could not quickly react in response to B-LCL neither *in vitro* nor *in vivo*, probably because of their inability to give a sufficient response to the antigen (B-LCL) and subsequently sustain the generation of T effector cell subsets. One possible explanation for that could be a very strong glucose deprivation caused by too long treatment with 2-DG. Sukumar et al. reported on successful generation of murine memory T cells *in vitro* treated with 2-DG for four days. Tumor-specific T cells infiltrated tumors three days after transfer (Sukumar et al. 2013). In contrast, according to our settings naive T cells were cultured with 2-DG in DMEM (low Glucose) medium for three weeks, which might have negatively affected the priming of naive T cells.

In contrast, mice transferred with TWS119 treated EBV-CTL_{SCM/CM} cells survived up to 80 days. The sacrificed mice contained tumor cells as well but the longer survival of mice indicated that the *in vitro* TWS119 treatment of naive CD8⁺ T cells didn't affect their EBV activity *in vivo*, resulting in controlled tumor growth. Thus, TWS119 treatment appeared to be more effective as compared to rapamycin and 2-DG treatment for the generation of functional EBV reactive memory T cells. EBV-specific CTL_{SCM/CM} cells generated under the

impact of TWS119 showed a T_{SCM}^- and T_{CM}^- like phenotype, *in vitro* migration capacity and metabolic features comparable to the 2-DG treated T cells but displayed two times higher proliferative capacity *in vitro* than 2-DG treated cells. Moreover, TWS119 treatment appeared not to compromise initial priming of naive $CD8^+$ T cells, as the TWS119 treated EBV- $CTL_{SCM/CM}$ cells perfectly recognized B-LCL targets *in vitro*.

By now a lot of studies to characterize the role and function of stem cell like memory T cells were performed in murine models, whereby the cells showed the ability to survive and promoted tumor regression (Sukumar et al. 2013); (Gattinoni et al. 2009). However, the latest study performed by Biasco et al. showed a safe use and longevity of genetically modified stem cell memory T cells *in vivo* in humans, however, the functional and phenotypic properties of these cells were not investigated (Biasco et al. 2015).

This work reveals a potential strategy to generate antigen specific memory T cells with a self-renewal capacity and a robust long-term persistence and functionality *in vivo*.

Nevertheless, the application of antigen specific $CTL_{SCM/CM}$ cells in adoptive immunotherapy might be hampered by the necessity of *in vitro* expansion prior to transfer and the use of antigen-presenting cells, notably dendritic cells to stimulate antigen-specific immune responses in naive T cells. The proliferative potential and longevity of $CTL_{SCM/CM}$ cells might differ from patient to patient because naive $CD8^+$ T cells used in this work to generate $CTL_{SCM/CM}$ cells were isolated from PBMC which have patient specific T cells subset composition. The issues related to the quality, expenses and time needed for the customized isolation and culture of the cells for individual patients might evolve as limiting factors for the clinical application of $CTL_{SCM/CM}$ cells.

6. Summary and outlook

Immunological memory is perhaps the most important consequence of an adaptive immune response, because it enables the immune system to respond more rapidly and effectively to pathogens (various viruses and bacteria) that have been encountered previously, and prevents them from causing disease. However, this secondary immune response is seriously impaired in individuals lacking a fully functional immune system after HSCT. One possibility to improve immunity in immunosuppressed patients is to administer *in vitro* generated antigen specific long-lasting memory T cells. Therefore, the focus of this study was to find a robust approach to generate antigen specific T_{SCM}^- and T_{CM}^- like T cells *in vitro*. In particular, as proof of concept it was decided to generate T cells against Epstein-Barr virus as one of the immunologically best studied viruses. Most adults older than 30 years are EBV positive and thus carry EBV-specific memory T cells for their entire life to control a latent and persisting virus infection. However, in the case of HSCT the opportunistic viruses, such as EBV can be life-threatening.

Therefore, T_{SCM} and T_{CM} cells were generated by manipulating the metabolism of naive $CD8^+$ T cells with RAPA and 2-DG. In addition, naive $CD8^+$ T cells were treated with the Wnt-signaling pathway modifier TWS119 to induce elevated expression of β -catenin. Treatment with all three drugs resulted in the expression of a T_{SCM}^- and T_{CM}^- like phenotype, but as rapamycin strongly inhibited cell proliferation and antigen specificity, it was not further applied to generate EBV-CTL_{SCM/CM} cells.

In line with T_{SCM}^- and T_{CM}^- like phenotype, 2-DG or TWS119 treated naive $CD8^+$ T cells exhibited T_{SCM}^- and T_{CM}^- like quiescent metabolism by utilizing mainly OXPHOS to generate energy. Besides they expressed high levels of the homing markers (CCR7 and CD62L) and showed increased migration capacity when compared to T_{EFF} (T_N w/o 2-DG or w/o TWS119, T_{total} w/o 2-DG or w/o TWS119 treatment and T_{total} plus 2-DG). 2-DG treated EBV-CTL_{SCM/CM} cells were capable of secreting IFN- γ *in vitro* in the presence of B-LCL but unfortunately failed to exert cytotoxic activity to the same targets as shown in chromium-51 release assays. In contrast, TWS119 treated EBV-CTL_{SCM/CM} cells elicited superior IFN- γ production *in vitro* and demonstrated about 40% cytotoxicity towards B-LCL.

EBV-CTL_{SCM/CM} cells generated in presence of 2-DG or TWS119 were transferred into NOD/SCID/IL2R γ^{null} (NSG)-mice to test for their long-term survival in the absence of antigen. After 1 week post transfer 4% of 2-DG treated EBV-CTL_{SCM/CM} cells were identified in the peripheral blood and after 2 weeks the number of T cells reduced to 1.8%. In contrast, around 30% of TWS119 treated CTL_{SCM/CM} cells could be detected in spleen and blood of mice sacrificed on day 28. To determine the therapeutic potential of EBV-specific CTL_{SCM/CM} cells, they were used for adoptive transfer into NSG-mice engrafted with human B-LCL.

Unfortunately, 2-DG treated EBV-specific CTL_{SCM/CM} cells could not inhibit or control tumor development. However, mice transferred with TWS119 treated EBV-CTL_{SCM/CM} cells survived for up to 80 days. The sacrificed mice contained tumor cells as well, but longer survival of mice indicated that *in vitro* TWS119 treatment of naive CD8⁺ T cells significantly augmented their activity towards EBV-peptide antigens, resulting in controlled tumor growth.

Prospectively, *in vitro* generated CTL_{SCM/CM} cells might represent an attractive tool to generate genetically modified T_{SCM} or T_{CM} cells with chimeric antigen receptors, like for example, CD19-CAR (Sabatino et al. 2016), (Cieri et al. 2012). The huge advantage of T_{SCM} and T_{CM} cells is that they have high proliferative and survival capacity. T_{SCM} and T_{CM} cells generated from a naive CD8⁺ T cell fraction display relatively homogenous antigen specificity when compared to the memory T cells generated from PBMC. These features and their ability to replenish a pool of potent effector T cells thus deploy T_{SCM} and T_{CM} cells as promising tools for an improved adoptive cellular immunotherapy.

7. References

- Abraham, R.T. & Wiederrecht, G.J., 1996. Immunopharmacology of rapamycin. *Annual review of immunology*, 14, pp.483–510. Available at: <http://www.ncbi.nlm.nih.gov/pubmed/8717522> [Accessed November 1, 2015].
- Alinikula, J. et al., 2011. Alternate pathways for Bcl6-mediated regulation of B cell to plasma cell differentiation. *European journal of immunology*, 41(8), pp.2404–13. Available at: <http://www.ncbi.nlm.nih.gov/pubmed/21674482> [Accessed November 17, 2015].
- Anon, 2007. *Fields' Virology, Volume 1*, Lippincott Williams & Wilkins. Available at: <https://books.google.com/books?id=5O0somr0w18C&pgis=1> [Accessed August 6, 2015].
- Antsiferova, O. et al., 2014. Adoptive Transfer of EBV Specific CD8+ T Cell Clones Can Transiently Control EBV Infection in Humanized Mice. *PLoS Pathogens*, 10(8), p.e1004333. Available at: <http://dx.plos.org/10.1371/journal.ppat.1004333>.
- Araki, K. et al., 2009. mTOR regulates memory CD8 T-cell differentiation. *Nature*, 460(7251), pp.108–12. Available at: <http://www.pubmedcentral.nih.gov/articlerender.fcgi?artid=2710807&tool=pmcentrez&rendertype=abstract> [Accessed November 9, 2015].
- Araki, K., Youngblood, B. & Ahmed, R., 2010. The role of mTOR in memory CD8 T-cell differentiation. *Immunological reviews*, 235(1), pp.234–43. Available at: <http://www.pubmedcentral.nih.gov/articlerender.fcgi?artid=3760155&tool=pmcentrez&rendertype=abstract> [Accessed January 26, 2016].
- Barton, E., Mandal, P. & Speck, S.H., 2011. Pathogenesis and host control of gammaherpesviruses: lessons from the mouse. *Annual review of immunology*, 29, pp.351–97. Available at: <http://www.ncbi.nlm.nih.gov/pubmed/21219186> [Accessed September 18, 2015].
- Beier, C.P. & Schulz, J.B., 2009. CD95/Fas in the brain--not just a killer. *Cell stem cell*, 5(2), pp.128–30. Available at: <http://www.ncbi.nlm.nih.gov/pubmed/19664983> [Accessed December 15, 2015].
- Biasco, L. et al., 2015. In vivo tracking of T cells in humans unveils decade-long survival and activity of genetically modified T memory stem cells. *Science translational medicine*, 7(273), p.273ra13. Available at: <http://stm.sciencemag.org/content/7/273/273ra13.full-text.pdf+html> [Accessed January 4, 2016].
- Bøyum, A., 1976. Isolation of lymphocytes, granulocytes and macrophages. *Scandinavian journal of immunology*, Suppl 5, pp.9–15. Available at: <http://www.ncbi.nlm.nih.gov/pubmed/1052391> [Accessed July 17, 2015].
- Brentjens, R.J. et al., 2011. Safety and persistence of adoptively transferred autologous

- CD19-targeted T cells in patients with relapsed or chemotherapy refractory B-cell leukemias. *Blood*, 118(18), pp.4817–28. Available at: <http://www.pubmedcentral.nih.gov/articlerender.fcgi?artid=3208293&tool=pmcentrez&rendertype=abstract> [Accessed December 16, 2015].
- Buller, C.L. et al., 2008. A GSK-3/TSC2/mTOR pathway regulates glucose uptake and GLUT1 glucose transporter expression. *American journal of physiology. Cell physiology*, 295(3), pp.C836-43. Available at: <http://www.pubmedcentral.nih.gov/articlerender.fcgi?artid=2544442&tool=pmcentrez&rendertype=abstract> [Accessed November 23, 2015].
- Bustamante, E. & Pedersen, P.L., 1977. High aerobic glycolysis of rat hepatoma cells in culture: role of mitochondrial hexokinase. *Proceedings of the National Academy of Sciences of the United States of America*, 74(9), pp.3735–3739.
- Butcher, E.C. & Picker, L.J., 1996. Lymphocyte homing and homeostasis. *Science (New York, N.Y.)*, 272(5258), pp.60–6. Available at: <http://www.ncbi.nlm.nih.gov/pubmed/8600538> [Accessed February 2, 2016].
- Buzon, M.J. et al., 2014. HIV-1 persistence in CD4+ T cells with stem cell-like properties. *Nature Medicine*, 20(2), pp.139–142. Available at: <http://www.ncbi.nlm.nih.gov/pubmed/24412925> [Accessed January 12, 2016].
- Caldwell, R.G. et al., 1998. Epstein-Barr virus LMP2A drives B cell development and survival in the absence of normal B cell receptor signals. *Immunity*, 9(3), pp.405–11. Available at: <http://www.ncbi.nlm.nih.gov/pubmed/9768760> [Accessed June 20, 2015].
- Campo, E. et al., 2011. The 2008 WHO classification of lymphoid neoplasms and beyond: evolving concepts and practical applications. *Blood*, 117(19), pp.5019–32. Available at: <http://www.pubmedcentral.nih.gov/articlerender.fcgi?artid=3109529&tool=pmcentrez&rendertype=abstract> [Accessed November 3, 2014].
- Cheng, L.E. et al., 2002. Enhanced signaling through the IL-2 receptor in CD8+ T cells regulated by antigen recognition results in preferential proliferation and expansion of responding CD8+ T cells rather than promotion of cell death. *Proceedings of the National Academy of Sciences of the United States of America*, 99(5), pp.3001–6. Available at: <http://www.ncbi.nlm.nih.gov/pubmed/11867736> [Accessed July 24, 2016].
- Chi, H., 2012. Regulation and function of mTOR signalling in T cell fate decisions. *Nature reviews. Immunology*, 12(5), pp.325–38. Available at: <http://www.pubmedcentral.nih.gov/articlerender.fcgi?artid=3417069&tool=pmcentrez&rendertype=abstract> [Accessed November 5, 2015].
- Christensen, K.L.Y. et al., 2009. Infectious disease hospitalizations in the United States. *Clinical infectious diseases : an official publication of the Infectious Diseases Society of America*, 49(7), pp.1025–35. Available at: <http://www.ncbi.nlm.nih.gov/pubmed/19708796> [Accessed September 29, 2015].

- Cieri, N. et al., 2012. IL-7 and IL-15 instruct the generation of human memory stem T cells from naive precursors. *Blood*, 121(4), pp.573–584. Available at: <http://www.bloodjournal.org/content/121/4/573.abstract> [Accessed January 11, 2016].
- Crotty, S., Johnston, R.J. & Schoenberger, S.P., 2010. Effectors and memories: Bcl-6 and Blimp-1 in T and B lymphocyte differentiation. *Nature immunology*, 11(2), pp.114–20. Available at: <http://www.pubmedcentral.nih.gov/articlerender.fcgi?artid=2864556&tool=pmcentrez&rendertype=abstract> [Accessed February 18, 2016].
- Damania, B. & Pipas, J.M. eds., 2009a. *DNA Tumor Viruses*, New York, NY: Springer US. Available at: <http://link.springer.com/10.1007/978-0-387-68945-6> [Accessed July 3, 2015].
- Damania, B. & Pipas, J.M. eds., 2009b. *DNA Tumor Viruses*, New York, NY: Springer US. Available at: <http://www.springerlink.com/index/10.1007/978-0-387-68945-6> [Accessed July 3, 2015].
- Ding, S. et al., 2003. Synthetic small molecules that control stem cell fate. *Proceedings of the National Academy of Sciences of the United States of America*, 100(13), pp.7632–7. Available at: <http://www.pnas.org/content/100/13/7632.full> [Accessed November 20, 2015].
- Djenidi, F. et al., 2015. CD8+CD103+ Tumor-Infiltrating Lymphocytes Are Tumor-Specific Tissue-Resident Memory T Cells and a Prognostic Factor for Survival in Lung Cancer Patients. *The Journal of Immunology*, 194(7), pp.3475–3486. Available at: <http://www.ncbi.nlm.nih.gov/pubmed/25725111> [Accessed January 9, 2016].
- Düvel, K. et al., 2010. Activation of a metabolic gene regulatory network downstream of mTOR complex 1. *Molecular cell*, 39(2), pp.171–83. Available at: <http://www.pubmedcentral.nih.gov/articlerender.fcgi?artid=2946786&tool=pmcentrez&rendertype=abstract> [Accessed October 19, 2015].
- EPSTEIN, M.A., ACHONG, B.G. & BARR, Y.M., 1964. VIRUS PARTICLES IN CULTURED LYMPHOBLASTS FROM BURKITT'S LYMPHOMA. *Lancet*, 1(7335), pp.702–3. Available at: <http://www.ncbi.nlm.nih.gov/pubmed/14107961> [Accessed April 21, 2015].
- Farber, D.L., Yudanin, N. a & Restifo, N.P., 2014. Human memory T cells: generation, compartmentalization and homeostasis. *Nature reviews. Immunology*, 14(1), pp.24–35. Available at: http://www.nature.com/nri/journal/v14/n1/full/nri3567.html?WT.mc_id=FBK_NatureReviewsEdit
<http://www.ncbi.nlm.nih.gov/pubmed/24336101>.
- Flynn, J.K. et al., 2014. Quantifying susceptibility of CD4+ stem memory T-cells to infection by laboratory adapted and clinical HIV-1 strains. *Viruses*, 6(2), pp.709–26. Available at: <http://www.pubmedcentral.nih.gov/articlerender.fcgi?artid=3939479&tool=pmcentrez&rendertype=abstract> [Accessed January 14, 2016].

- Frauwirth, K.A. & Thompson, C.B., 2004. Regulation of T lymphocyte metabolism. *Journal of immunology (Baltimore, Md. : 1950)*, 172(8), pp.4661–5. Available at: <http://www.ncbi.nlm.nih.gov/pubmed/15067038> [Accessed November 2, 2015].
- Fuertes Marraco, S.A. et al., 2015. Long-lasting stem cell-like memory CD8+ T cells with a naïve-like profile upon yellow fever vaccination. *Science translational medicine*, 7(282), p.282ra48. Available at: <http://www.ncbi.nlm.nih.gov/pubmed/25855494> [Accessed January 14, 2016].
- Fujiwara, S., Imadome, K.-I. & Takei, M., 2015. Modeling EBV infection and pathogenesis in new-generation humanized mice. *Experimental & molecular medicine*, 47, p.e135. Available at: <http://dx.doi.org/10.1038/emm.2014.88> [Accessed September 2, 2015].
- Gattinoni, L. et al., 2011a. A human memory T cell subset with stem cell-like properties. , 17(10). Available at: <http://dx.doi.org/10.1038/nm.2446>.
- Gattinoni, L. et al., 2011b. A human memory T cell subset with stem cell-like properties. Available at: <http://dx.doi.org/10.1038/nm.2446>.
- Gattinoni, L. et al., 2009. Wnt signaling arrests effector T cell differentiation and generates CD8+ memory stem cells. *Nature medicine*, 15(7), pp.808–813.
- Gottschalk, S., Rooney, C.M. & Heslop, H.E., 2005. Post-transplant lymphoproliferative disorders. *Annual review of medicine*, 56, pp.29–44. Available at: <http://www.ncbi.nlm.nih.gov/pubmed/15660500> [Accessed July 21, 2015].
- Halloran, P.F., 2004. Immunosuppressive drugs for kidney transplantation. *The New England journal of medicine*, 351(26), pp.2715–29. Available at: <http://www.ncbi.nlm.nih.gov/pubmed/15616206> [Accessed June 28, 2015].
- He, S., Kato, K., Jiang, J., Wahl, D.R., et al., 2011. Characterization of the metabolic phenotype of rapamycin-treated CD8+ T cells with augmented ability to generate long-lasting memory cells. *PLoS ONE*, 6(5).
- He, S., Kato, K., Jiang, J., Wahl, D.R., et al., 2011. Characterization of the metabolic phenotype of rapamycin-treated CD8+ T cells with augmented ability to generate long-lasting memory cells. *PLoS one*, 6(5), p.e20107. Available at: <http://www.pubmedcentral.nih.gov/articlerender.fcgi?artid=3096660&tool=pmcentrez&rendertype=abstract> [Accessed February 16, 2016].
- Heufler, C. et al., 1996. Interleukin-12 is produced by dendritic cells and mediates T helper 1 development as well as interferon-gamma production by T helper 1 cells. *European journal of immunology*, 26(3), pp.659–68. Available at: <http://www.ncbi.nlm.nih.gov/pubmed/8605935> [Accessed July 24, 2016].
- Hinrichs, C.S. et al., 2008. IL-2 and IL-21 confer opposing differentiation programs to CD8+ T cells for adoptive immunotherapy. *Blood*, 111(11), pp.5326–33. Available at: <http://www.pubmedcentral.nih.gov/articlerender.fcgi?artid=2396726&tool=pmcentrez&rendertype=abstract> [Accessed November 19, 2015].

- Hong, G.K. et al., 2005. Epstein-Barr virus lytic infection contributes to lymphoproliferative disease in a SCID mouse model. *Journal of virology*, 79(22), pp.13993–4003. Available at: <http://www.pubmedcentral.nih.gov/articlerender.fcgi?artid=1280209&tool=pmcentrez&rendertype=abstract> [Accessed July 3, 2015].
- Ichii, H. et al., 2002. Role for Bcl-6 in the generation and maintenance of memory CD8+ T cells. *Nature immunology*, 3(6), pp.558–63. Available at: <http://dx.doi.org/10.1038/ni802> [Accessed February 4, 2016].
- Itzhaki, O. et al., 2011. Establishment and large-scale expansion of minimally cultured “young” tumor infiltrating lymphocytes for adoptive transfer therapy. *Journal of immunotherapy (Hagerstown, Md. : 1997)*, 34(2), pp.212–20. Available at: <http://www.ncbi.nlm.nih.gov/pubmed/21304398> [Accessed January 22, 2016].
- Jochum, S. et al., 2012. RNAs in Epstein-Barr virions control early steps of infection. *Proceedings of the National Academy of Sciences of the United States of America*, 109(21), pp.E1396-404. Available at: <http://www.pubmedcentral.nih.gov/articlerender.fcgi?artid=3361417&tool=pmcentrez&rendertype=abstract> [Accessed July 5, 2015].
- Kaech, S.M. & Ahmed, R., 2001. Memory CD8+ T cell differentiation: initial antigen encounter triggers a developmental program in naïve cells. *Nature immunology*, 2(5), pp.415–22. Available at: <http://www.pubmedcentral.nih.gov/articlerender.fcgi?artid=3760150&tool=pmcentrez&rendertype=abstract> [Accessed September 24, 2015].
- Kirschner, A.N. et al., 2006. Soluble Epstein-Barr Virus Glycoproteins gH, gL, and gp42 Form a 1:1:1 Stable Complex That Acts Like Soluble gp42 in B-Cell Fusion but Not in Epithelial Cell Fusion. *Journal of Virology*, 80(19), pp.9444–9454. Available at: <http://www.pubmedcentral.nih.gov/articlerender.fcgi?artid=1617263&tool=pmcentrez&rendertype=abstract> [Accessed July 5, 2015].
- Klebanoff, C.A., Gattinoni, L. & Restifo, N.P., 2012. Sorting Through Subsets. *Journal of Immunotherapy*, 35(9), pp.651–660. Available at: <http://www.pubmedcentral.nih.gov/articlerender.fcgi?artid=3501135&tool=pmcentrez&rendertype=abstract> [Accessed January 19, 2016].
- Kochenderfer, J.N. et al., 2012. B-cell depletion and remissions of malignancy along with cytokine-associated toxicity in a clinical trial of anti-CD19 chimeric-antigen-receptor-transduced T cells. *Blood*, 119(12), pp.2709–20. Available at: <http://www.pubmedcentral.nih.gov/articlerender.fcgi?artid=3327450&tool=pmcentrez&rendertype=abstract> [Accessed November 20, 2015].
- Kochenderfer, J.N. et al., 2015. Chemotherapy-refractory diffuse large B-cell lymphoma and indolent B-cell malignancies can be effectively treated with autologous T cells

- expressing an anti-CD19 chimeric antigen receptor. *Journal of clinical oncology : official journal of the American Society of Clinical Oncology*, 33(6), pp.540–9. Available at: <http://jco.ascopubs.org/content/early/2014/08/25/JCO.2014.56.2025.short> [Accessed September 18, 2015].
- Kubota, N. et al., 2008. One-step multiplex real-time PCR assay to analyse the latency patterns of Epstein-Barr virus infection. *Journal of Virological Methods*, 147(1), pp.26–36.
- Laplante, M. & Sabatini, D.M., 2009. mTOR signaling at a glance. *Journal of cell science*, 122(Pt 20), pp.3589–94. Available at: <http://jcs.biologists.org/content/122/20/3589.abstract> [Accessed July 11, 2014].
- Lee, D.W. et al., 2014. T cells expressing CD19 chimeric antigen receptors for acute lymphoblastic leukaemia in children and young adults: a phase 1 dose-escalation trial. *The Lancet*, 385(9967), pp.517–28. Available at: <http://www.ncbi.nlm.nih.gov/pubmed/25319501> [Accessed October 14, 2014].
- Li, Y., Bleakley, M. & Yee, C., 2005. IL-21 influences the frequency, phenotype, and affinity of the antigen-specific CD8 T cell response. *Journal of immunology (Baltimore, Md. : 1950)*, 175(4), pp.2261–9. Available at: <http://www.ncbi.nlm.nih.gov/pubmed/16081794> [Accessed February 15, 2016].
- Lugli, E. et al., 2013. Identification, isolation and in vitro expansion of human and nonhuman primate T stem cell memory cells. *Nature protocols*, 8(1), pp.33–42. Available at: <http://www.ncbi.nlm.nih.gov/pubmed/23222456>.
- Mackay, I.R. et al., 2000. The Immune System. *New England Journal of Medicine*, 343(1), pp.37–49. Available at: <http://www.nejm.org/doi/abs/10.1056/NEJM200007063430107> [Accessed August 28, 2016].
- Maude, S.L. et al., 2014. Chimeric Antigen Receptor T Cells for Sustained Remissions in Leukemia. *New England Journal of Medicine*, 371(16), pp.1507–1517. Available at: <http://www.pubmedcentral.nih.gov/articlerender.fcgi?artid=4267531&tool=pmcentrez&rendertype=abstract> [Accessed October 16, 2014].
- Mockler, M.B., Conroy, M.J. & Lysaght, J., 2014. Targeting T cell immunometabolism for cancer immunotherapy; understanding the impact of the tumor microenvironment. *Frontiers in oncology*, 4, p.107. Available at: <http://www.pubmedcentral.nih.gov/articlerender.fcgi?artid=4032940&tool=pmcentrez&rendertype=abstract> [Accessed September 10, 2015].
- Mucha, K. et al., 2010. Post-transplant lymphoproliferative disorder in view of the new WHO classification: a more rational approach to a protean disease? *Nephrology, dialysis, transplantation : official publication of the European Dialysis and Transplant Association - European Renal Association*, 25(7), pp.2089–98. Available at: <http://ndt.oxfordjournals.org/content/25/7/2089.full> [Accessed July 28, 2015].

- Nagai, Y. et al., 2015. T memory stem cells are the hierarchical apex of adult T-cell leukemia. *Blood*, 125(23), pp.3527–35. Available at: <http://www.ncbi.nlm.nih.gov/pubmed/25847015> [Accessed December 11, 2015].
- Nemerow, G.R. et al., 1987. Identification of gp350 as the viral glycoprotein mediating attachment of Epstein-Barr virus (EBV) to the EBV/C3d receptor of B cells: sequence homology of gp350 and C3 complement fragment C3d. *Journal of virology*, 61(5), pp.1416–20. Available at: <http://www.pubmedcentral.nih.gov/articlerender.fcgi?artid=254117&tool=pmcentrez&rendertype=abstract> [Accessed July 5, 2015].
- Obar, J.J. & Lefrançois, L., 2010. Memory CD8+ T cell differentiation. *Annals of the New York Academy of Sciences*, 1183, pp.251–66. Available at: <http://www.pubmedcentral.nih.gov/articlerender.fcgi?artid=2836783&tool=pmcentrez&rendertype=abstract> [Accessed February 15, 2016].
- Pariante, M. et al., 2007. [Age distribution of serological profiles of Epstein-Barr virus infection: review of results from a diagnostic laboratory]. *Enfermedades infecciosas y microbiología clínica*, 25(2), pp.108–10. Available at: <http://www.ncbi.nlm.nih.gov/pubmed/17288908> [Accessed July 21, 2015].
- Parkin, D.M., 2006. The global health burden of infection-associated cancers in the year 2002. *International journal of cancer. Journal international du cancer*, 118(12), pp.3030–44. Available at: <http://www.ncbi.nlm.nih.gov/pubmed/16404738> [Accessed June 10, 2015].
- Paulsen, M. & Janssen, O., 2011. Pro- and anti-apoptotic CD95 signaling in T cells. *Cell communication and signaling: CCS*, 9, p.7. Available at: <http://www.ncbi.nlm.nih.gov/pubmed/21477291> [Accessed September 14, 2016].
- Pearce, E.L. et al., 2009. Enhancing CD8 T-cell memory by modulating fatty acid metabolism. *Nature*, 460(7251), pp.103–107. Available at: <http://www.pubmedcentral.nih.gov/articlerender.fcgi?artid=2803086&tool=pmcentrez&rendertype=abstract> [Accessed October 11, 2015].
- Pearce, E.L. et al., 2013. Fueling immunity: insights into metabolism and lymphocyte function. *Science (New York, N.Y.)*, 342(6155), p.1242454. Available at: <http://www.ncbi.nlm.nih.gov/pubmed/24115444>.
- Plas, D.R., Rathmell, J.C. & Thompson, C.B., 2002. Homeostatic control of lymphocyte survival: potential origins and implications. *Nature immunology*, 3(6), pp.515–21. Available at: <http://dx.doi.org/10.1038/ni0602-515> [Accessed October 23, 2015].
- Porter, D.L. et al., 2015. Chimeric antigen receptor T cells persist and induce sustained remissions in relapsed refractory chronic lymphocytic leukemia. *Science translational medicine*, 7(303), p.303ra139. Available at: <http://stm.sciencemag.org/content/7/303/303ra139> [Accessed November 21, 2015].

- Restifo, N.P., 2014. Big bang theory of stem-like T cells confirmed. *Blood*, 124(4), pp.476–7. Available at: <http://www.pubmedcentral.nih.gov/articlerender.fcgi?artid=4110654&tool=pmcentrez&rendertype=abstract> [Accessed August 27, 2015].
- Robbins, P.F. et al., 2013. Mining exomic sequencing data to identify mutated antigens recognized by adoptively transferred tumor-reactive T cells. *Nature medicine*, 19(6), pp.747–52. Available at: <http://www.pubmedcentral.nih.gov/articlerender.fcgi?artid=3757932&tool=pmcentrez&rendertype=abstract> [Accessed January 21, 2016].
- Rosenberg, S.A. et al., 2011. Durable Complete Responses in Heavily Pretreated Patients with Metastatic Melanoma Using T-Cell Transfer Immunotherapy. *Clinical Cancer Research*, 17(13), pp.4550–4557. Available at: <http://www.pubmedcentral.nih.gov/articlerender.fcgi?artid=3131487&tool=pmcentrez&rendertype=abstract> [Accessed August 8, 2014].
- Rossignol, R. et al., 2004. Energy Substrate Modulates Mitochondrial Structure and Oxidative Capacity in Cancer Cells. *Cancer Research*, 64(3), pp.985–993.
- Rowe, M. et al., 1991. Epstein-Barr virus (EBV)-associated lymphoproliferative disease in the SCID mouse model: implications for the pathogenesis of EBV-positive lymphomas in man. *The Journal of experimental medicine*, 173(1), pp.147–58. Available at: <http://www.pubmedcentral.nih.gov/articlerender.fcgi?artid=2118756&tool=pmcentrez&rendertype=abstract> [Accessed August 11, 2015].
- Sabatino, M. et al., 2016. Generation of clinical-grade CD19-specific CAR-modified CD8+ memory stem cells for the treatment of human B-cell malignancies. *Blood*, 128(4), pp.519–28. Available at: <http://www.ncbi.nlm.nih.gov/pubmed/27226436> [Accessed July 31, 2016].
- Sarbasov, D.D. et al., 2006. Prolonged rapamycin treatment inhibits mTORC2 assembly and Akt/PKB. *Molecular cell*, 22(2), pp.159–68. Available at: <http://www.ncbi.nlm.nih.gov/pubmed/16603397> [Accessed July 29, 2014].
- Saule, P. et al., 2006. Accumulation of memory T cells from childhood to old age: central and effector memory cells in CD4(+) versus effector memory and terminally differentiated memory cells in CD8(+) compartment. *Mechanisms of ageing and development*, 127(3), pp.274–81. Available at: http://www.researchgate.net/publication/7418304_Saule_P._et_al._Accumulation_of_memory_T_cells_from_childhood_to_old_age_Central_and_effector_memory_cells_in_CD4_versus_effector_memory_and_terminally_differentiated_memory_cells_in_CD8_compartment._Mech._Ageing_Dev._127_274-281 [Accessed September 29, 2015].
- Shope, T., Dechairo, D. & Miller, G., 1973. Malignant lymphoma in cottontop marmosets after inoculation with Epstein-Barr virus. *Proceedings of the National Academy of Sciences of*

- the United States of America*, 70(9), pp.2487–91. Available at: <http://www.pubmedcentral.nih.gov/articlerender.fcgi?artid=427039&tool=pmcentrez&rendertype=abstract> [Accessed September 18, 2015].
- Shultz, L.D. et al., 2005. Human lymphoid and myeloid cell development in NOD/LtSz-scid IL2R gamma null mice engrafted with mobilized human hemopoietic stem cells. *Journal of immunology (Baltimore, Md.: 1950)*, 174(10), pp.6477–89. Available at: <http://www.ncbi.nlm.nih.gov/pubmed/15879151> [Accessed February 24, 2016].
- Sinclair, L. V et al., 2008. Phosphatidylinositol-3-OH kinase and nutrient-sensing mTOR pathways control T lymphocyte trafficking. *Nature immunology*, 9(5), pp.513–21. Available at: <http://www.pubmedcentral.nih.gov/articlerender.fcgi?artid=2857321&tool=pmcentrez&rendertype=abstract> [Accessed January 25, 2016].
- Staal, F.J.T., Luis, T.C. & Tiemessen, M.M., 2008. WNT signalling in the immune system: WNT is spreading its wings. *Nature reviews. Immunology*, 8(8), pp.581–93. Available at: <http://www.ncbi.nlm.nih.gov/pubmed/18617885> [Accessed October 26, 2015].
- Stemberger, C. et al., 2014. Lowest numbers of primary CD8+ T cells can reconstitute protective immunity upon adoptive immunotherapy. *Blood*, 124(4), pp.628–637.
- Stevanović, S. et al., 2015. Complete regression of metastatic cervical cancer after treatment with human papillomavirus-targeted tumor-infiltrating T cells. *Journal of clinical oncology: official journal of the American Society of Clinical Oncology*, 33(14), pp.1543–50. Available at: <http://www.ncbi.nlm.nih.gov/pubmed/25823737> [Accessed January 5, 2016].
- Steven, N.M. et al., 1997. Immediate early and early lytic cycle proteins are frequent targets of the Epstein-Barr virus-induced cytotoxic T cell response. *The Journal of experimental medicine*, 185(9), pp.1605–17. Available at: <http://www.pubmedcentral.nih.gov/articlerender.fcgi?artid=2196300&tool=pmcentrez&rendertype=abstract> [Accessed June 17, 2015].
- Sukumar, M. et al., 2013. Inhibiting glycolytic metabolism enhances CD8+ T cell memory and antitumor function. *Journal of Clinical Investigation*, 123(10), pp.4479–4488.
- Surh, C.D. & Sprent, J., 2008. Homeostasis of naive and memory T cells. *Immunity*, 29(6), pp.848–62. Available at: <http://www.ncbi.nlm.nih.gov/pubmed/19100699> [Accessed February 15, 2016].
- Taylor, G.S. et al., 2014. The Immunology of Epstein-Barr Virus–Induced Disease. *Annual Review of Immunology*, 33(1), p.150223151939000. Available at: <http://www.annualreviews.org/doi/abs/10.1146/annurev-immunol-032414-112326>.
- Théry, C. & Amigorena, S., 2001. The cell biology of antigen presentation in dendritic cells. *Current opinion in immunology*, 13(1), pp.45–51. Available at: <http://www.ncbi.nlm.nih.gov/pubmed/11154916> [Accessed August 28, 2016].

- Thorley-Lawson, D. a, 2001. Epstein-Barr virus: exploiting the immune system. *Nature reviews. Immunology*, 1(1), pp.75–82.
- Touitou, R. et al., 2003. Heterogeneous Epstein-Barr virus latent gene expression in AIDS-associated lymphomas and in type I Burkitt's lymphoma cell lines. *The Journal of general virology*, 84(Pt 4), pp.949–57. Available at: <http://jgv.microbiologyresearch.org/content/journal/jgv/10.1099/vir.0.18687-0> [Accessed November 9, 2015].
- van der Windt, G.J.W. et al., 2012. Mitochondrial Respiratory Capacity Is a Critical Regulator of CD8+ T Cell Memory Development. *Immunity*, 36(1), pp.68–78. Available at: <http://dx.doi.org/10.1016/j.immuni.2011.12.007>.
- Vandesompele, J. et al., 2002. Accurate normalization of real-time quantitative RT-PCR data by geometric averaging of multiple internal control genes. *Genome biology*, 3(7), p.RESEARCH0034.
- Weerkamp, F. et al., 2006. Wnt signaling in the thymus is regulated by differential expression of intracellular signaling molecules. *Proceedings of the National Academy of Sciences of the United States of America*, 103(9), pp.3322–6. Available at: <http://www.pubmedcentral.nih.gov/articlerender.fcgi?artid=1413930&tool=pmcentrez&rendertype=abstract> [Accessed December 14, 2015].
- Weinberg, S.E. & Chandel, N.S., 2014. Futility Sustains Memory T Cells. *Immunity*, 41(1), pp.1–3. Available at: <http://dx.doi.org/10.1016/j.immuni.2014.06.009>.
- Willinger, T. et al., 2006a. Human naive CD8 T cells down-regulate expression of the WNT pathway transcription factors lymphoid enhancer binding factor 1 and transcription factor 7 (T cell factor-1) following antigen encounter in vitro and in vivo. *Journal of immunology (Baltimore, Md. : 1950)*, 176(3), pp.1439–1446.
- Willinger, T. et al., 2006b. Human naive CD8 T cells down-regulate expression of the WNT pathway transcription factors lymphoid enhancer binding factor 1 and transcription factor 7 (T cell factor-1) following antigen encounter in vitro and in vivo. *Journal of immunology (Baltimore, Md. : 1950)*, 176(3), pp.1439–46. Available at: <http://www.ncbi.nlm.nih.gov/pubmed/16424171> [Accessed November 19, 2015].
- Xu, X. et al., 2012. mTOR, linking metabolism and immunity. *Seminars in Immunology*, 24(6), pp.429–435. Available at: <http://dx.doi.org/10.1016/j.smim.2012.12.005>.
- Young, L.S. & Rickinson, A.B., 2004. Epstein-Barr virus: 40 years on. *Nature reviews. Cancer*, 4(10), pp.757–768.
- Zhou, X. et al., 2010. Differentiation and persistence of memory CD8(+) T cells depend on T cell factor 1. *Immunity*, 33(2), pp.229–40. Available at: <http://www.pubmedcentral.nih.gov/articlerender.fcgi?artid=2928475&tool=pmcentrez&rendertype=abstract> [Accessed January 28, 2016].

8. Appendix

8.1 Abbreviations

2-DG	2-deoxy-D-glucose
⁵¹Cr	chromium-51
AIDS	acquired immunodeficiency syndrome
APC	antigen presenting cell
ATL	adult T cell leukemia
ATP	adenosine triphosphate
Bcl-6	B cell CLL/lymphoma 6
BCR	B cell receptor
BL	Burkitt's lymphoma
B-LCL	B lymphoblastoid cell line
CAR	chimeric antigen receptor
CLL	chronic lymphocytic leukemia
CPTI	carnitine palmitoytransferase I
DC	dendritic cell
DMSO	dimethyl sulphoxide
DVL	<i>Drosophila Dishevelled</i>
EBNA	Epstein-Barr nuclear antigen
EBV	Epstein-Barr virus
ECAR	extracellular acidification rate
EDTA	ethylene-diamine-tetraacetic-acid
ELISpot	enzyme linked immune spot
FACS	fluorescence activated cell sorting
FAO	fatty acid oxidation
FSC	forward scatter
GaCa	gastric carcinoma
GC	germinal center
Glut-1	glucose transporter-1
GvHD	graft-versus-host disease
HEV	high endothelial venules
HIV-1	immunodeficiency virus type I
HL	Hodgkin's lymphoma
HLA	human leucocyte antigen
HRP	horse radish peroxidase
HSCT	hematopoietic stem cell transplantation

HTVL-1	human T cell leukemia virus type 1
(i.v.)	intra venous
IFN-γ	interferon- γ
IM	infectious mononucleosis
IS	integration site
LAL	lysosomal acid lipase
LCMV	lymphocytic choriomeningitis virus
Lef-1	lymphoid enhancer-binding factor-1
LMP1	latent membrane protein 1
LMP2A	latent membrane protein 2A
LPD	lymphoproliferative disease
MACS	magnetic activated cell sorting
MFI	mean fluorescence intensity
MHC	major histocompatibility complex
MHV-68	γ murine herpesvirus-68
mTOR	mammalian target of rapamycin
NADH	nicotinamide adenine dinucleotide
NK	natural killer cells
NPC	nasopharyngeal carcinoma
NSG	NOD-SCID IL-2R gamma null
OCR	oxygen consumption rate
OXPHOS	oxidative phosphorylation
PBMC	peripheral blood mononuclear cell
PBS	phosphate buffered saline
PPP	pentose phosphate pathway
PTLD	post-transplant lymphoproliferative disease
RAPA	rapamycin
SCID	severe combined immunodeficiency
SNAT-2	glutamine transporter-2
SOT	solid organ transplantation
SRC	spare respiratory capacity
SSC	side scatter
Tcf-7	T cell factor-7
T_{CM}	T central memory
TCR	T cell receptor
T_{EFF}	T effector cell
T_{EM}	T effector memory cell
TIL	tumor-infiltrating lymphocytes

T_N	T naive cell
TNF	tumor necrosis factor
T_{SCM}	T stem cell memory
UCNT	undifferentiated carcinoma of the nasopharyngeal type
VAHS	virus associated hemophagocytic syndrome
VEGF	vascular endothelial growth factor

8.1 Index of figures

Figure 1: Memory T cell frequency pathogen susceptibility and mortality throughout human life.	4
Figure 2: “Linear” or “developmental” model of T cell differentiation..	5
Figure 3: Active and inactive stage of Wnt-β-catenin signaling..	7
Figure 4: mTOR-signaling cascade	8
Figure 5: Dynamic of T cell metabolism during an immune response.	10
Figure 6: Memory T cells engage in fatty-acid synthesis and oxidation.....	12
Figure 7: Hypothetical model of EBV persistence in human organism.	14
Figure 8: Generation of EBV-specific CTL _{SCM/CM} cells from naïve CD8 ⁺ T cells.....	32
Figure 9: Accumulation of 2-DG6P in the cell.	34
Figure 10: Transmigration assay..	39
Figure 11: EBV-specific CTL _{SCM/CM} transfer into NSG-mice.....	41
Figure 12: Phenotype of naïve CD8 ⁺ T cells examined on day of isolation and on day 21 after RAPA treatment	43
Figure 13: Phenotype of total CD8 ⁺ T cells examined on day of isolation and on day 21 in the culture.	44
Figure 14: Phenotype of naïve CD8 ⁺ T cells examined on day of isolation and on day 21 after 2-DG treatment.....	46
Figure 15: Phenotype of total CD8 ⁺ T cells examined on day of isolation and on day 21 after 2-DG treatment.....	47
Figure 16: Phenotype of naïve CD8 ⁺ T cells examined on day of isolation and on day 21 after TWS119 treatment	48
Figure 17: Phenotype of total CD8 ⁺ T cells examined on day of isolation and on day 21 in the culture	49
Figure 18: <i>In vitro</i> proliferation of EBV-CTL _{SCM/CM} cells after RAPA treatment.....	50
Figure 19: <i>In vitro</i> proliferation of EBV-CTL _{SCM/CM} cells after 2-DG treatment.....	50
Figure 20: <i>In vitro</i> proliferation of EBV-CTL _{SCM/CM} cells after TWS119 treatment	51
Figure 21: Expression pattern of EBV encoded proteins in B-LCL.	52
Figure 22: IFN-γ secretion from rapamycin treated CTL _{SCM/CM} cells	53
Figure 23: IFN-γ secretion from 2-DG and TWS119 treated CTL _{SCM/CM} cells.	53
Figure 24: Lytic activity of 2-DG treated CTL _{SCM/CM} cells.....	54
Figure 25: Lytic activity of TWS119 treated CTL _{SCM/CM} cells.....	55
Figure 26: Manipulation of naïve CD8 ⁺ T cell metabolism.....	56
Figure 27: CD36 expression in naïve and total CD8 ⁺ T cell populations	57
Figure 28: Manipulation of total CD8 ⁺ T cell metabolism.....	57
Figure 29: Glucose uptake measured in 2-DG and TWS119 treated T cells.....	58

Figure 30: Lactate production measured in 2-DG and TWS119 treated T cells.	59
Figure 31: OCR and ECAR measured in 2-DG treated T cells.....	60
Figure 32: OCR and ECAR measured in TWS119 treated T cells.	61
Figure 33: Lef-1, Tcf-7 and Bcl-6 expression in 2-DG and TWS119 treated T cells	62
Figure 34: Transmigration potential of 2-DG and TWS119 treated CTL _{SCM/CM} cells <i>in vitro</i> . ..	63
Figure 35: <i>In vivo</i> persistence of 2-DG treated EBV-specific CTL _{SCM/CM} cells in NSG-mice. ..	64
Figure 36: <i>In vivo</i> persistence of TWS119 treated EBV-specific CTL _{SCM/CM} in NSG-mice.	65
Figure 37: <i>In vivo</i> EBV-reactivity of 2-DG treated EBV-CTL _{SCM/CM} cells.....	66
Figure 38: Survival of 2-DG treated EBV-CTL _{SCM/CM} and T _{EFF} cells <i>in vivo</i>	67
Figure 39: Prolonged survival of mice post transfer of TWS119 treated EBV-CTL _{SCM/CM}	68
Figure 40: Increased engraftment of TWS119 treated EBV-CTL _{SCM/CM} cells.....	68

8.2 Index of tables

Table 1: Latency transcription programs.....	15
Table 2: Overview of EBV-associated malignancies.....	16
Table 3: The pipetting schema for glucose uptake assay	34
Table 4: Master reaction mix for lactate production assay	36
Table 5: The pipetting schema for transwell assay	39

9. Addendum

9.1 Acknowledgments

Acknowledgements were removed for reasons of data protection

9.2 Curriculum vitae

The curriculum vitae was removed for reasons of data protection.